Nagra
Nationale
Genossenschaft
für die Lagerung
radioaktiver Abfälle

Cédra
Société coopérative
nationale
pour l'entreposage
de déchets radioactifs

Cisra
Società cooperativa
nazionale
per l'immagazzinamento
di scorie radioattive

TECHNICAL REPORT 85-31

Model Calculation of the Groundwater Flow at Oberbauenstock

B. Grundfelt
B. Lindbom
A. Markström

June 1987

KEMAKTA Konsult AB, Stockholm

Parkstrasse 23 5401 Baden/Schweiz Telephon 056/20 55 11

Nagra
Nationale
Genossenschaft
für die Lagerung
radioaktiver Abfälle

Cédra
Société coopérative
nationale
pour l'entreposage
de déchets radioactifs

Cisra
Società cooperativa
nazionale
per l'immagazzinamento
di scorie radioattive

TECHNICAL REPORT 85-31

Model Calculation of the Groundwater Flow at Oberbauenstock

B. Grundfelt
B. Lindbom
A. Markström

June 1987

KEMAKTA Konsult AB, Stockholm

Parkstrasse 23 5401 Baden/Schweiz Telephon 056/20 55 11

Der vorliegende Bericht wurde im Auftrag der Nagra erstellt. Die Autoren haben ihre eigenen Ansichten und Schlussfolgerungen dargestellt. Diese müssen nicht unbedingt mit denjenigen der Nagra übereinstimmen.

Le présent rapport a été préparé sur demande de la Cédra. Les opinions et conclusions présentées sont celles des auteurs et ne correspondent pas nécessairement à celles de la Cédra.

This report was prepared as an account of work sponsored by Nagra. The viewpoints presented and conclusions reached are those of the author(s) and do not necessarily represent those of Nagra.

SUMMARY

Model calculations of the groundwater flow at a potential site for an intermediate-level waste repository at Oberbauen Stock in the Swiss prealps have been performed. The study comprises two steps; modelling of the position of the groundwater table and modelling of the groundwater flow in the host rock.

The calculations in the first case indicate that much of the sedimentary rock above the host rock is partially drained. The highest groundwater table obtained is about 100 m above the surface of the host rock.

The second step shows that the flow through the host rock is directed downwards. Because the quantification of flow rate etc is very sensitive to boundary conditions, it is deemed essential that a thorough understanding of the hydrology of the site be developed.

ZUSAMMENFASSUNG

Es wurden Modellberechnungen der Grundwasserströmung am potentiellen Standort für ein Endlager mittelaktiver Abfälle am Oberbauenstock in den schweizerischen Voralpen durchgeführt. Die Studie besteht aus zwei Phasen: die Modellierung der Höhe des Grundwasserspiegels und jene der Grundwasserströmung im Wirtgestein.

Die Berechnungen der ersten Phase zeigen, dass ein Grossteil des Sedimentgesteins oberhalb des Wirtgesteins teilweise entwässert ist. Der höchste Grundwasserspiegel befindet sich etwa 100 m über der Wirtgesteinsoberfläche.

Die zweite Phase zeigt eine Abwärtsströmung des Grundwassers durch das Wirtgestein. Weil die Quantifizierung der Fliessrate usw. in starkem Masse von den Randbedingungen abhängt, wird die Erarbeitung eines eingehenden Verständnisses der Hydrologie des Standorts für wesentlich gehalten.

RESUME

On a effectué des calculs sur modèle relatifs à l'écoulement des eaux souterraines en un site potentiel de dépôt final pour déchets de faible et moyenne activité, l'Oberbauenstock, situé dans les Préalpes suisses. L'étude s'est faite en deux étapes: modélisation de la position de la nappe phréatique et modélisation de l'écoulement des eaux souterraines dans la roche d'accueil.

Dans le premier cas, les calculs indiquent qu'une grande partie des roches sédimentaires surincombantes à la roche d'accueil est partiellement drainée. La nappe phréatique la plus élévée est située à environ 100 m au-dessus de la surface de la roche d'accueil.

La seconde étape révèle un écoulement descendant à travers la roche d'accueil. Etant donné que la quantification du taux d'écoulement, etc. dépend fortement des conditions aux limites, on estime essentiel d'approfondir les connaissances sur l'hydrologie du site.

CONTENTS

1 INTRODUCTION AND SUMMARY

Mathematical modelling of groundwater flow is an essential and central part of the safety assessment of repositories for radioactive waste. In this report, model calculations of the flow conditions at the Oberbauen Stock site in the Swiss prealps are presented. The calculations have been performed as part of the Swiss Project Gewähr 1985 on contract from NAGRA.

The calculations are based on data interpreted from the documentation of construction of a road tunnel, the Seelisberg tunnel. The repository is situated in marl surrounded by various limestones and shales.

The study is divided into two parts:

- modelling of the groundwater table in the limestones above the marl
- modelling of the flow in the marl with a reduced domain.

The results from the first part, which is a two-dimensional calculation of groundwater flow, show that the limestones above the marl are probably drained. For some parameter combinations, the resulting groundwater table is situated about 100 m above the marl surface.

The second part comprises a number of calculations with a three-dimensional model. In general, the calculated flow in the marl is directed downwards. It is shown that quantification of the flow rate, the flow paths and water travel times is strongly dependent on the boundary conditions assumed.

2 A SHORT DESCRIPTION OF OBERBAUEN STOCK

Oberbauen Stock is situated on the western shore of the Urnersee, the southern most part of the Vierwaldstättersee, in central Switzerland (see Figure 2.1). The area has an alpine character with topographic differences of almost 2,000 metres.

The host rock is a marl (Valanginian marl) which forms part of the Drusberg nappe in the prealps. The marl is surrounded above and below by various limestones of more or less marly character. Figure 2.2 shows a profile from west to east of the site geology.

In the south the marl is bounded by a Tertiary shale and some limestone formations of the Axen nappe. The northern boundary of the marl is formed by the Oberbauen fold of the Drusberg nappe. Figure 2.3 shows a geologic profile from south to north.

The permeabilities of the various formations are poorly investigated. The legend in Figure 4.5 gives some quantitative indications of the current understanding of the permeability relationships between the layers. Some more quantitative conclusions can be drawn on the basis of one observation in the pilot tunnel for construction of the Seelisberg tunnel, a road tunnel runs through the host rock. The quantification is based on general observations combined with ventilation calculations (see Chapter 5).

The water that infiltrates through the topmost layers of the site percolates through the permeable formations. Some of the formations are fractured and karstified. These features will, because of the less permeable marly layers, drain some of the water sideways and thereby reduce the amount of water infiltrating into the host rock.

The modelling of the groundwater flow situation is performed in two steps:

- modelling of the groundwater formation in the partially saturated sedimentary series above the host rock and

- modelling of the flow situation in the host rock assuming fully saturated conditions.

The inclination of the layers at the site indicate that part of the water could be drained westwards instead of flowing to the Urnersee. In the modelling presented in this report, however, all the water is assumed to go into the Urnersee.

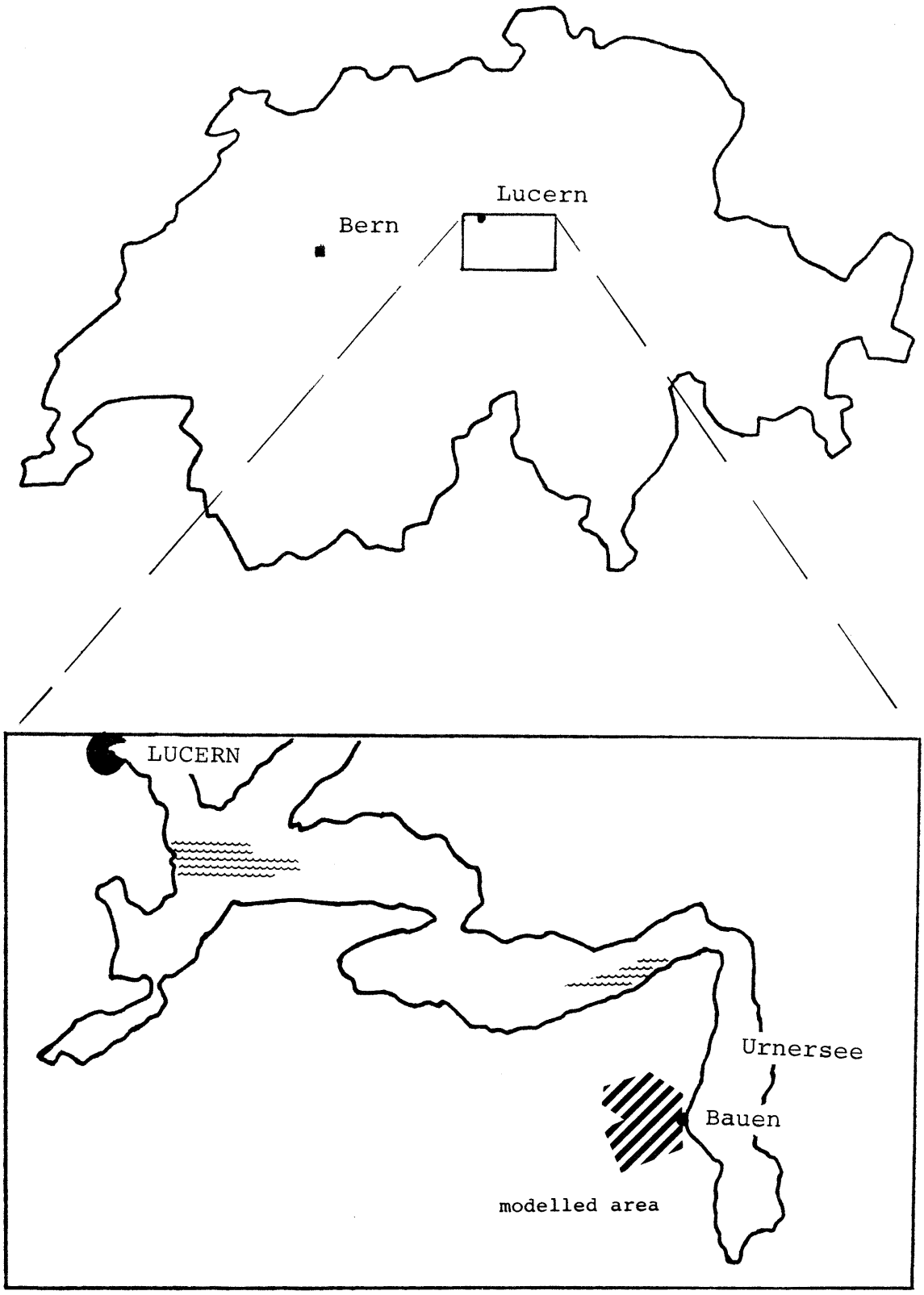

Figure 2.1 Location of the modelled area at Oberbauen Stock in central Switzerland

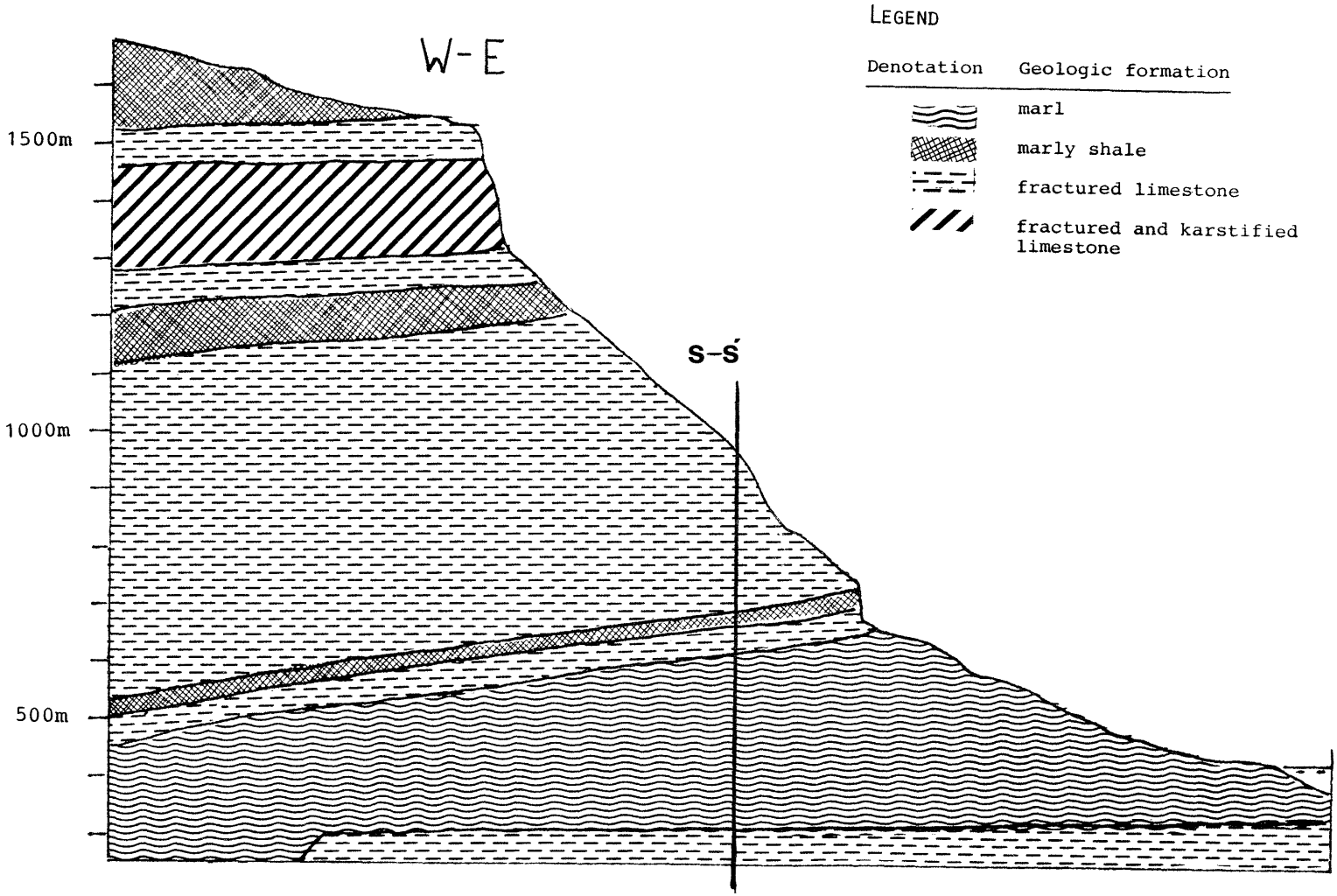

Figure 2.2 Simplified geologic profile from east to west.
(Based of Section B-B' in Figure 7b in NTB 84-20)

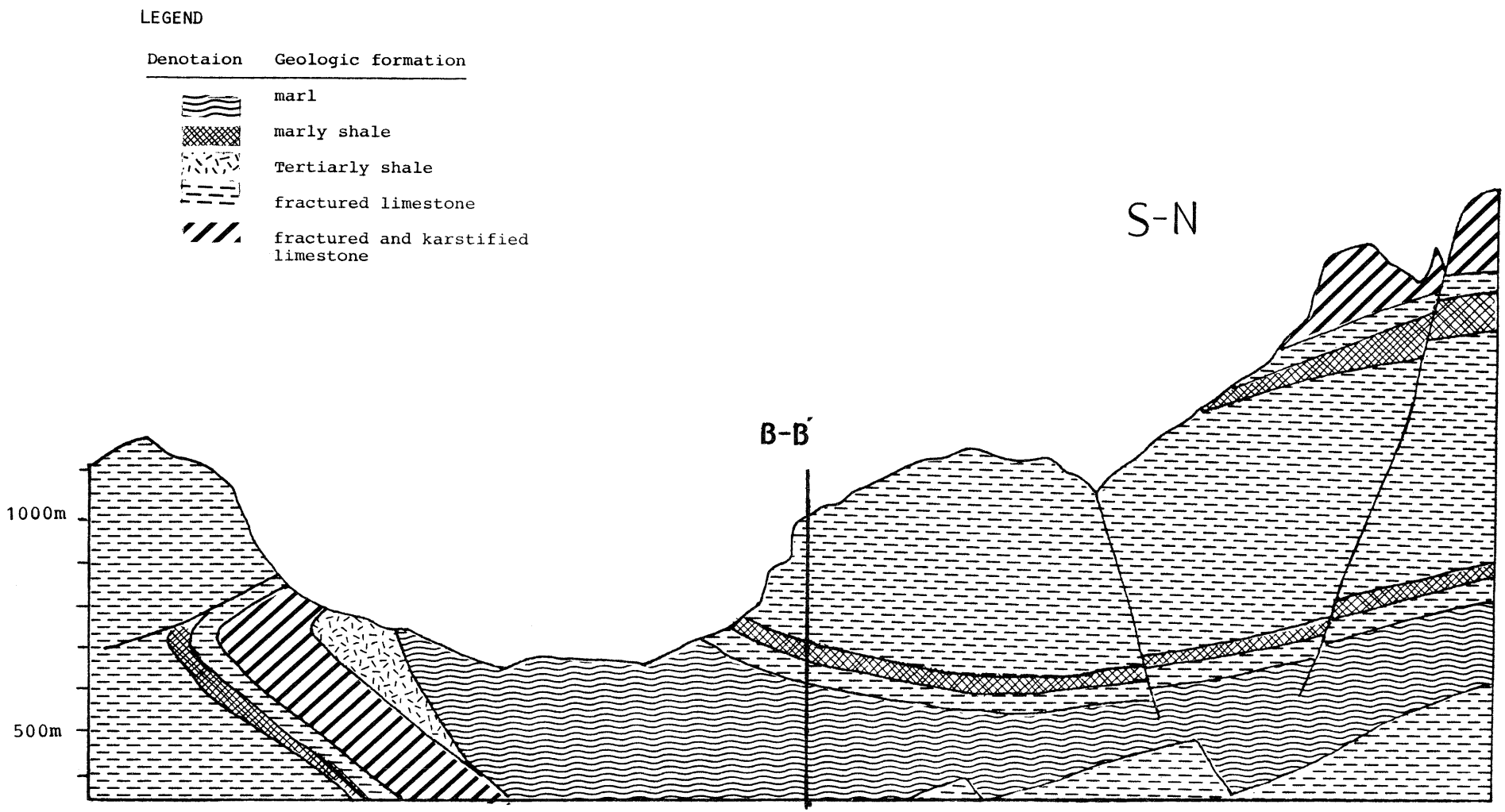

Figure 2.3 Simplified geologic profile from south to north.
(Based on Section S-S' in Figure 7F in NTB 84-20)

3 MODEL DESCRIPTION

3.1 General

The mathematical model used for the hydrological calculations is a one, two and three dimensional model based on the finite element method /1/ for calculation of groundwater pressure.

A program package for pre- and post-processing of data from the finite element model has been developed /4/. It is schematically shown in Figure 3.1 below.

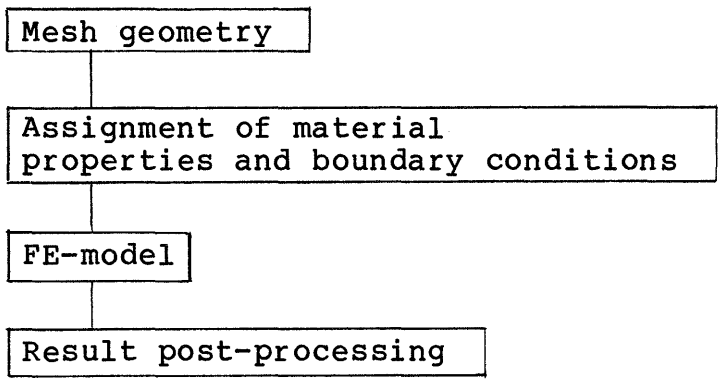

Figure 3.1. Flow sheet of the HYPAC-program package.

3.2 Mesh geometry

The generation of the geometric data is automated in three steps:

- Definition of the geometry of special geological features (e.g. fracture zones) and underground constructions (e.g. tunnels, repositories).
- Mesh generation using a special program, FEMGEN, developed at the University of Lund.
- Mesh post-processing by optimizing the band and front widths to minimize the calculation costs and control of the element distortion.

3.3 Assignment of material properties and boundary conditions

A subroutine package has been developed in order to facilitate the assignment of the material properties and boundary conditions. The package is designed to operate interactively. The model can handle boundary conditions of the types "prescribed pressure" and "prescribed flux".

3.4 FE-model

The model is based on the flow equation (flow through porous media) derived from Darcy's law and the equation of continuity.

A general formulation of the flow equation including saturated/unsaturated flow is:

$$\rho\varepsilon \left[S_w \left(c^f + c^r\right) + \frac{dS_w}{dp} \right] \frac{\partial p}{\partial t} = \bar{\nabla} \cdot \frac{\bar{\bar{k}} \cdot k_{rw} \cdot \rho}{\eta} \left(\bar{\nabla} p - \rho \bar{g}\right)$$

where:

ε	=	porosity	(m^3/m^3)
ρ	=	fluid density	(kg/m^3)
η	=	dynamic viscosity of the fluid	$(Pa \cdot s)$
S_w	=	saturation	(m^3/m^3)
c_f	=	compressibility of fluid = $\frac{1}{\rho} \frac{\partial \rho}{\partial p}$	(Pa^{-1})
c^r	=	compressibility of the rock = $\frac{1}{\varepsilon} \frac{\partial \varepsilon}{\partial p}$	(Pa^{-1})
p	=	groundwater pressure = P_{total}	(Pa)
k	=	intrinsic permeability	(m^2)
k_{rw}	=	relative permeability (wet phase)	
$\bar{g}$	=	gravitational acceleration	(m/s^2)

In this study two series of calculations have been performed. The position of the groundwater table in the sedimentary series overlying the host rock has been studied using a 2D saturated/unsaturated flow model, while the flow in the host rock was modelled assuming a fully saturated 3D formation. In both cases the flow equation was simplified as described below.

2D-model:

In the two-dimensional calculations (Chapter 4), the flow equation has been simplified assuming:

- Steady-state conditions.
- That the relative permeability is uniform over the whole saturation range.

Under these simplifying assumptions, the flow equation may be written:

$$\bar{\nabla} \frac{\rho \bar{\bar{k}}}{\eta} \left(\bar{\nabla} p - \rho \bar{g} \right) = 0$$

3D-model:

In the three-dimensional modelling of the host rock (Chapter 5), the flow equation has been simplified assuming:

- Steady-state conditions in a saturated medium.

The flow equation may be written:

$$\bar{\nabla} \frac{\rho \bar{\bar{k}}}{\eta} \left(\bar{\nabla} p - \rho \bar{g} \right) = 0$$

The equations are solved using the Galerkin formulation of the Finite Element Method.

3.5 Result post-processing

HYPAC contains the following principal post-processing programs:

- CLG/CPL for contouring of hydraulic head on element faces.

- TRG/TPL for particle tracking. The program can also be used for contouring of heads and flow rates at arbitrary cross-sections or for recording hydraulic heads and fluxes along a line (e.g. a borehole).

The post-processing also includes programs for checking the relevance of the results. These programs are:

- REC for checking that all calculated heads are within an interval defined by the extremes of heads assigned as boundary conditions.

- MBC for checking the mass conservation of the solution. This program can also be used to calculate flow rates across arbitrary element faces (e.g. the percolation rate on the top surface). The MBC program is briefly described in Section 5.4.2.

Description of CLG/CPL

The CLG program (Contour Line Generator) calculates contours of hydraulic heads (or any other function defined at the nodal points) and writes the coordinates of successive points of the contour on a file. The CPL program is used for plotting of these contours.

A plot plane is defined as a cross-section running along an arbitrary number of element faces, either projected on one of the three principal planes of the coordinate system or straightened out by calculating one or both of the plot plane coordinates as the distance along the plane.

The main steps of the CLG program are:

- Definition of a plot plane consisting of a mesh of element faces to be contoured.

- Contouring of the mesh.

- Calculation of projected vectors on the element faces.

- Plotting the results (CPL).

The contouring is done using an algorithm that utilizes the same interpolation functions as the finite element mesh. This means that the contours describe the actual calculated heads without smoothing.

The flow vectors are presented in the form of arrows. The length of the arrows is proportional to the logarithm of the Darcy velocity.

Description of TRG/TPL, IPL

The TRG program (Trajectory Generator) was originally used only for particle tracking, but it can also be used for contouring of flow rates and heads in an arbitrary cross-section or for recording hydraulic heads and fluxes along a line. TPL and IPL are the corresponding plotting programs for presentation of the path lines and isocurves.

The main steps of the program are (path lines):

- Locate the element and find the local coordinates of the starting point given in global coordinates.
- Compute potentials, gradients and fluxes.
- Stepping along the trajectory.
- Plotting the path lines (TPL).

The tracking of the trajectories is done using a simple Euleran stepping method. The endpoint of a step is used as a starting point for the next step. An attempt to locate the current element is made. Should this fail, the above program steps are run through once again. After each step the local coordinates of the new starting point must be calculated.

The corresponding steps for contouring potentials and flow rates are:

- Input of a rectangular grid out of an arbitrary cross-section (global coordinates).
- Find the elements and local coordinates.
- Compute potentials, gradients and flow rates.
- Plotting the contours (IPL).

The algorithm used for contouring is a simple first order interpolation on a regular, rectangular grid.

4 SIMULATION OF THE GROUNDWATER TABLE POSITION IN THE LIMESTONE OVERBURDEN

4.1 General

As mentioned in Chapter 2, the geological system at Oberbauen Stock is very complicated due to the large number of different materials and their complex geometry. This means that the boundary conditions for the hydraulic system in the host rock are difficult to estimate, especially considering the lack of adequate field measurements.

As a tool for judging the groundwater head at the top surface of the host rock, two-dimensional modelling of the partially saturated flow in the sedimentary series overlying the host rock has been performed. The study was designed as a parameter variation exercise varying the permeabilities of the various geological media within reasonable intervals.

The calculations have been performed using the finite element model GWHRT described in Chapter 3 and /1,2/.

As a basis for the calculations, a vertical cut through the Oberbauen Stock was chosen.

4.2 Modelling strategy

4.2.1 Geometry of the modelled units

As a basis for the modelling of the partially saturated flow through sedimentary series above the host rock, a two-dimensional cut corresponding to B-B' in Figure 7b in /NTB 84-20/ was chosen. The geographic location of this cut is shown in Figure 4.1.

The modelled cut differs from the original B-B' cut in /NTB 84-20/ in two ways: firstly it has been extended towards the west, in order that the western edge of the cut might coincide with the topographic water divide, slightly north of the summit of Oberbauen Stock (the dashed line in Figure 4.1), and secondly, the sedimentary layers have been made horizontal instead of sloping towards the west. The latter alteration was made to avoid an artificial build-up of a groundwater basin at the western end of the cut because of the no-flow boundary along this edge (see Section 4.2.3).

The sedimentary series as interpreted in /NTB 84-20/ is shown in Figure 4.2. The essential property from a groundwater hydrology point of view is the hydraulic conductivity of the various layers. In Figure 4.5 the hydraulic conductivity of the various layers has been qualitatively indicated. For modelling purposes, the sedimentary series has been simplified as indicated in Figure 4.3, which shows the modelled domain, the finite element mesh and the material property areas.

Apart from the host rock (the Valanginian marl), the domain contains three aquifers ("Schrattenkalk", siliceous limestone and Valanginian limestone) and two aquitards (marly Drusberg layer and marly shale).

The host rock has been extended downwards compared to the description in cut B-B'. This extension of impervious material puts the groundwater at a higher level than would be the case with a permeable material. The introduction of a pervious bottom layer connected to the Urnersee would decrease the pressure drop across the marl and hence also lower the level of the groundwater table. The vertical extension of the domain also decreases the influence of the bottom boundary condition on the flow field (see Section 4.2.3).

4.2.2 Finite element mesh

The finite element mesh used consists of 272 rectangular 8-node elements and a total of 889 nodal points. The mesh is shown in Figure 4.3.

Along the eastern (right hand side in Figure 4.3) slope of the sedimentary series and the host rock, two thin element layers have been introduced to describe a seepage face. This is further described below.

4.2.3 Boundary conditions

Figure 4.4 shows the applied boundary conditions. At the top of the "Schrattenkalk" aquifer, an infiltration rate of 420 mm/yr, corresponding to 30% of the precipitation in the region, is applied. The western and bottom boundaries are no-flow boundaries.

Along the eastern slope a seepage face is modelled above the lake surface. Below the lake surface a hydrostatic pressure corresponding to the hydraulic head of the lake surface (433 m.a.s.l.) is applied.

The seepage face is modelled using two thin element layers with a high hydraulic conductivity compared to the rest of the media. The boundary condition on the outside of these elements is a no-flow boundary.

4.2.4 Material properties

The governing material properties in a partially saturated flow model are the hydraulic conductivity at full saturation, the relative permeability as a function of the saturation and the capillary suction head as a function of the degree of saturation (see Chapter 3). The latter two parameters are specific to the partially saturated flow problem whereas the hydraulic conductivity appears in most flow model applications.

In a steady-state system, the capillary suction results in a negative pressure in the unsaturated zone, the hydraulic head being less than the level above a given datum. From this pressure the degree of saturation and hence the relative permeability can be solved iteratively.

The limestones in the sedimentary series are usually cracked. The main portion of the flow in these layers will occur in the fractures where the capillary suction is low and the variation in permeability due to different degrees of saturation is small. In this study it has therefore been assumed that the relative permeability is uniform, regardless of the degree of saturation. This also linearises the flow equation and thus simplifies the solution.

Consequently the essential material property for the problem stated in this chapter is the hydraulic conductivity at full saturation. Figure 4.5 shows reasonable ranges for the conductivity of the various media modelled. Because there is no field data available, the values in the Figure have been based on common hydrogeologic experience of similar media /3/.

The hydraulic conductivity of the seepage face elements is not shown in Figure 4.5. It has been varied in the interval 10^{-5}-10^{-2} m/s and is two orders of magnitude higher than the conductivity of the "Schrattenkalk" layer. Cases 1 and 2 are regarded as reference cases and the value of the hydraulic conductivity for the seepage elements is not within this range.

4.2.5 Overview of parameter variations performed

In this report, 10 different calculations with varying hydraulic conductivities are presented. In two of these runs the whole domain has the same hydraulic conductivity, except for the seepage face elements. The other eight runs aim at demonstrating the influence of different conductivities in the different layers. Table 4.1 shows the hydraulic conductivities used in the 10 runs. The results are discussed in Section 4.3.

Table 4.1 Variation of the hydraulic conductivities for the different layers and runs. For explanation of K_1-K_6 see Figure 4.5.

K m/s Case no.	1	2	3	4	5	6	7	8	9	10
K_1	$5\cdot10^{-8}$	$5\cdot10^{-8}$	10^{-4}	10^{-4}	10^{-5}	10^{-5}	10^{-5}	10^{-7}	10^{-7}	10^{-7}
K_2	$5\cdot10^{-8}$	$5\cdot10^{-8}$	10^{-7}	10^{-7}	10^{-7}	10^{-9}	10^{-9}	10^{-9}	10^{-9}	10^{-9}
K_3	$5\cdot10^{-8}$	$5\cdot10^{-8}$	10^{-5}	10^{-5}	10^{-5}	10^{-6}	10^{-6}	10^{-6}	10^{-7}	10^{-7}
K_4	$5\cdot10^{-8}$	$5\cdot10^{-8}$	10^{-6}	10^{-6}	10^{-8}	10^{-8}	10^{-6}	10^{-6}	10^{-6}	10^{-6}
K_5	$5\cdot10^{-8}$	$5\cdot10^{-8}$	10^{-4}	10^{-4}	10^{-5}	10^{-5}	10^{-6}	10^{-5}	10^{-7}	10^{-6}
K_6	$5\cdot10^{-8}$	$5\cdot10^{-8}$	10^{-8}	10^{-10}	10^{-10}	10^{-10}	10^{-10}	10^{-10}	10^{-10}	10^{-8}
K_{seep}	$5\cdot10^{-8}$	$5\cdot10^{-6}$	10^{-2}	10^{-2}	10^{-3}	10^{-3}	10^{-3}	10^{-5}	10^{-5}	10^{-5}

4.3 Results

4.3.1 General

As mentioned above, the object of primary interest in this study is the hydraulic head at the top surface of the Valanginian marl. The position of the groundwater table gives a conservative (high) estimate of this head, given that it is located above the top surface of the marl. In this section, plots of the groundwater table and flow vectors are shown for a selection of the runs. Furthermore the calculated infiltration rates into the aquitards (the marly Drusberg layer and the marly shale) and the host rock are given for all runs.

The cases for which no plots are depicted (cases 5-7) show results that are similar to cases 3 and 4, i.e. they yield a low groundwater table.

The velocity vectors are shown as arrows with a length proportional to the logarithm of the Darcy velocity.

4.3.2 The position of the groundwater table

In Figures 4.6-4.10 the results from cases 3,4,8,9 and 10 are shown. These cases can be divided into two groups, cases 3 and 4 representing a system with a low groundwater table where the top of the host rock is unsaturated and cases 8-10 representing a system with a fully saturated host rock and a groundwater table lying slightly above the marl top surface.

The main difference between the two groups is that, in the first group (cases 3 and 4), the hydraulic conductivities are all at the high end of the intervals in Figure 4.5, whereas in the second group the conductivities are low.

It appears that the most important parameters in the calculations are the hydraulic conductivities of the "Schrattenkalk" and the way the seepage face is modelled (K_1 and K_{seep}). When these conductivities are high, more water is drained to the steep eastern flank and hence less water remains to infiltrate into the host rock. This is demonstrated in Table 4.2 which shows the infiltration rate for the aquitards and the host rock for the different cases. In cases 3 and 10, the hydraulic conductivity of the host rock is two orders of magnitude higher than in the other runs. If this is compensated for, one sees in the Table that, in the cases presented, the rate of infiltration into the Valanginian marl appears to be almost inversely proportional to the conductivities of the "Schrattenkalk" and the seepage face.

The influence of the hydraulic conductivity of the Valanginian marl can be seen from a comparison between cases 9 and 10 and between cases 3 and 4. In cases 3 and 10 the conductivity of the marl is two orders of magnitude higher than in cases 4 and 9 respectively. This has resulted in almost a 100 times higher infiltration rate into the marl but the position of the groundwater table is almost unaffected by the change. Most of the water needed to maintain the groundwater table in these cases is taken from recharge to the siliceous limestone aquifer from the seepage face. In the calculations this infiltration occurs as a consequence of the pressure drop over the marly Drusberg layer being greater than that in the seepage face. This infiltration may be artificial or at least exaggerated. There is currently no consensus on how to model a seepage face in the undersaturated zone.

Table 4.2 Calculated infiltration rates into the aquitards in the sedimentary series and into the host rock.

Case no.	"Schrattenkalk"	Infiltration (mm/yr) to unit: Marly Drusberglayer	Marly shale	Valanginian Marl
1	420	382	296	242
2	|	235	138	134
3	|	7	13	0.02
4	|	24	9	0.0003
5	|	65	7	0.003
6	|	1	3	0.002
7	|	1	3	0.003
8	|	81	245	0.2
9	|	75	88	0.3
10	420	79	141	23

4.3.3 The effect of the seepage face

As mentioned in Section 4.2.4, the hydraulic conductivity of the seepage face was taken to be 100 times the conductivity of the "Schrattenkalk" layer in cases 3-10. The effects of the "Schrattenkalk" conductivity and the seepage face conductivity on the drainage of the system cannot therefore be decoupled in these cases. Cases 1 and 2 were run to illustrate the effect of the seepage face in a simplified situation where, for all media, the same hydraulic conductivity has been chosen in order to balance the infiltration, thus yielding a relatively high groundwater table.

Figures 4.11 and 4.12 show the groundwater table and the flow field for cases 1 and 2. In case 2, the hydraulic conductivity in the seepage face is two orders of magnitude higher than in the rest of the domain, whereas in case 1 the whole domain is homogeneous. The conductivity increase in the seepage face causes a lowering of the groundwater table from approximately 1400 m to around 900 m, i.e. a drop of 500 m. This is an artefact of the model.

As mentioned in the previous subsection, the model representation of the seepage face is probably inappropriate. The most obvious sign of this is the significant infiltration into the siliceous limestone layer from the seepage face.

4.4 Discussion

An attempt has been made to estimate the highest and lowest position of the groundwater table in the sedimentary series overlying the host rock at Oberbauen Stock using a partially saturated flow model and varying the hydraulic conductivities of the various layers in the series.

The results show a maximum level of the groundwater table at about 100 m above the host rock top surface (700 m.a.s.l.). This maximum level occurs when the hydraulic conductivities of all media are at the low end of the reasonable intervals. If the conductivities increase, the groundwater table is lowered. Moreover the results indicate that the numerical model system is particularly sensitive to the conductivity of the topmost layer of the series and to the implementation of the seepage face describing the eastern flank of the series.

Because the sub-regional hydraulic system of Oberbauen Stock has been poorly investigated, there are several uncertainties of which the most important are:

- the description of the boundary condition at the eastern flank of the domain (seepage face)
- the omission of the influence of capillary forces and other effects of the partial saturation on the hydraulic conductivity
- the potential for strong seasonal variations in the infiltration at the top of the system
- the assignment of an infiltration rate at the top surface independently of the hydraulic conductivity of the topmost layer

The seepage face at the eastern flank does not describe evapotranspiration. Including evapotranspiration would decrease the amount of water available to infiltrate the host rock. Furthermore, modelling the seepage face as a channel retains too high ahead in the seepage face. This causes an artificial infiltration into the siliceous limestone layer. The calculations presented are thus conservative, i.e. they give too high a groundwater table with respect to this phenomenon.

The omission of the influence of capillary forces on the permeability probably exaggerates the tendency to drain the system. This assumption is therefore not conservative. Also, the seasonal infiltration variation could cause at least a temporary rise in the groundwater table. The steady-state assumption is therefore not necessarily a conservative one.

In reality, the rate of infiltration at the top of the formation is a balance between the hydraulic conductivity of the topmost layer and the precipitation rate. Accounting for this would decrease the tendency of the groundwater table to rise when the conductivity is lowered.

In some of the runs, the top of the host rock is unsaturated mainly because of a very low rate of infiltration into the host rock. Observations during the construction of the Seelisberg tunnel /NTB 84-20/, /3/, however, indicate that the host rock is saturated. It must therefore be deemed probable that the infiltration into the host rock is underestimated in the case with a very low groundwater table.

In conclusion, given the above-mentioned uncertainties, the accuracy of the results is limited. It is, however, reasonable to assume that the groundwater table varies between the top surface of the host rock and about 700 m.a.s.l., although other assumptions regarding hydraulic conductivities might yield a still higher groundwater table.

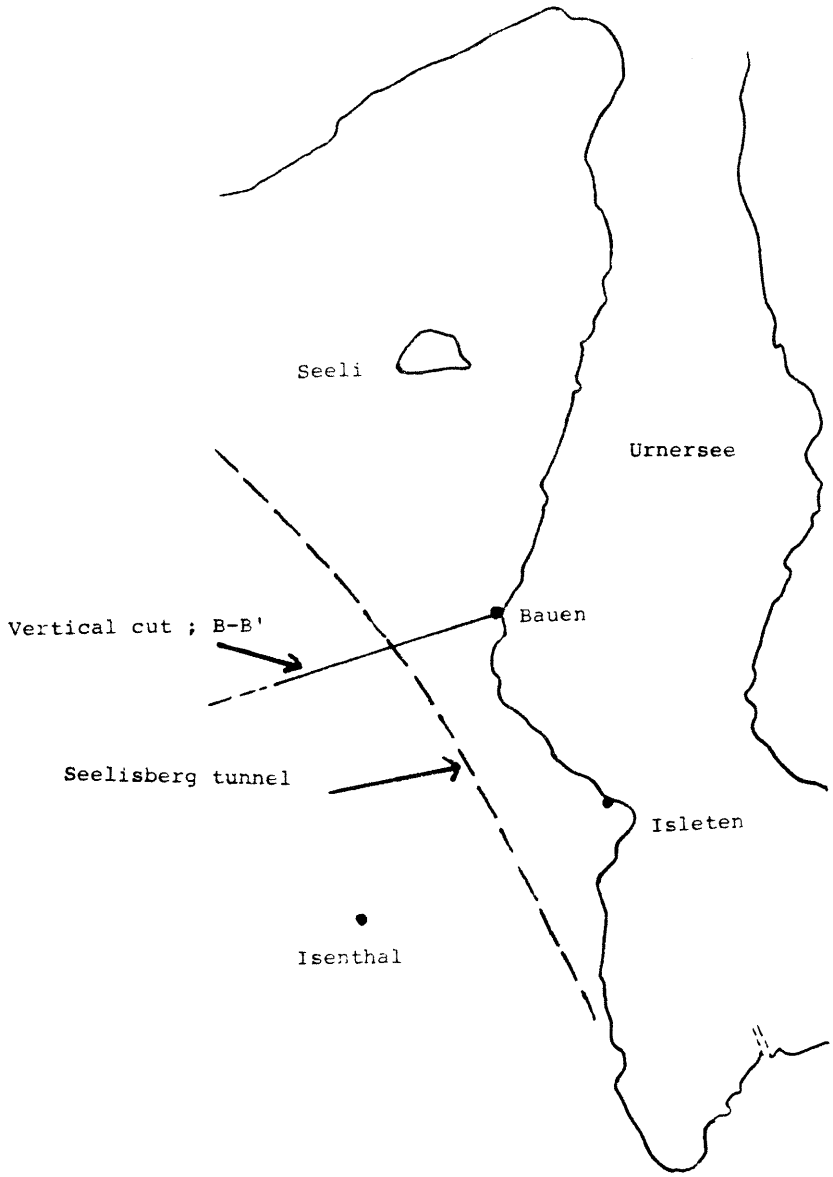

Figure 4.1 Position of the cut B-B' as modelled. The dashed line shows the extension of the cut towards the topographic water divide.

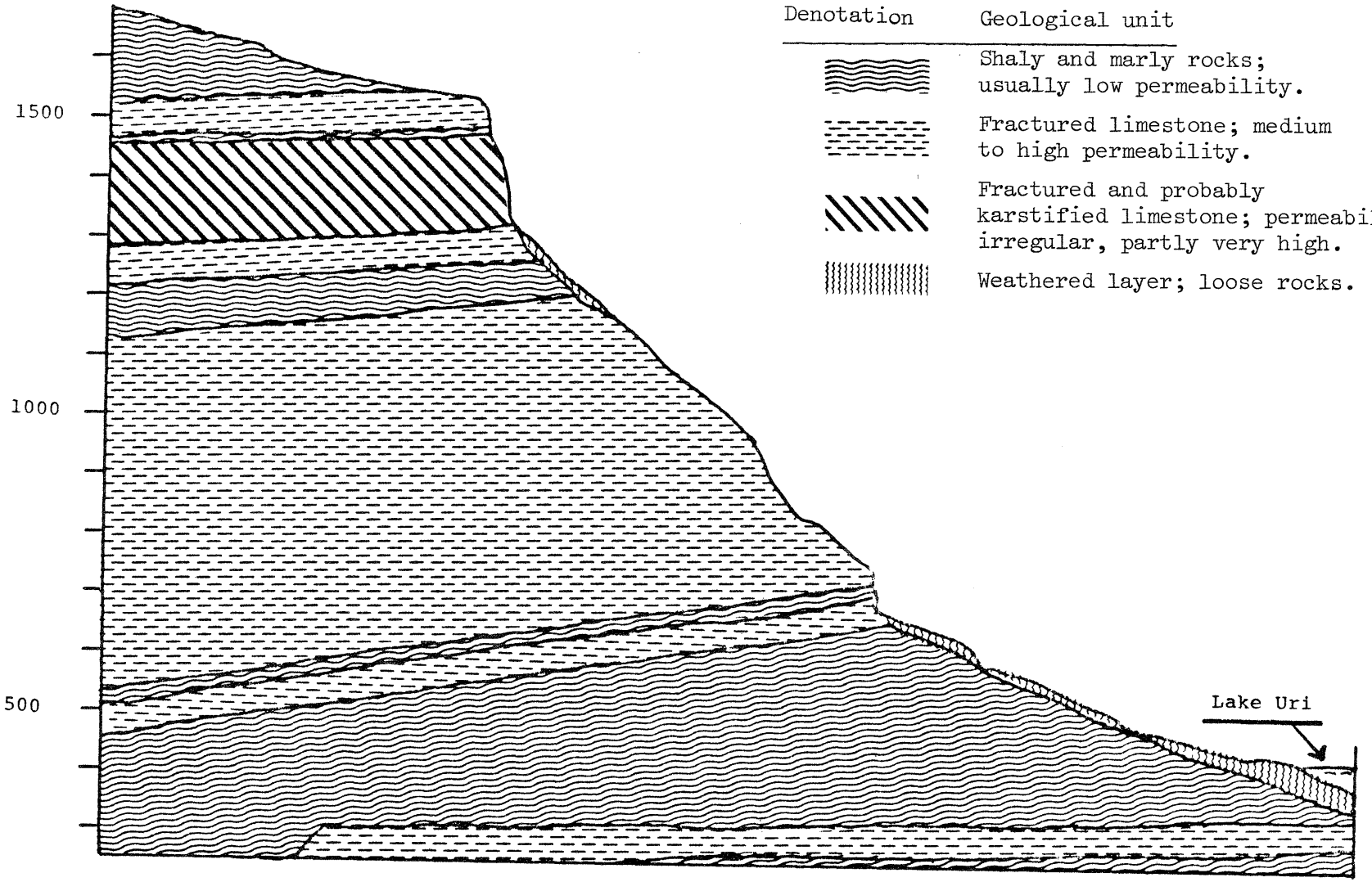

Figure 4.2 Schematic view of the sedimentary series and the host rock at Oberbauen Stock. The section corresponds to cut B-B'.

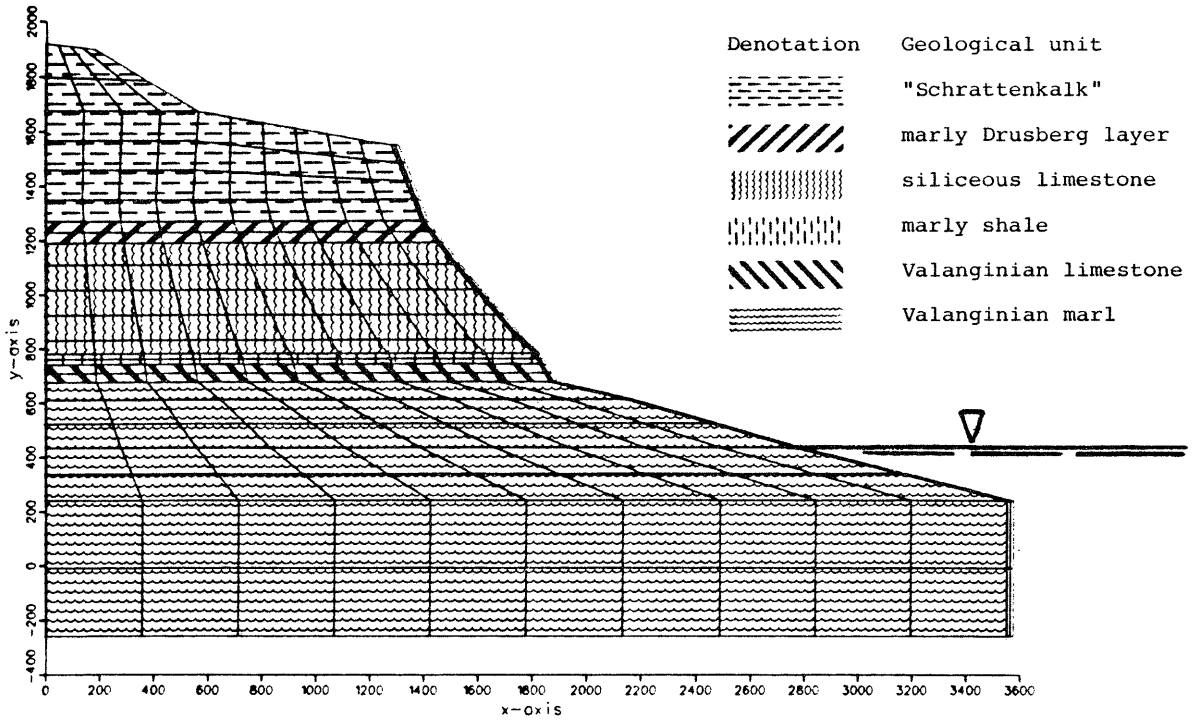

Figure 4.3 The modelled domain showing the finite element mesh and the material property areas.

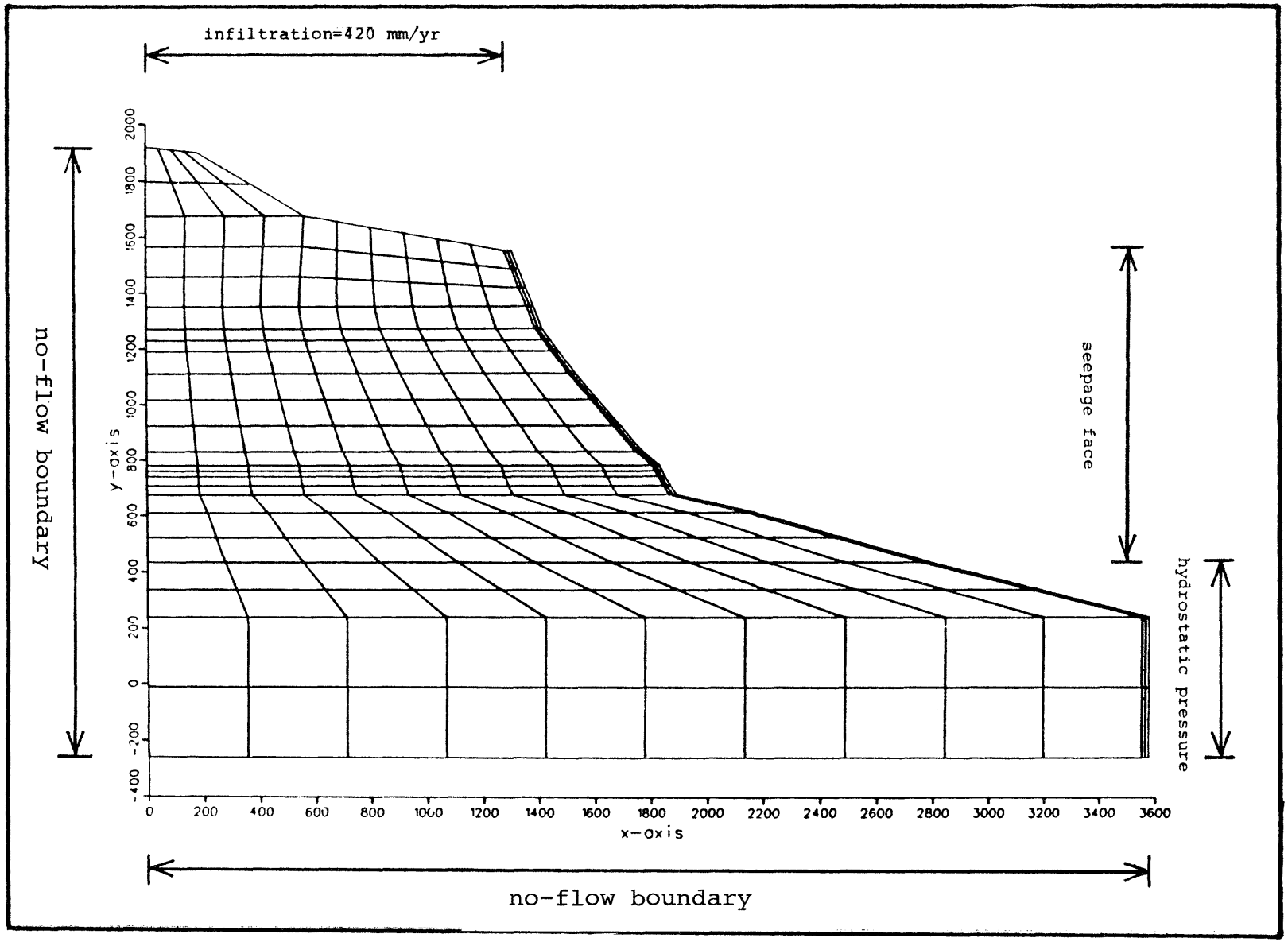

Figure 4.4 Assigned boundary conditions.

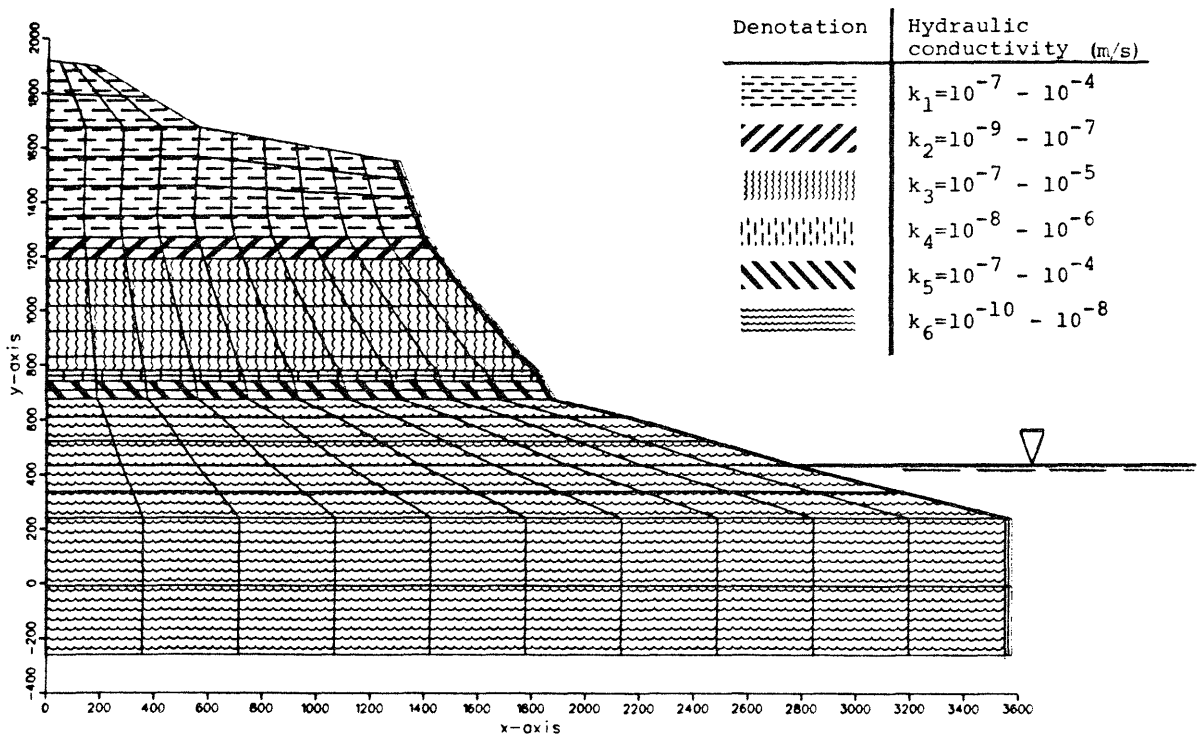

Figure 4.5 Reasonable ranges for the hydraulic conductivity of the strata as indicated in the legend.

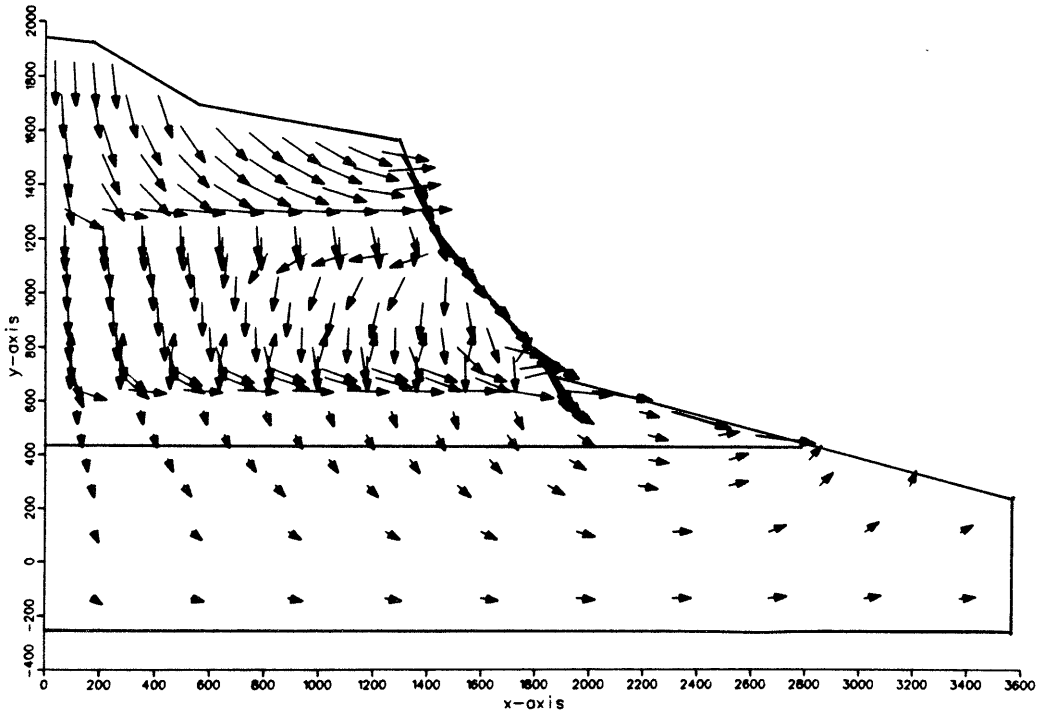

Figure 4.6 Calculated groundwater table and flow field for case 3.

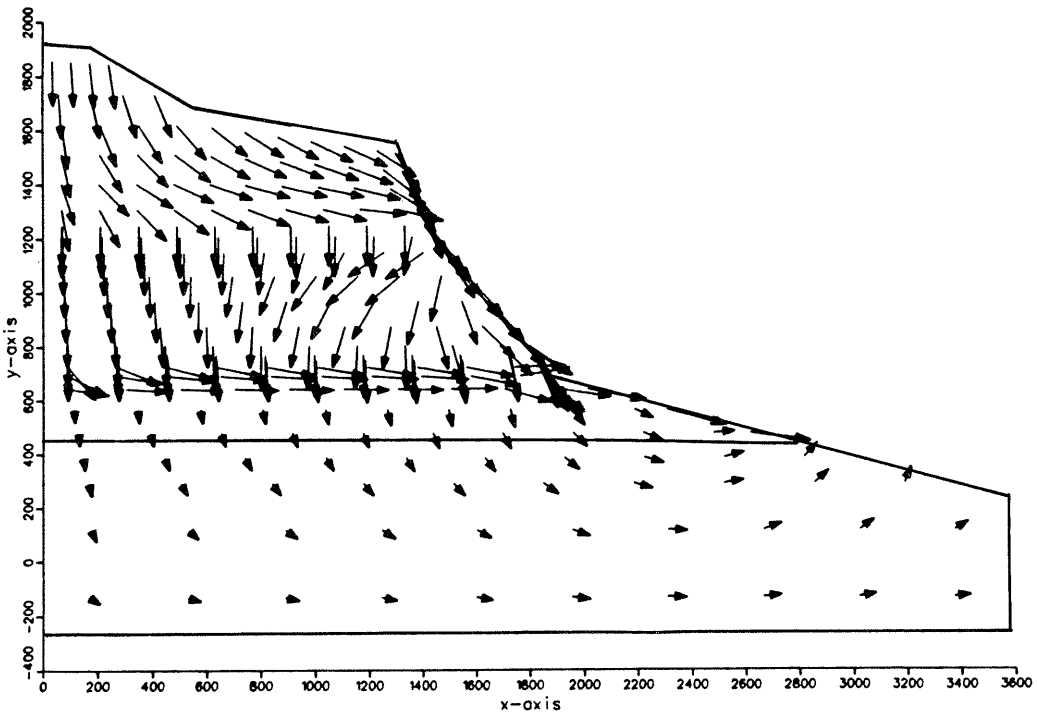

Figure 4.7 Calculated groundwater table and flow field for case 4.

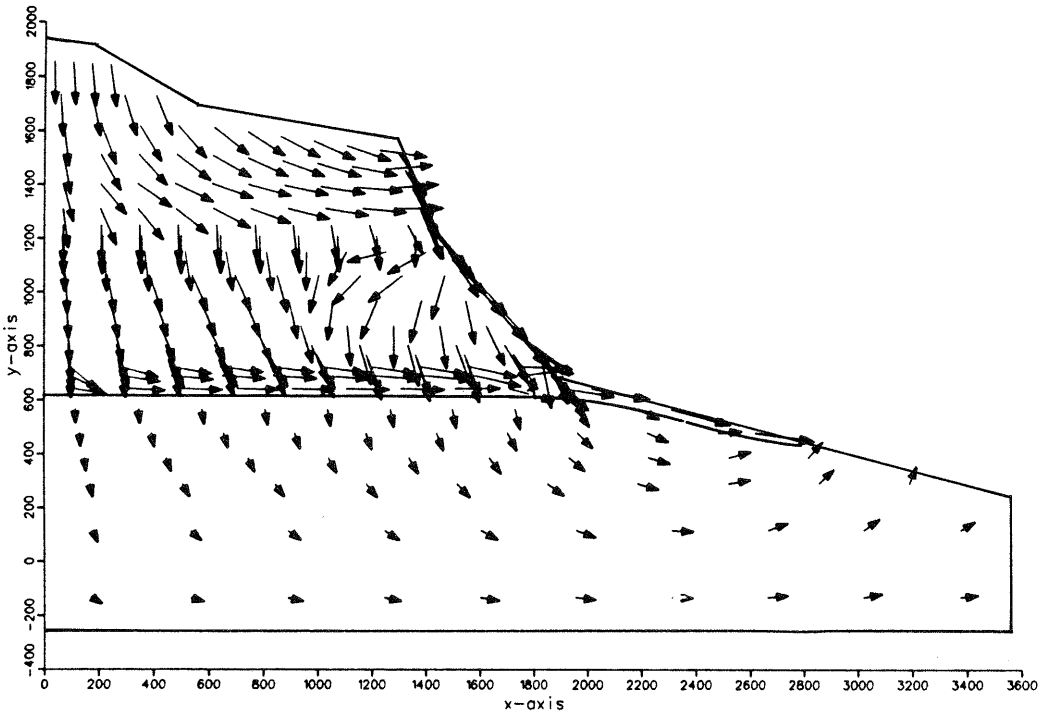

Figure 4.8 Calculated groundwater table and flow field for case 8.

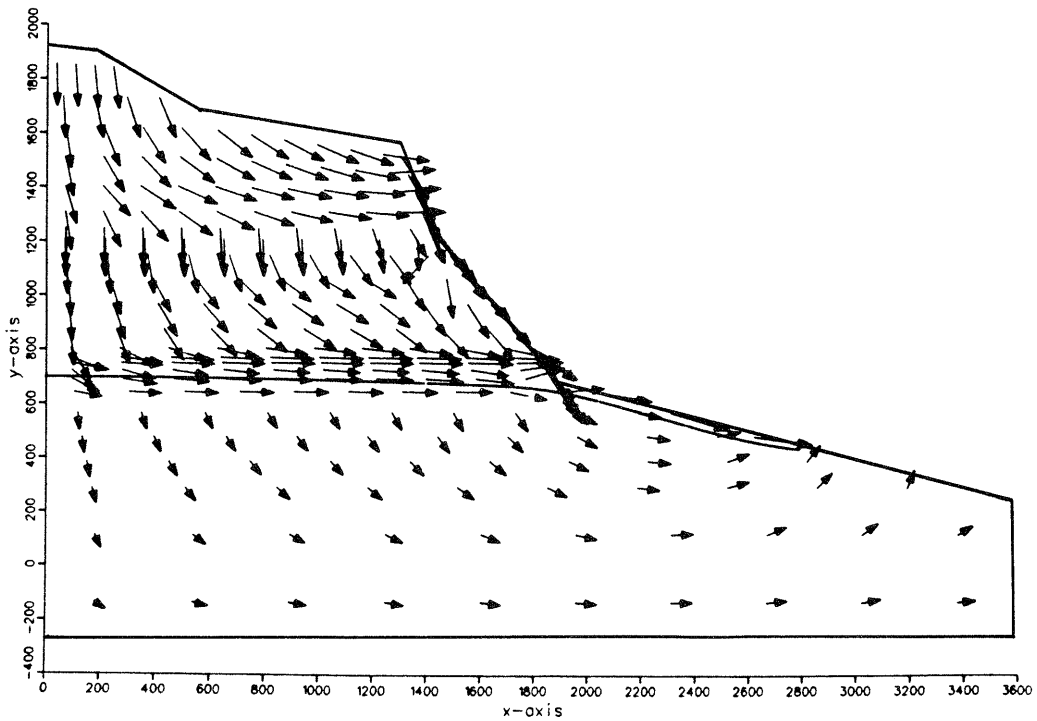

Figure 4.9 Calculated groundwater table and flow field for case 9.

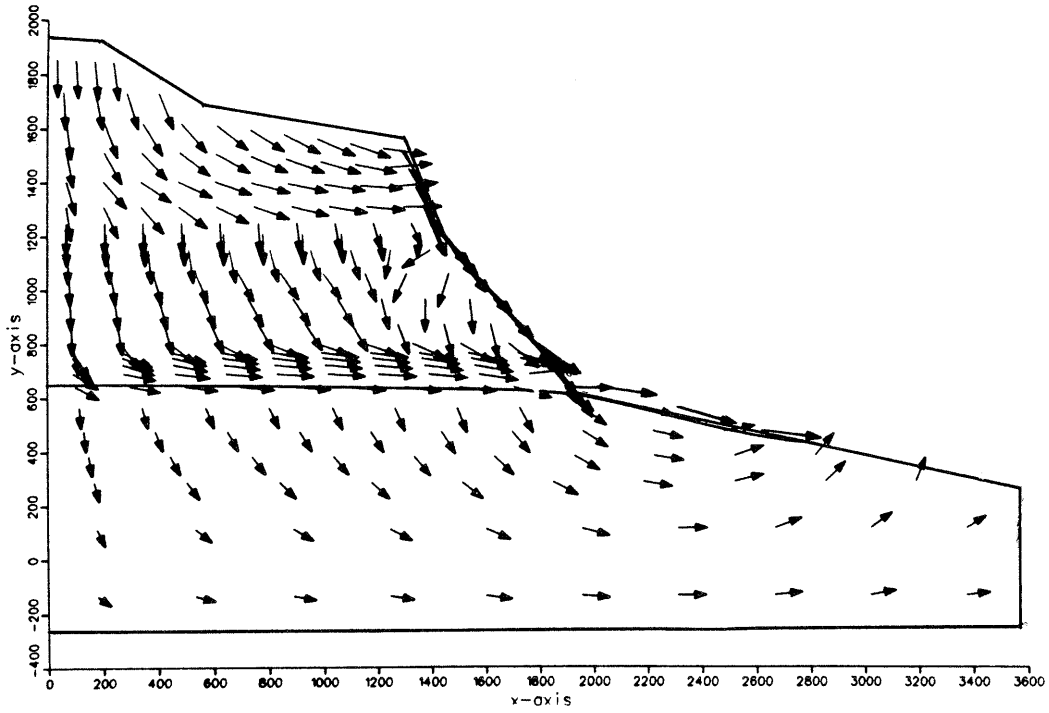

Figure 4.10 Calculated groundwater table and flow field for case 10.

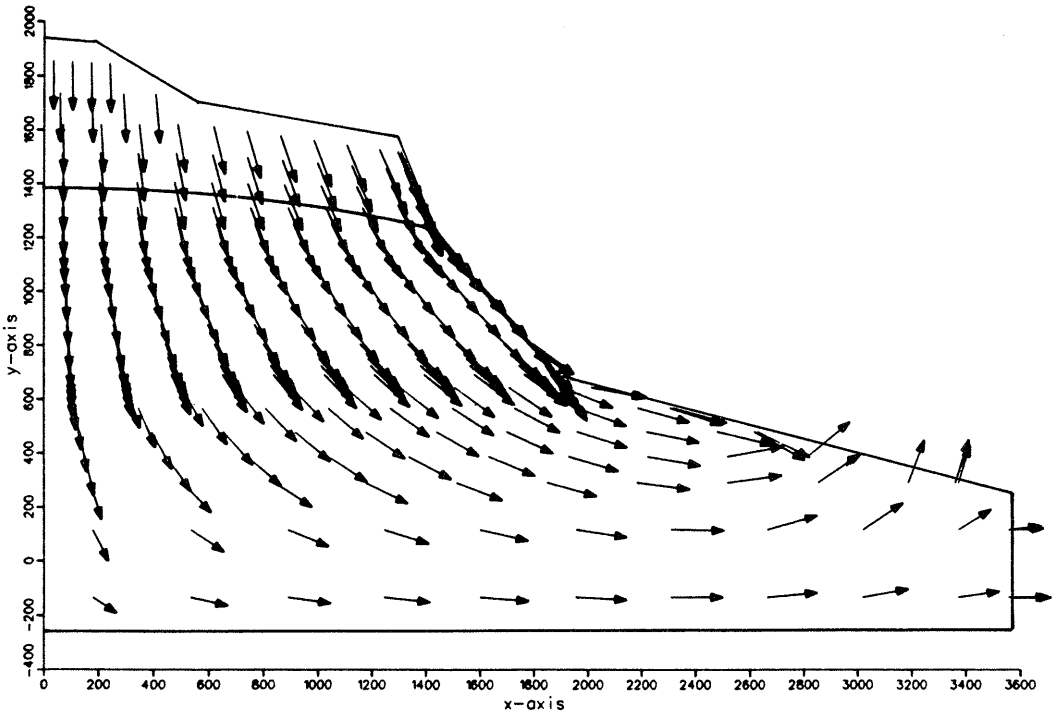

Figure 4.11 Calculated groundwater table and flow field for case 1.

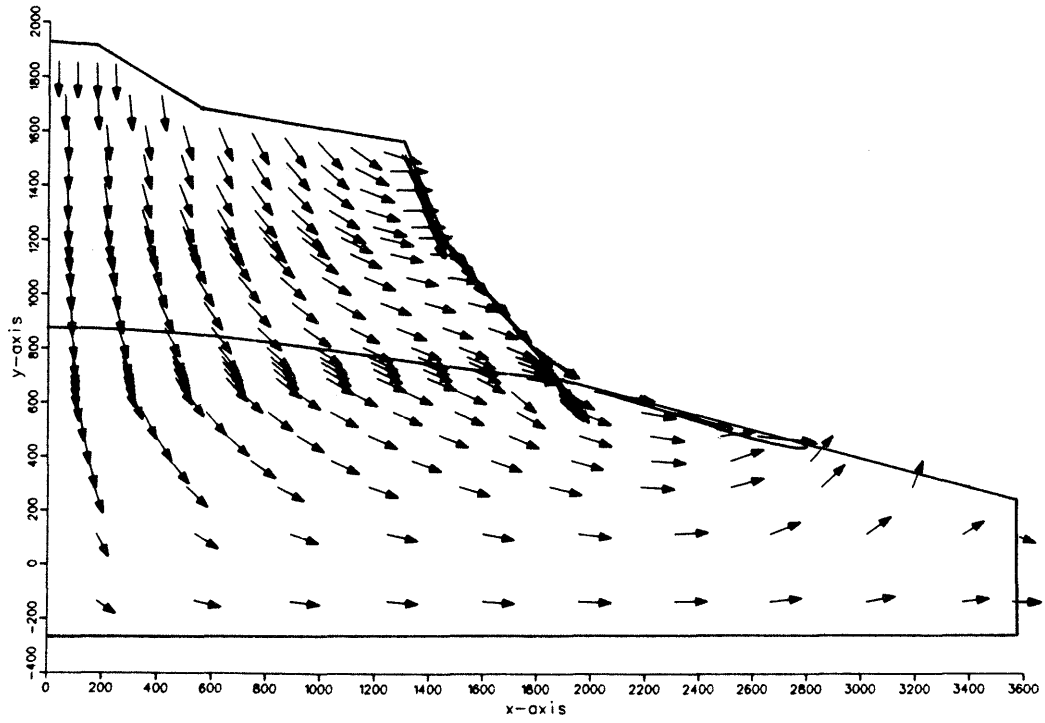

Figure 4.12 Calculated groundwater table and flow field for case 2.

5 THREE-DIMENSIONAL MODEL OF THE GROUNDWATER FLOW CONDITIONS IN THE MARL

5.1 General

The complex geometry of the host rock is difficult to represent in a two-dimensional model. Therefore, a three-dimensional model is used to take into account the complex flow situation in the marl body. Due to the lack of data from the site, several runs have been performed to evaluate the importance of different host rock extensions and different boundary conditions for the flow situation around the repository. The calculations are performed using a model based on the finite element method /1/, see Section 3.4. The program package for input and output handling is described by /4/, see Section 3.5.

The level of the groundwater table at the marl top surface is derived from the two-dimensional calculations described in Chapter 4.

5.2 Modelling strategy

5.2.1 Hydraulic units

The hydraulic units in the modelled domain comprise the marl body and the surrounding layers of varying properties. The lens-shaped host rock contains the potential repository with its access tunnel and the Seelisberg tunnel, including a ventilation tunnel as seen in Figures 5.1 and 5.2.

The major part of the marl surface forms a plateau at a level of 600 m.a.s.l. and a slope inclining slightly towards the west. The highest portion of the modelled domain is located at the southern boundary and corresponds to the marl outcrop at Choltal (800 m.a.s.l.). The eastern boundary slopes steeply towards the Urnersee, the major drainage area in the model. The marl body is modelled down to 350 m.a.s.l. Underneath the repository, this will be an underestimation of about 70 m of the anticipated real marl thickness.The influence of this discrepancy on the flow pattern is further discussed in Section 5.3.3.

The total surface of the marl, apart from the two earlier mentioned plateaus (at 600 and 800 m.a.s.l.) and the eastern flank, is covered by surrounding layers representing limestone series and shales. The thickness of these layers varies between 200-600 metres.

The elevation of the Seelisberg tunnel is 500 m.a.s.l. The two tunnel pipes have been modelled as one single pipe with a square cross-section of 22 x 22 m. An 11 metre thick decompressed zone is modelled around the tunnel.

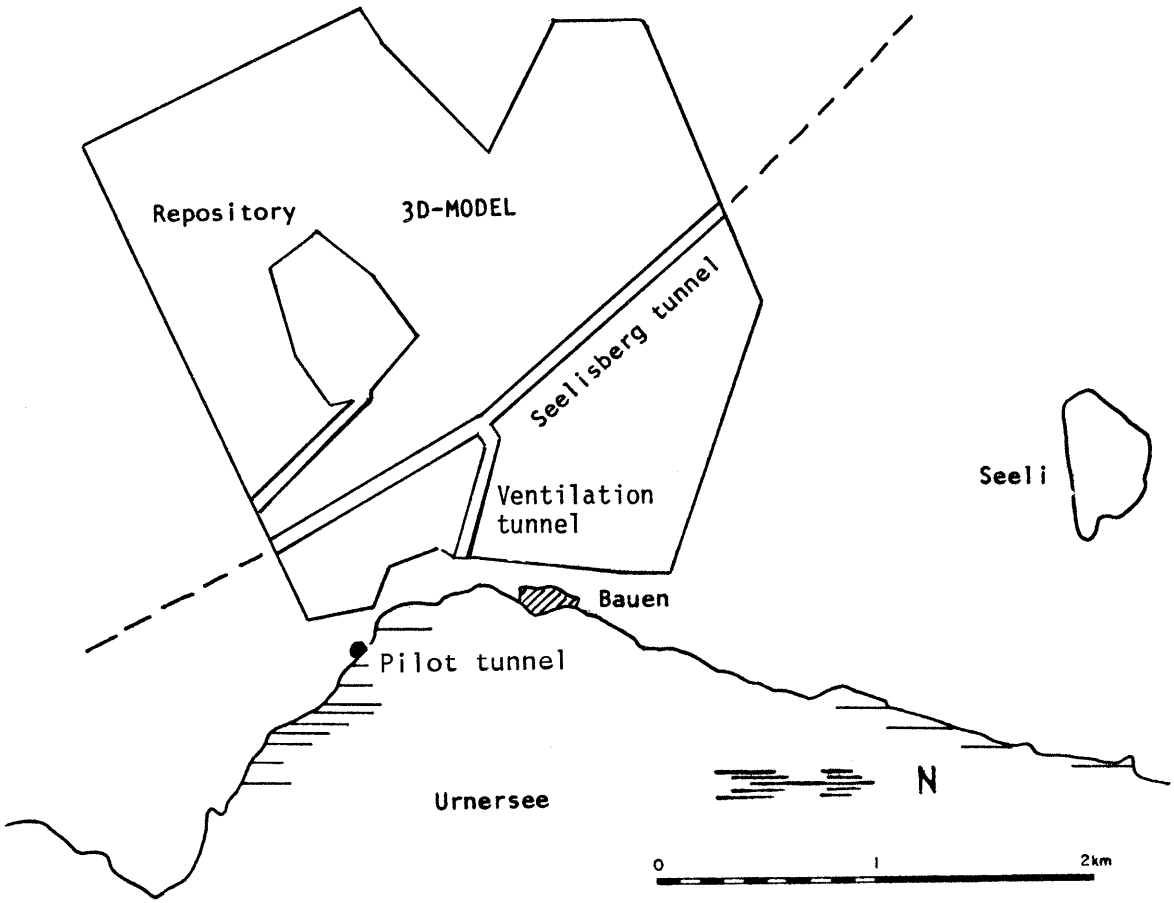

Figure 5.1 Plan view of the modelled area at Oberbauen.

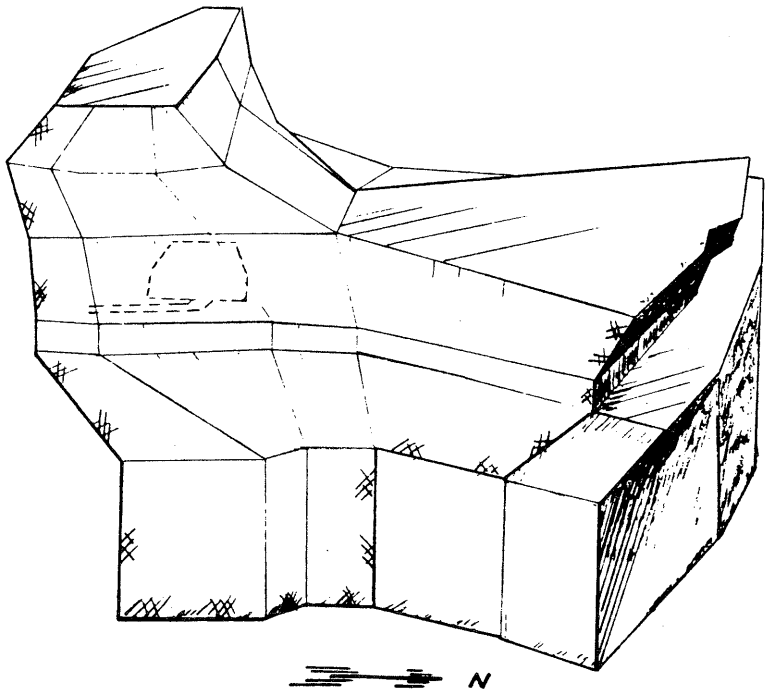

Figure 5.2 View of the mesh geometry used for modelling the groundwater hydrology of Oberbauen Stock. The boundaries of the host rock and the underlying Tertiary shale have been indicated. The approximate position of the repository is shown with a dashed contour.

It has not been possible to model the storage tunnel system. Instead, the repository area is modelled as a 12 metre thick flake, representing a decompressed zone at 450 m.a.s.l. The flake representation yields a conservative estimate of the influence of the decompressed zones. The corresponding access tunnel is modelled in the same way as the Seelisberg tunnel (a square cross-section of 22 x 22 m), but here the tunnel elements represent a comparatively impervious core corresponding to the tunnel backfill material. The access tunnel is modelled as if it were horizontal. Figure 5.3 shows the relative location of the above-mentioned facilities.

In one parameter variation the southern boundary consists of a comparatively impermeable Tertiary shale, Figure 5.4.

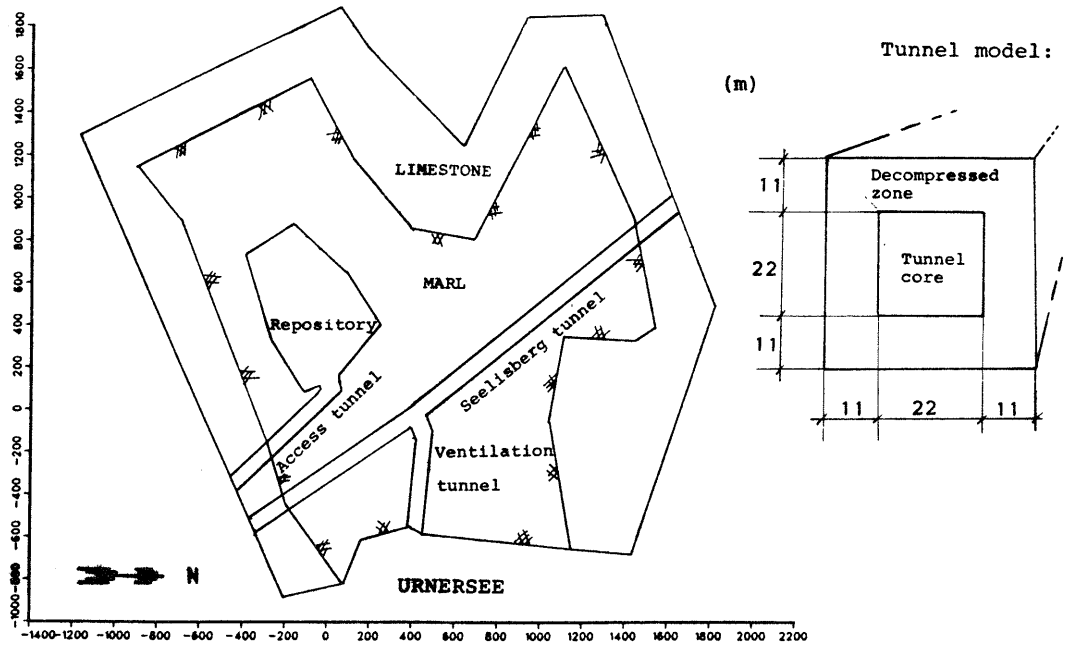

Figure 5.3 Illustration of the geometry of the repository and the access and Seelisberg tunnels as modelled

5.2.2 Mesh data

Three element meshes have been generated for the seven runs presented.

The largest mesh was used in the first two runs. It consists of 1584 elements in 12 layers. The number of nodal points is 7775.

In runs 3 and 4, the Seelisberg tunnel elements have been eliminated. The mesh contains 1569 elements and 7775 nodal points.

The mesh in runs 5-7 contains 1458 elements and 7279 nodal points. To simulate a water table elevation at 460 m.a.s.l. (in the surrounding layers), the limestone elements in the northern and western part of the model have been omitted above 460 m.a.s.l.

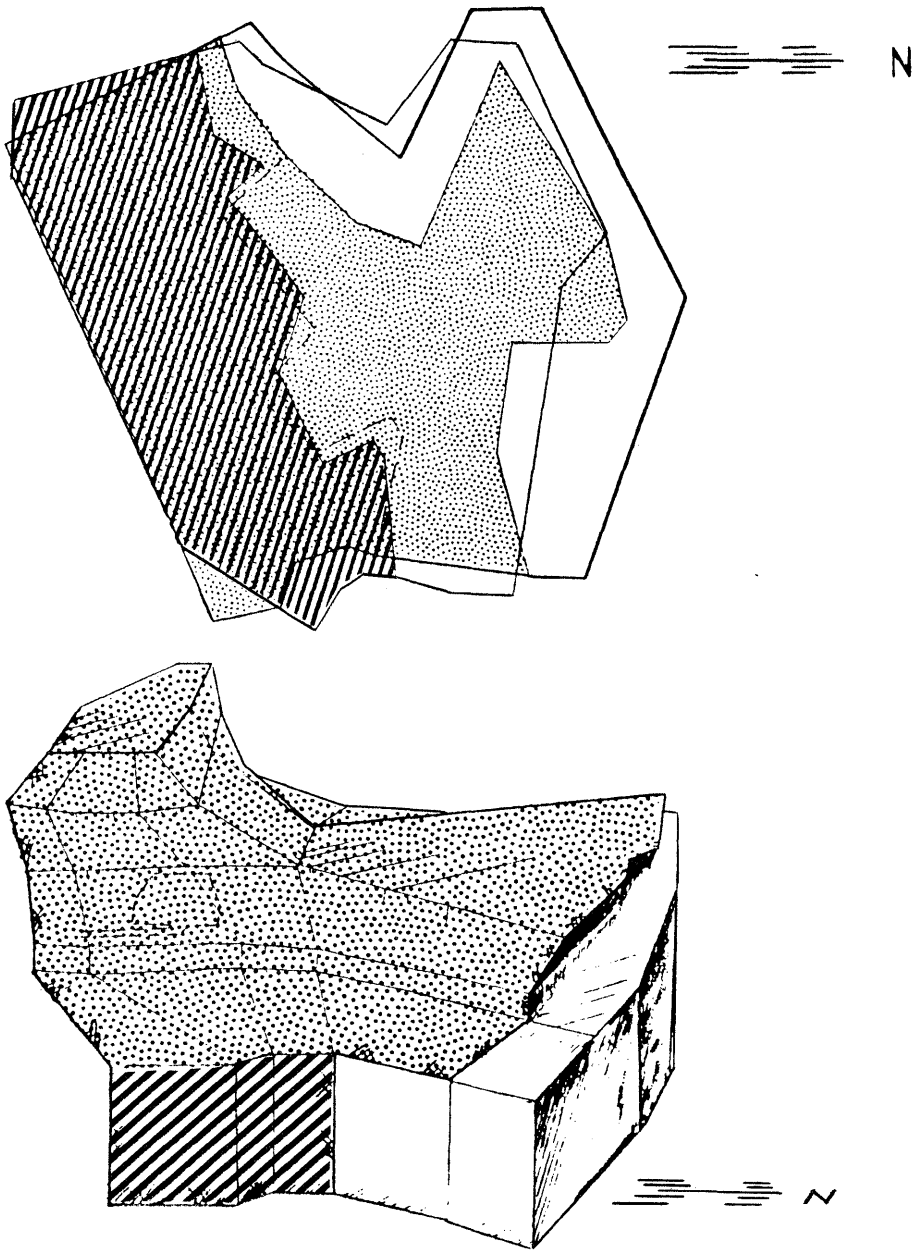

Figure 5.4 Illustration of the geometry of the Tertiary shale as modelled.
- top view at horizontal cross-sections at two levels (top figure)
- perspective view (bottom figure)

5.2.3 Boundary conditions

The boundary conditions applied to the model are shown schematically in Figure 5.5. The bottom surface of the mesh has been treated as a no-flow boundary.

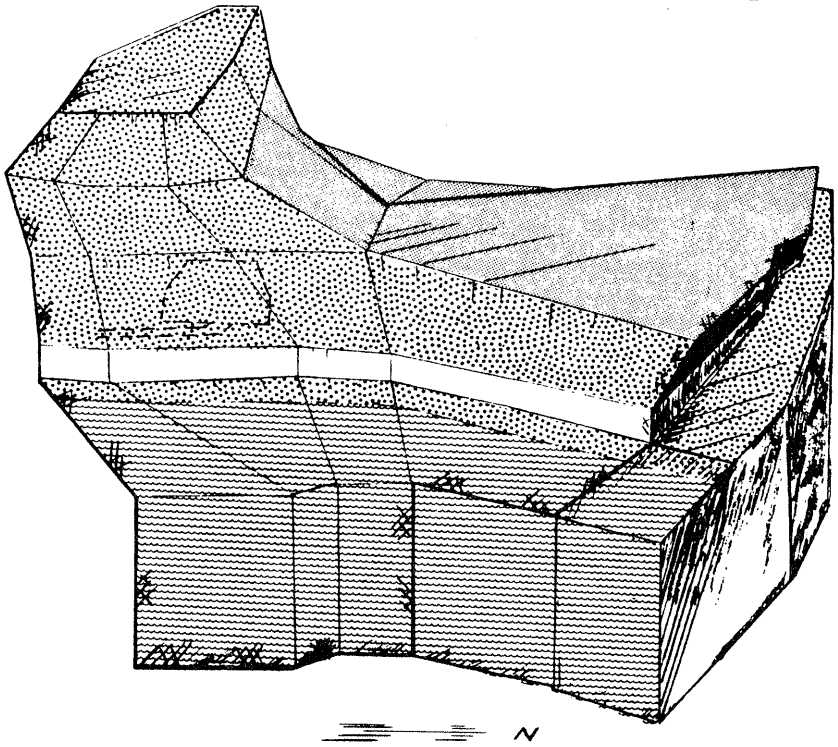

Figure 5.5 Boundary conditions for the three-dimensional groundwater modelling

All "vertical" boundaries, with the exception of the eastern boundary, are defined as no-flow boundaries located on the outer surface of the surrounding limestone/shale layers.

The portion of the eastern boundary situated below the water table of Urnersee is assigned a hydrostatic pressure corresponding to the lake surface at 433 m.a.s.l.

The top surface of the modelled domain including the eastern slope above the Urnersee is assigned atmospheric pressure; i.e. the level of the water table coincides with the level of the marl/limestone surface.

The eastern flank between 478-522 m.a.s.l. was modelled as vertical instead of sloping. In order to avoid unnaturally high gradients, this area has been treated as a no-flow boundary instead of setting an atmospheric pressure boundary. The influence of this contradiction on the calculated flow seems to be limited.

In one parameter variation (runs 3 and 5), a hydrostatic pressure corresponding to a water table located at 700 m.a.s.l. has been prescribed for the top surface in the northern part of the domain. This is an extreme value derived from the two-dimensional calculations (Chapter 4).

The northern and western boundaries of the marl are surrounded by an element layer representing pervious boundary formations. In the calculations the level of the water table is assumed to vary between 700-460 m.a.s.l. but as these boundary layers are more permeable then the marl they are probably drained almost down to the level of the Urnersee. To simulate this, the limestone elements above approximately 460 m.a.s.l. are omitted (runs 5 - 7).

In the first two runs, the Seelisberg tunnel is modelled as elements assigned a very high hydraulic conductivity, 10^{-2} m/s. In the subsequent runs these elements are eliminated. Instead the inner surface of the tunnel has been assigned atmospheric pressure. At the opening of the access tunnel the head is prescribed at atmospheric pressure.

5.2.4 Material properties

The governing material property is the hydraulic conductivity. The modelled domain comprises 5 property areas:

- the marl body and the backfilled portion of the access tunnel
- the Seelisberg tunnel including the ventilation tunnel (run 1 and run 2)
- the repository and the decompressed zones of the Seelisberg, ventilation and access tunnels
- the surrounding pervious layer
- the Tertiary shale in the southern part of the modelled domain.

Hydraulic conductivities assigned to the property areas are assumed to be isotropic and independent of depth.

From a geological point of view, the major part of the marl body consists of pure marl rock with a hydraulic conductivity less than 10^{-11} m/s. The host rock also comprises more permeable discontinuites in the form of vertical or slanted zones (Ruschelzonen) and thin horizontal limestone lenses /NTB 85-20/.

Calculations of the amount of water that can be evaporated and carried away with the ventilation air in the Seelisberg tunnel indicate that most of the discontinuities have a hydraulic conductivity of 3.10^{-9} m/s or less /NTB 85-29/.

In a conservatively estimated cross-section, these discontinuities account for approximately 3% of the total cross-section area. The hydraulic conductivity assigned to the marl body in the model is based on a large scale average value which can be written:

$10^{-11} \times 0.97 + 3 \cdot 10^{-9} \times 0.03 = 10^{-10}$ m/s.

This overall value is in good agreement with the value obtained from a mass balance of water in the ventilation air /NTB 85-17/.

The backfill elements of the access tunnel were assigned a conductivity of 10^{-10} m/s.

The core of Seelisberg tunnel (including the ventilation tunnel) was assigned a conductivity of 10^{-2} m/s, (run 1 and run 2). In the remaining runs the tunnel was, as mentioned, left open .

The hydraulic conductivity assigned to the decompressed zones (repository, access and Seelisberg tunnels) was assumed to vary between 10^{-9} - 10^{-7} m/s based on the probable rock mechanical behaviour of the open tunnels /NTB 85-30/.

The conductivity assigned to the permeable surrounding layers was assumed to vary between 10^{-7} - 10^{-5} m/s according to the hydraulic property of the "Drusbergkalk".

The underlying stratum in the southern part of the host rock was assumed to be a Tertiary shale with a conductivity of 10^{-10} m/s. Different extensions of the shale are modelled in runs 5-7. In these runs, the pervious boundary elements in the south above 350 m.a.s.l. were assigned a conductivity similar to that of the marl/shale, Figure 5.4.

5.2.5 Overview of calculations performed

In conclusion, the following boundary condition versions and parameter variations have been performed in the different runs:

Table 5.1. Boundary condition versions and parameter variations

	run 1	run 2	run 3 1)	run 4 1)	run 5 1)2)	run 6 1)2)	run 7 1)2)
Hydraulic conductivity (m/s)							
marl and access tunnel	10^{-10}	10^{-10}	10^{-10}	10^{-10}	10^{-10}	10^{-10}	10^{-10}
decompressed zones	10^{-7}	10^{-9}	10^{-8}	10^{-8}	10^{-8}	10^{-8}	10^{-8}
Drusbergkalk	10^{-5}	10^{-5}	10^{-5}	10^{-5}	10^{-7}	10^{-7}	10^{-7}
Tertiary shale	-	-	-	-	10^{-10}	10^{-10}	-
Seelisberg tunnel	10^{-2}	10^{-2}	-	-	-	-	-
Boundary conditions							
elevation of the water table: (m.a.s.l.)							
marl	z*	z	700	z	700	z	z
surrounding limestone layers	z	z	700	z	460	460	460

* z= the groundwater table coincides with the topography of the marl/limestone surface.

1) the inner surface of the Seelisberg tunnel is assigned atmospheric pressure.

2) -the northern and western elements at the boundary above 460 m.a.s.l. are omitted
-the hydraulic head assigned to the western marl surface can be somewhat lower in this run compared to runs 1-4, because of differences in the mesh topography, Fig. 5.6.
-the elements at the southern boundary above 350 m.a.s.l. are assigned a conductivity of 10^{-10} m/s.

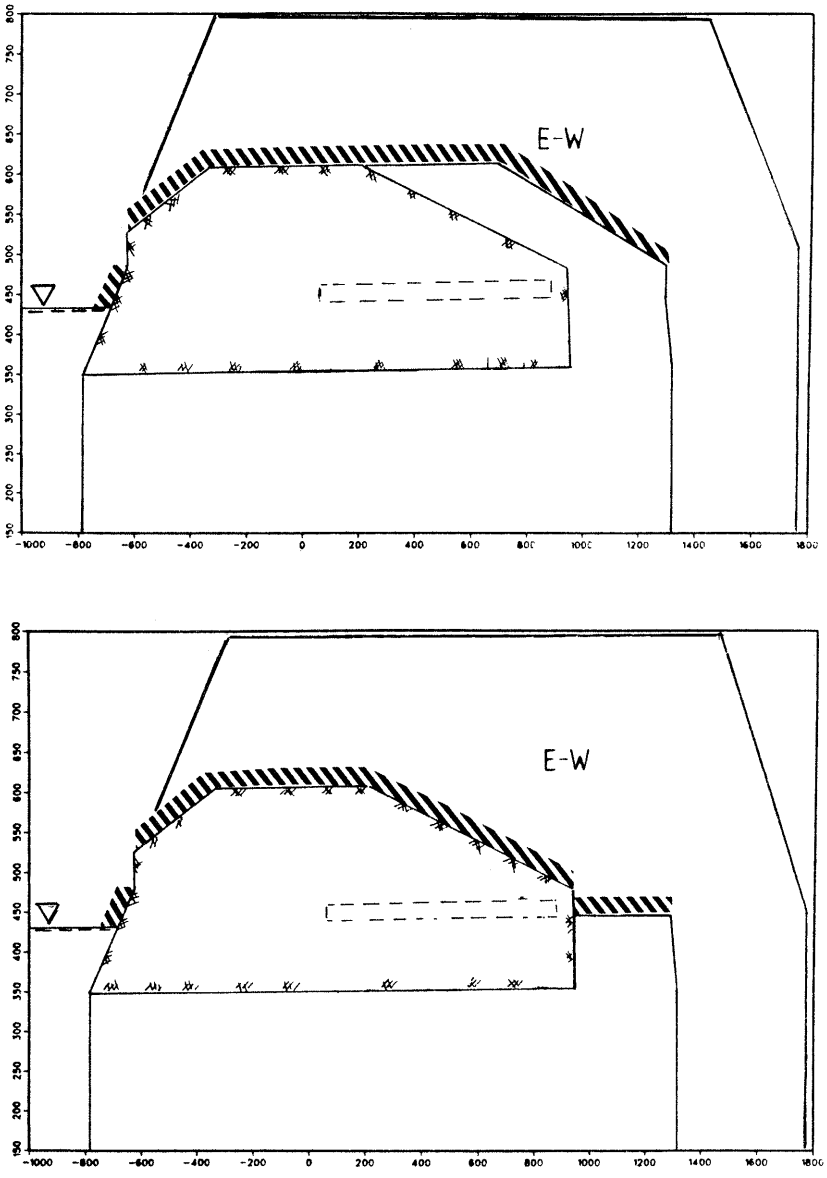

Figure 5.6 Vertical cross-section illustrating differences in the boundary conditions assigned to the western part of the model.

Top surface boundary condition for run:
- 1,2 and 4 (top)
- 6 and 7 (bottom)

5.3 Results

5.3.1 Head distribution and flow field

Figures 5.7-5.13 show the calculated groundwater potential distribution in 1 horizontal and 3 vertical cross-sections. The flow pattern and flow vector arrows in the cross-section show that the flow principally occurs in the surrounding pervious limestone layer while the water in the interlying body of the marl is relatively stagnant. The length of the flow vectors is proportional to the logarithm of the Darcy velocity. Note that the flow vectors are two-dimensional projections of the three-dimensional solution. The direction of the third vector component is indicated by the colour of the arrowhead. Unfilled (white) arrowheads mean that the third component points out of the paper plane towards the reader.

A comparison between the Figures shows:

Concerning the flow direction from the repository:

The potential in the pervious formation underneath the host rock is largely determined by the level of the groundwater table in the surrounding formations. The head is therefore higher in runs 1-4 than in runs 5-7. In runs 5 and 6 the introduction of the low-permeability Tertiary shale below the repository contributes to a rise in head in this region. However, in the limestone immediately to the north of the shale, the head is again determined by the boundary conditions applied to the surrounding medium. This is clearly seen in the cross-sections B-B' and C-C' in Figures 5.11 and 5.12.

As a consequence of the relatively low hydraulic head in the underlying strata, the general flow direction from the repository is downwards. The 600 m plateau in the northern part of the marl body adds a northerly component to the flow direction.

Concerning the influence of the groundwater level in the overlying strata:

In runs 3 and 5, the groundwater table in the overlying sedimentary series has been raised to 700 m.a.s.l. As a consequence of this, the hydraulic head in the repository is increased by about 50 m in case 3 (compared to case 4) and by about 25 m in case 5 (compared to case 6). The greater head increase in case 3 is due to the higher hydraulic head in the pervious boundary layer. In case 5 this head is kept constant and the variation of the boundary conditions thus only applies to the marl body.

In run 5 the rise in hydraulic head in the repository due to the rise the groundwater table corresponds to an increased head difference of about 20% between the repository and the underlying limestone. In run 3 the head difference remains essentially unaltered. The consequences of the high groundwater table are thus limited in the repository region. As can be seen in the cross-sections B-B' and C-C' in Figures 5.9 and 5.11, however, the gradient through the northern part of the marl is significantly increased.

Concerning the influence of the Tertiary shale:

The stratum underlying the host rock is assumed to consist of a highly pervious limestone in run 7. In runs 5 and 6 the southern part of this stratum is assumed to belong to the Tertiary shale, with a hydraulic conductivity equal to that of the host rock. Comparing Figures 5.12 and 5.13, one finds that the introduction of the shale adds a northerly component to the flow vectors. The consequences of this are discussed further in the subsequent sections.

Concerning the influence of the permeability contrast between the undisturbed marl and the decompressed zone:

As can be expected from the continuity condition implied by the flow equation (see Chapter 3), a comparison between runs 1, 2 and 3 shows that a high permeability in the decompressed zone leads to a low hydraulic gradient and a high flow rate. This is discussed further in Section 5.3.2.

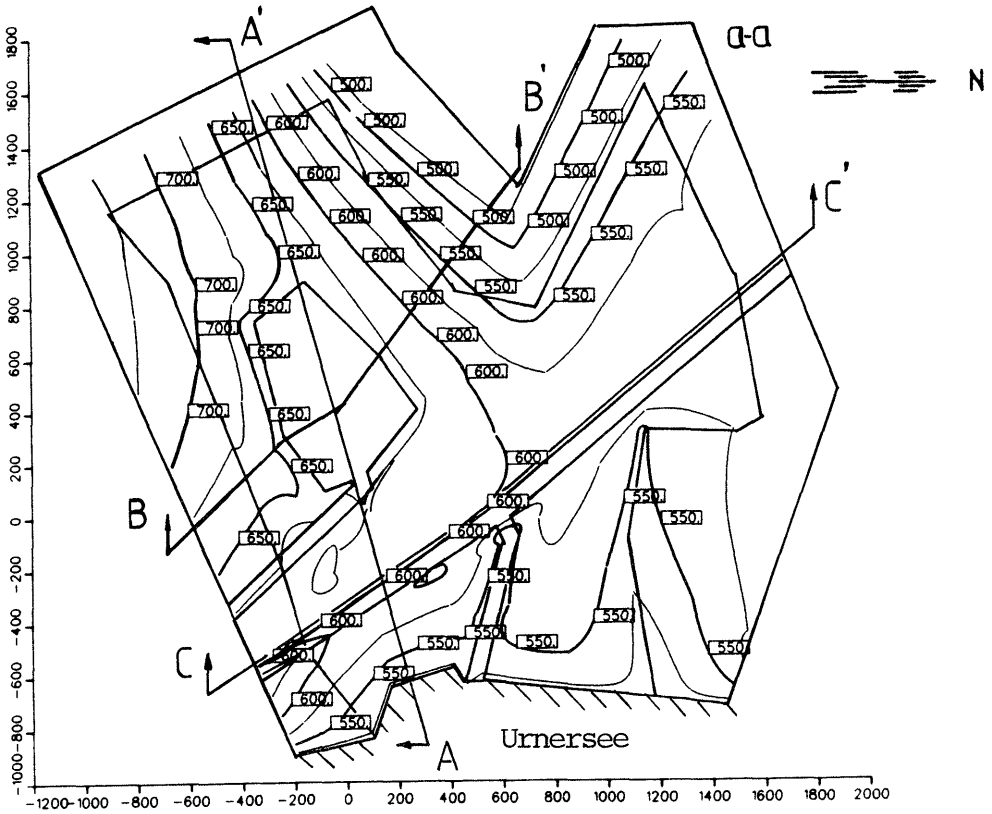

Figure 5.7.1

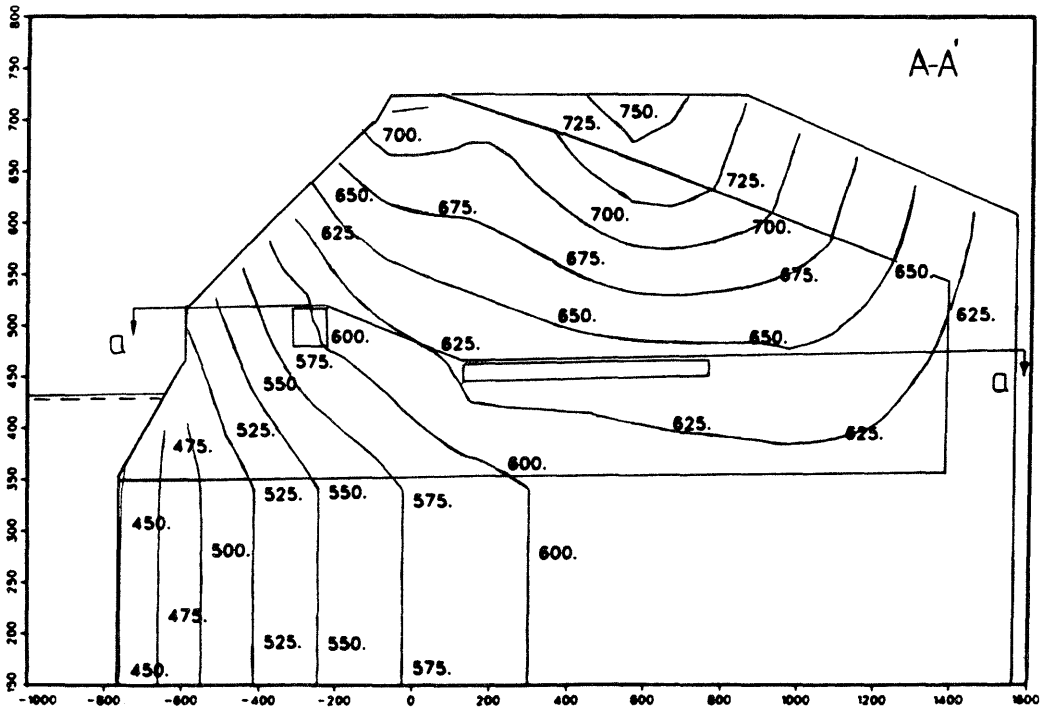

Figure 5.7.2

Figures 5.7.1-4 Isopotentials from run 1.
Figure 5.7.1 shows a horizontal cross-section (aa) through the repository and tunnel planes. Figures 5.7.2-4 show the vertical cross-sections AA, BB and CC indicated in view aa.

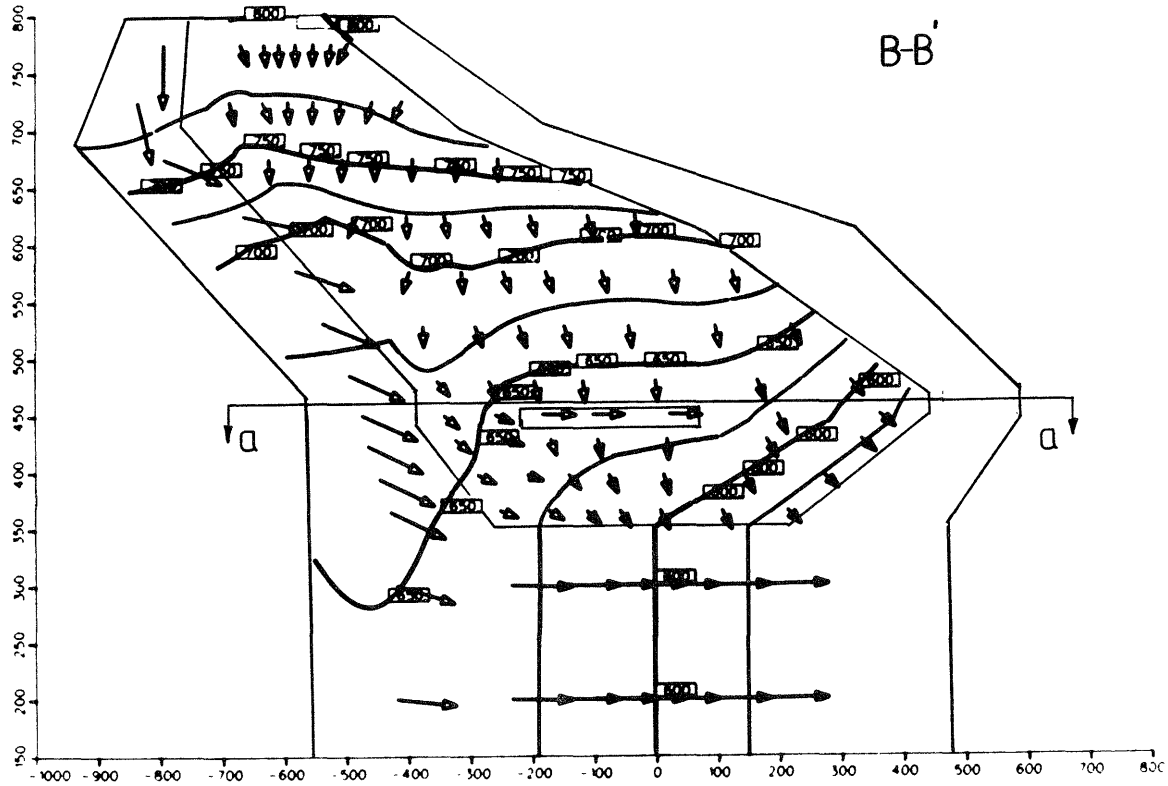

Figure 5.7.3

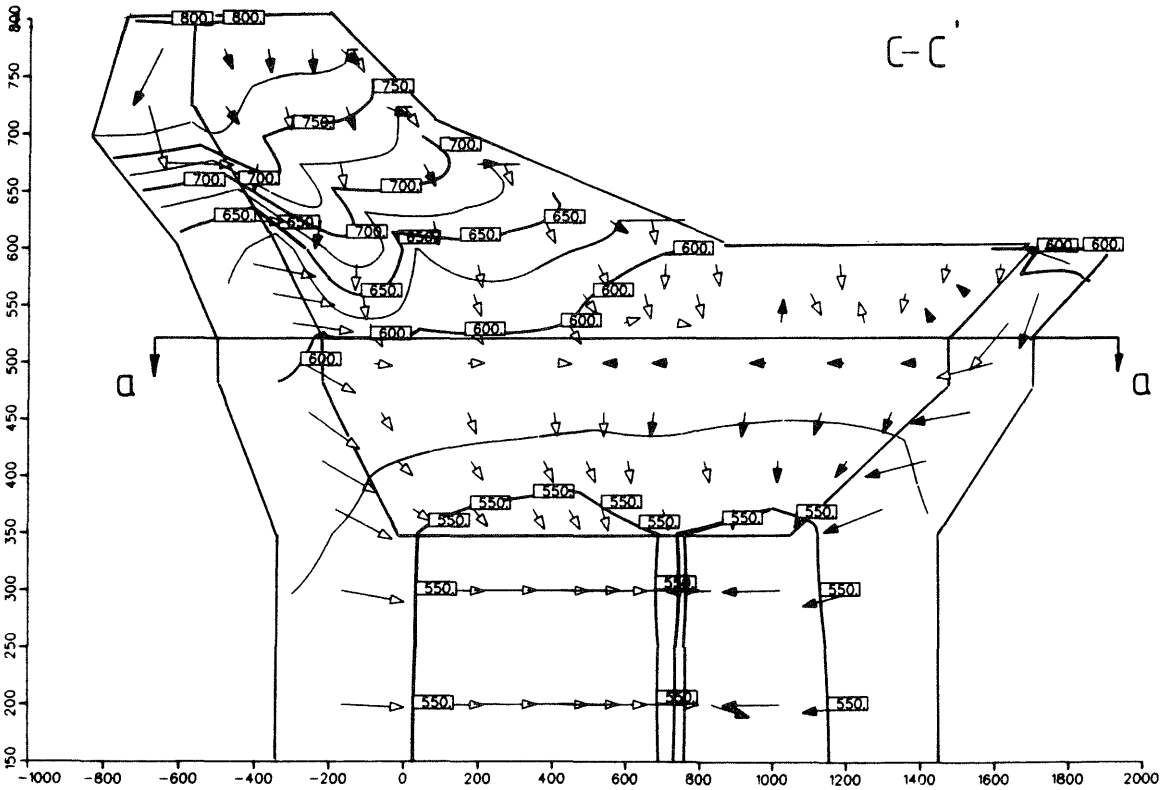

Figure 5.7.4

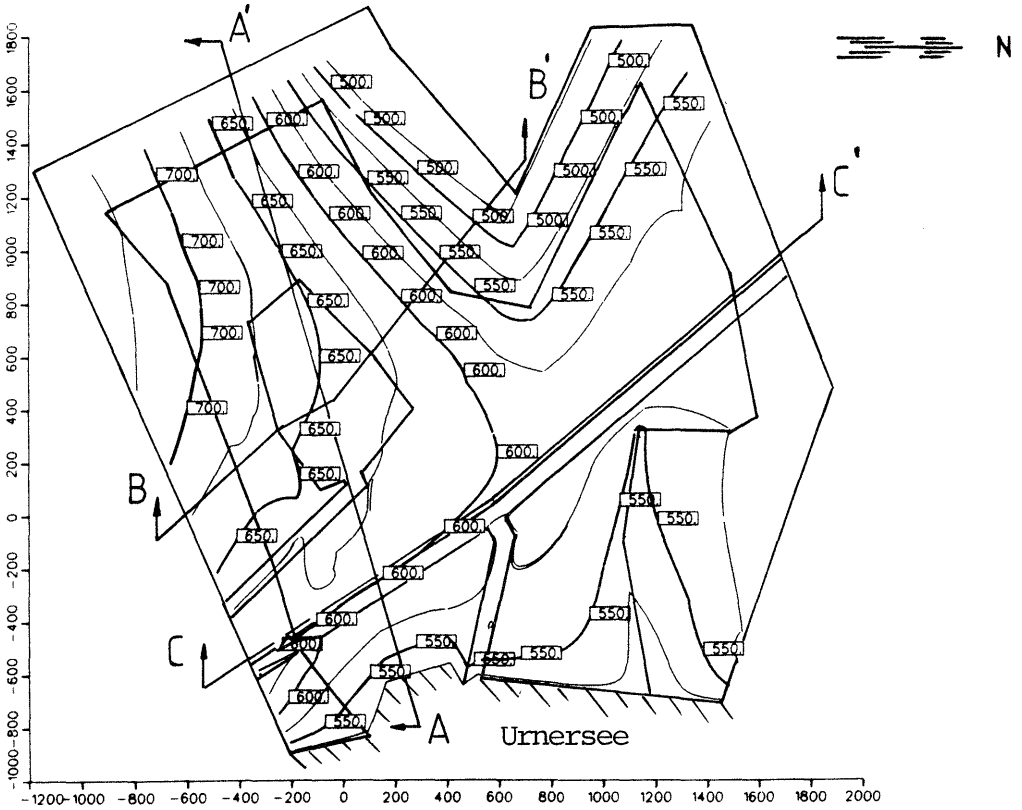

Figure 5.8.1

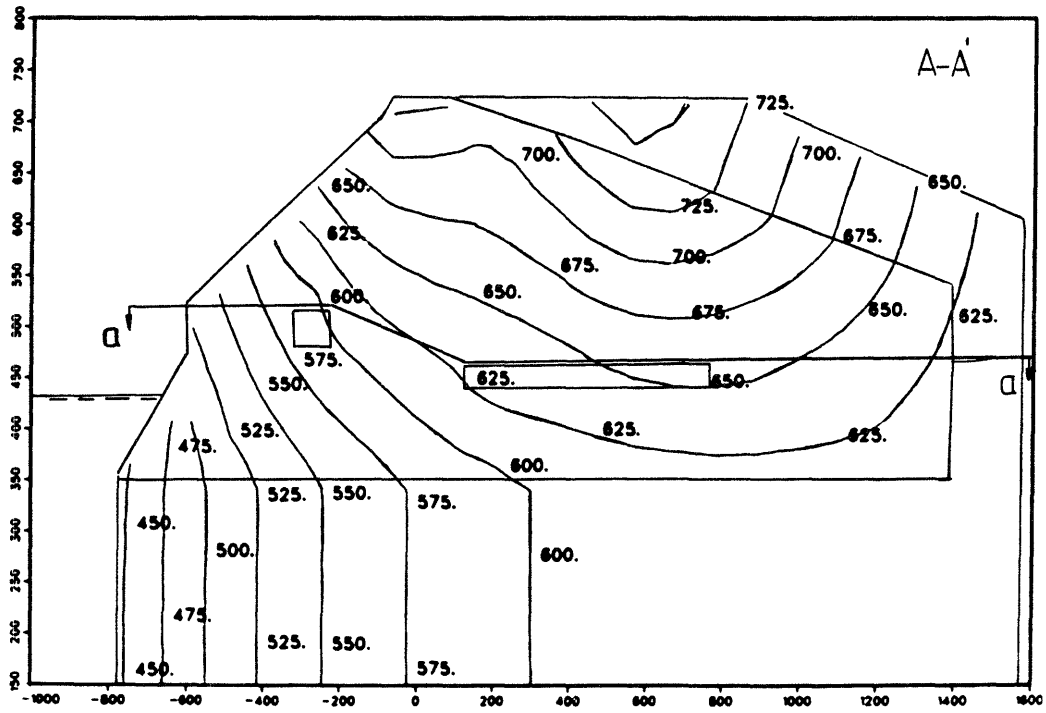

Figure 5.8.2

Figures 5.8.1-4 Isopotentials from run 2.
Figure 5.8.1 shows a horizontal cross-section (aa) through the repository and tunnel planes
Figures 5.8.2-4 show the vertical cross-sections AA, BB and CC indicated in view aa

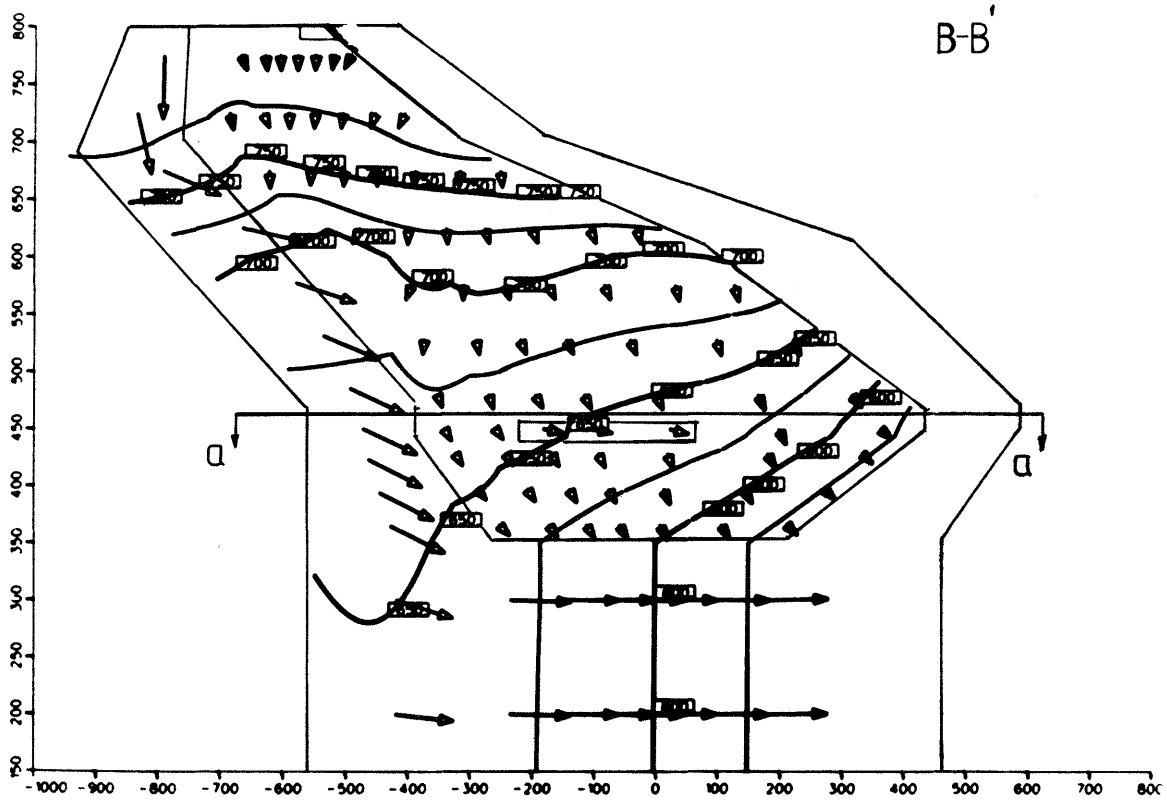

Figure 5.8.3

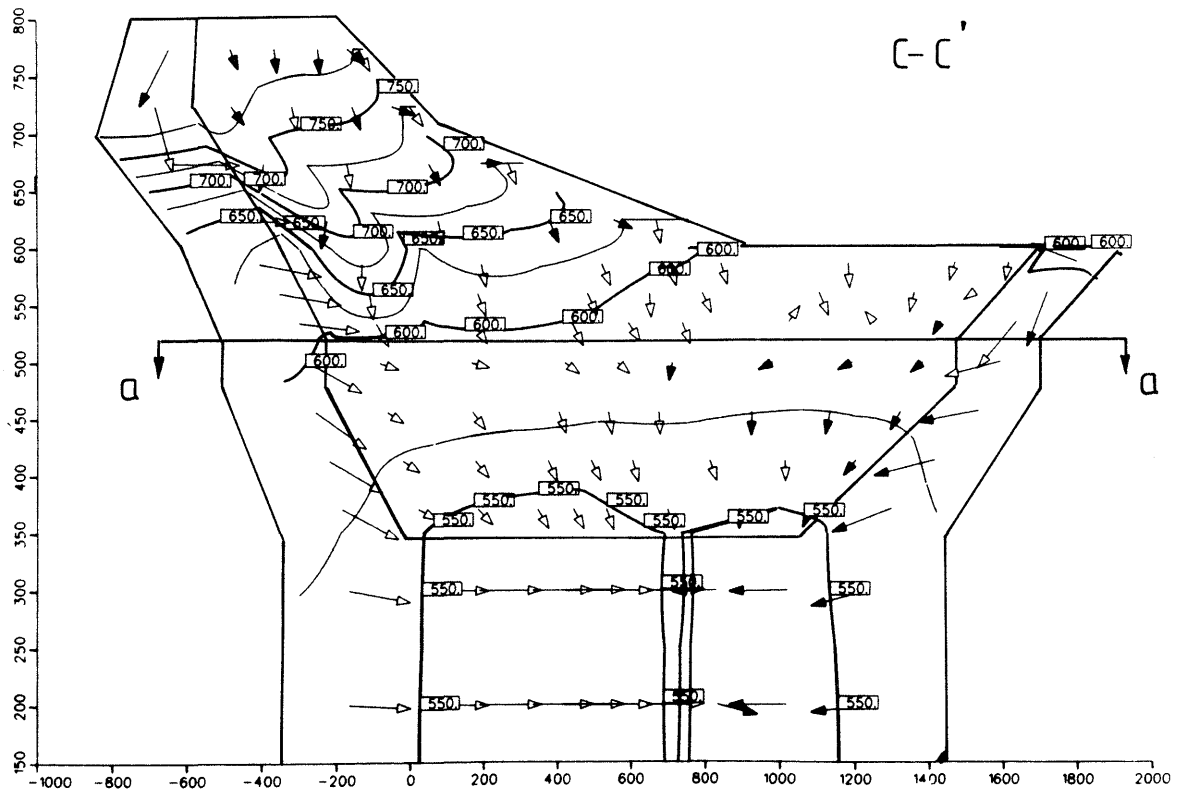

Figure 5.8.4

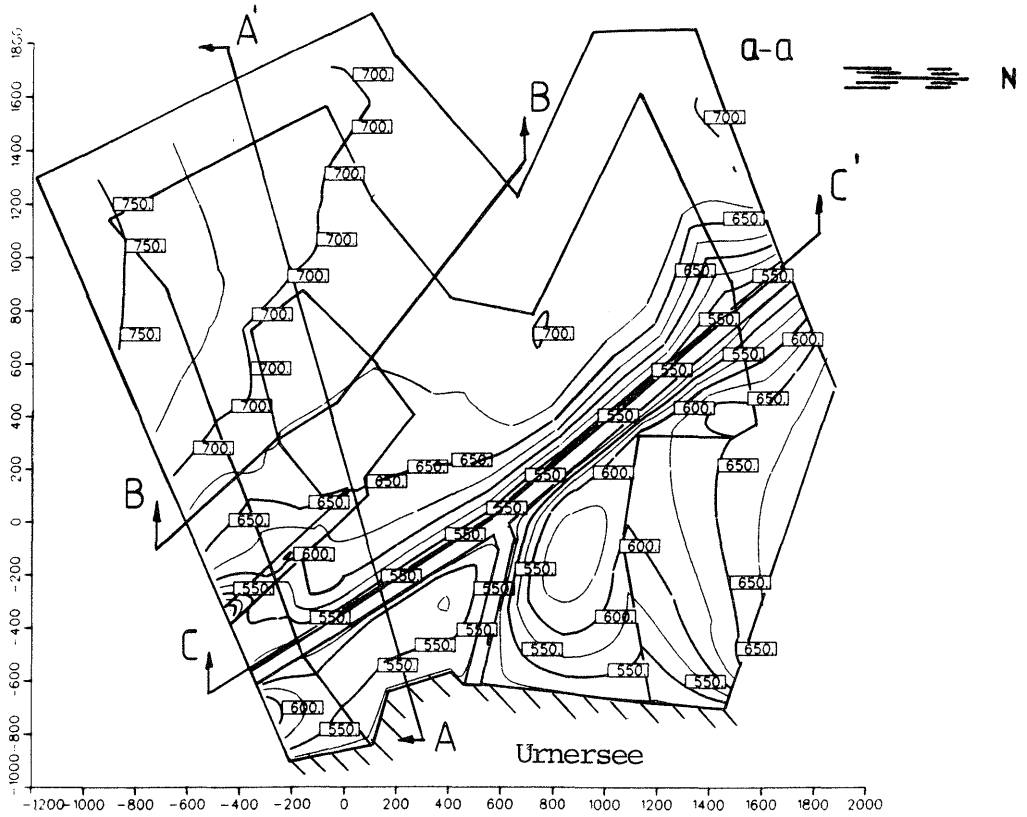

Figure 5.9.1

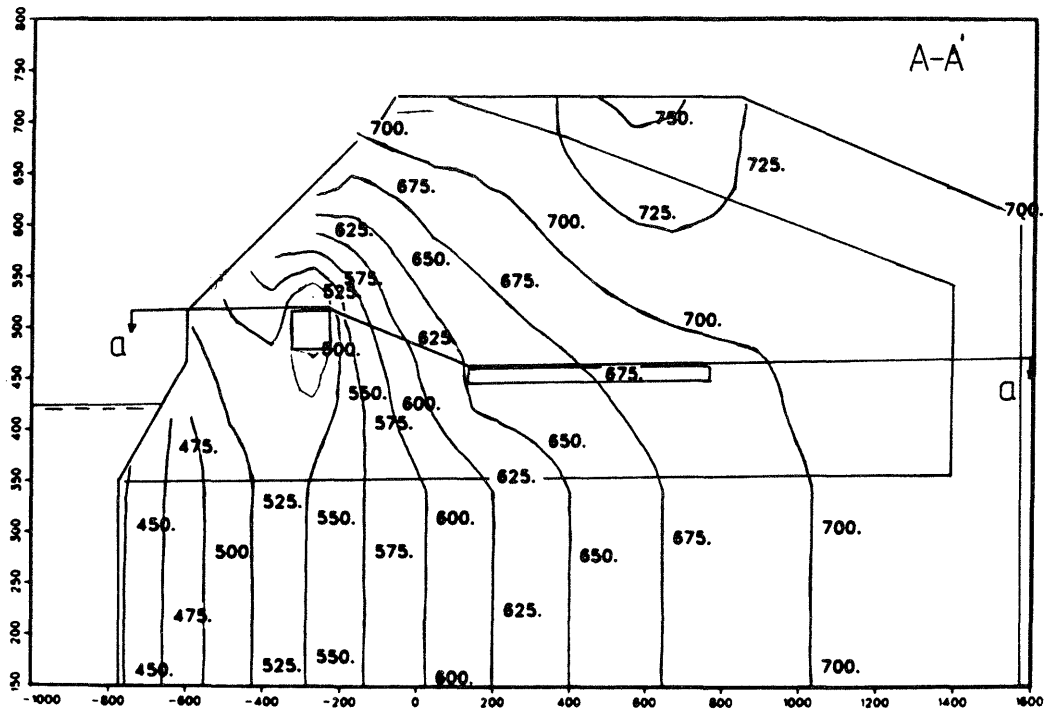

Figure 5.9.2

Figures 5.9.1-4 Isopotentials from run 3.
Figure 5.9.1 shows a horizontal cross-section (aa) through the repository and tunnel planes. Figures 5.9.2-4 show the vertical cross-sections AA, BB and CC indicated in view aa

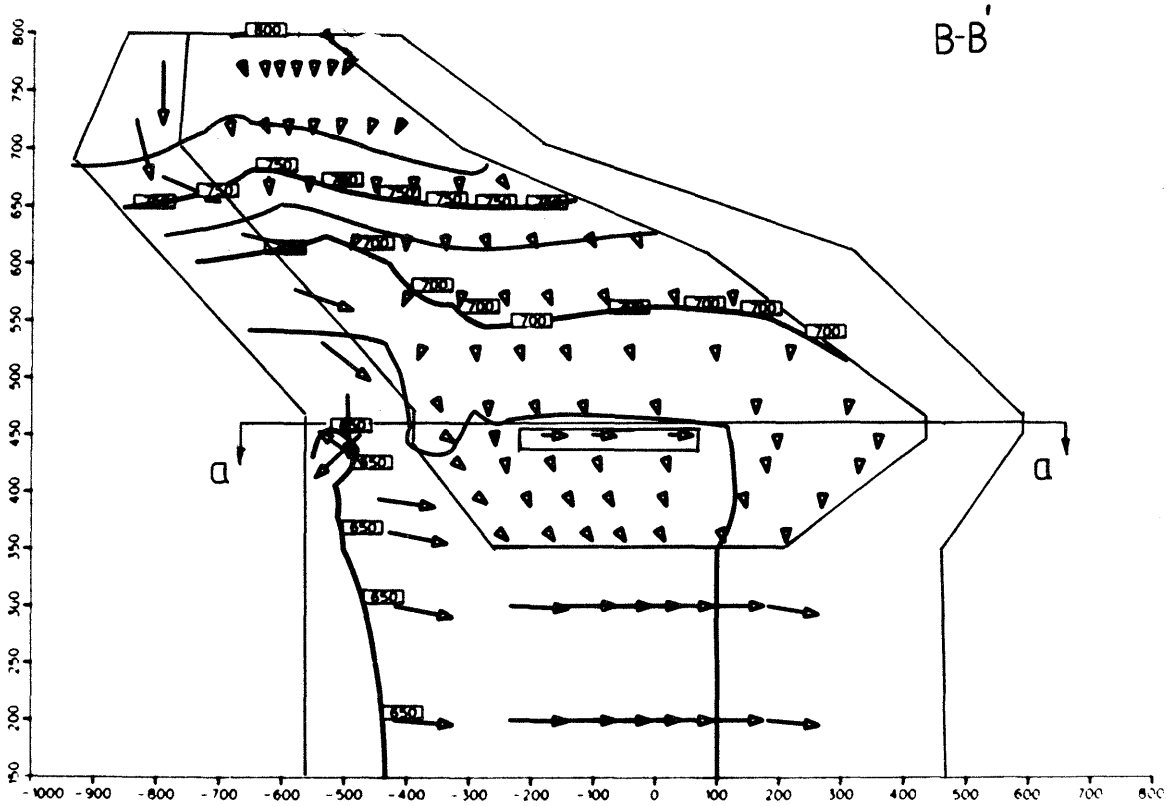

Figure 5.9.3

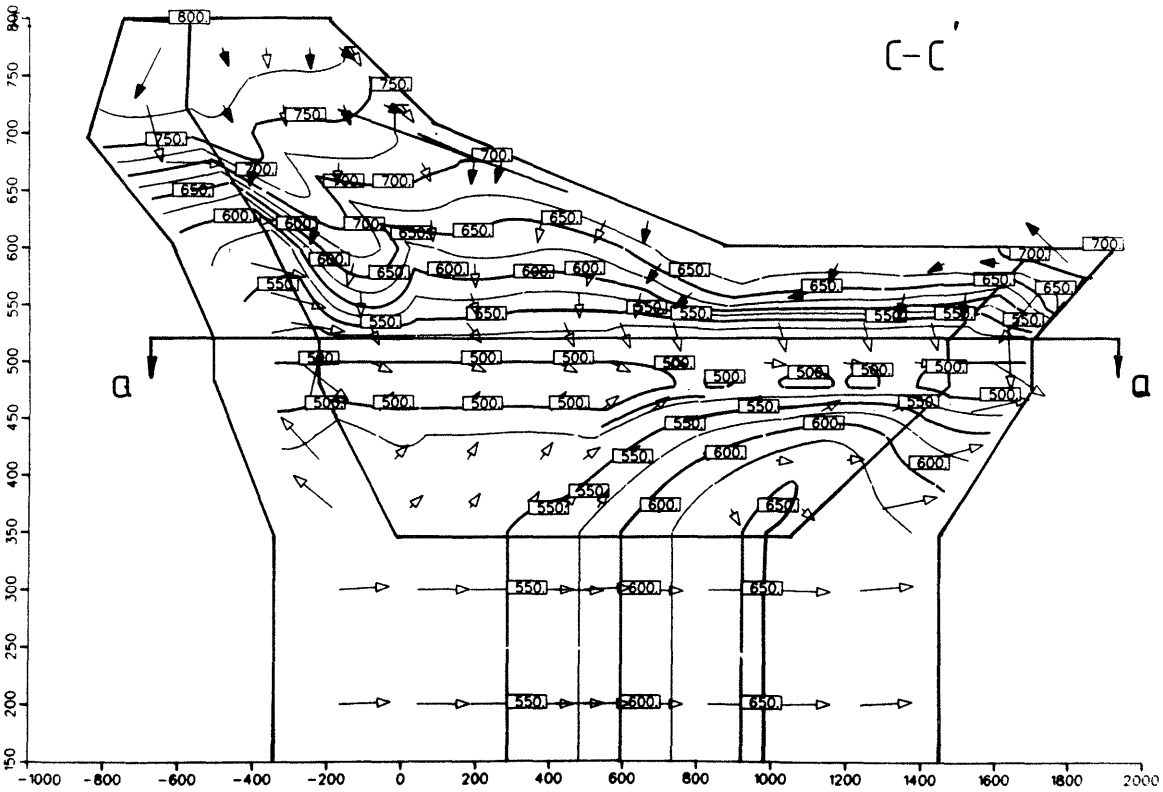

Figure 5.9.4

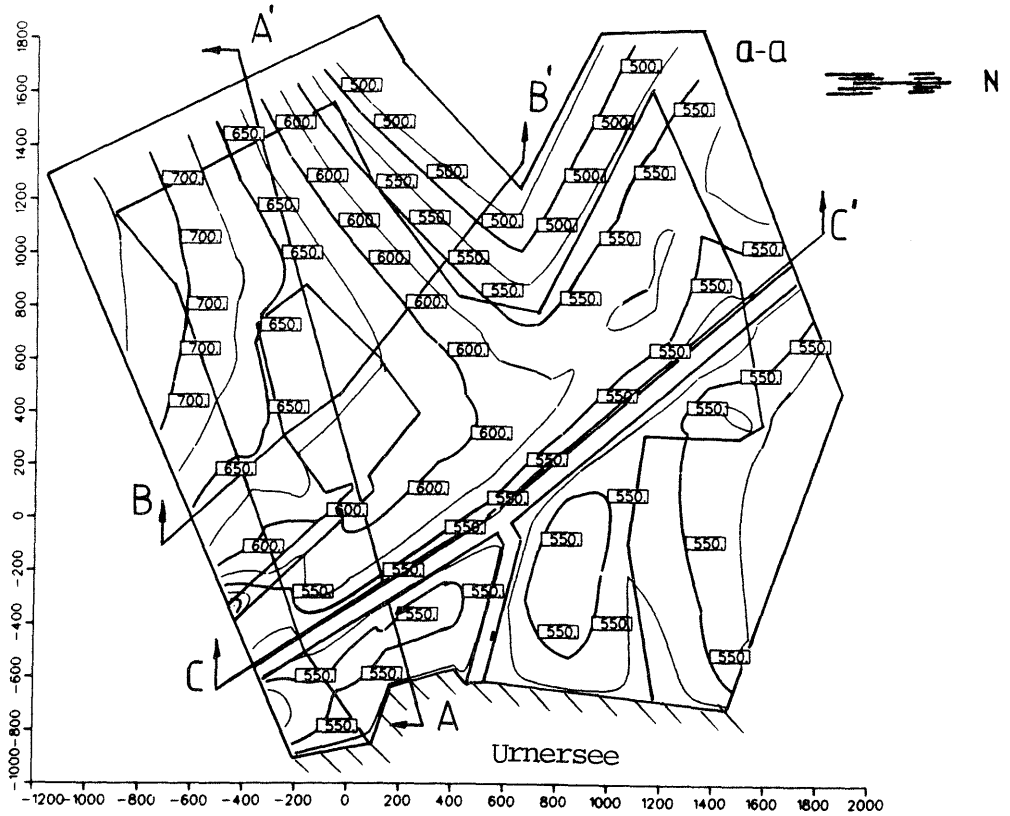

Figure 5.10.1

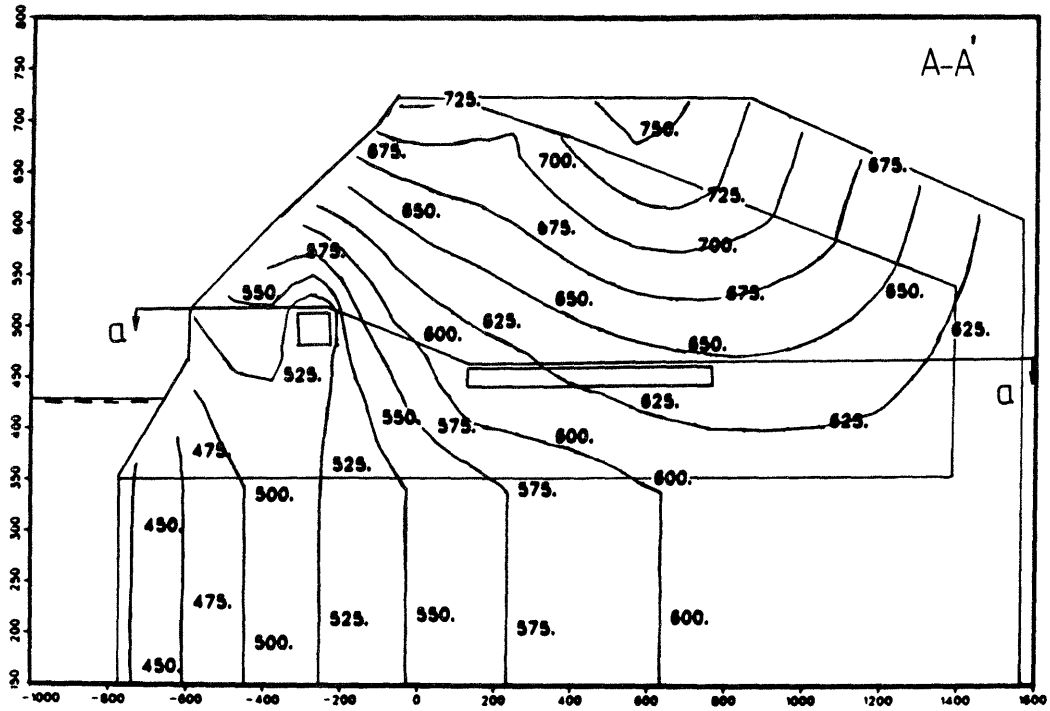

Figure 5.10.2

Figures 5.10.1-4 Isopotentials from run 4
Figure 5.10.1 shows a horizontal cross-section (aa) through the repository and tunnel planes. Figures 5.10.2-4 show the vertical cross-sections AA, BB and CC indicated in view aa

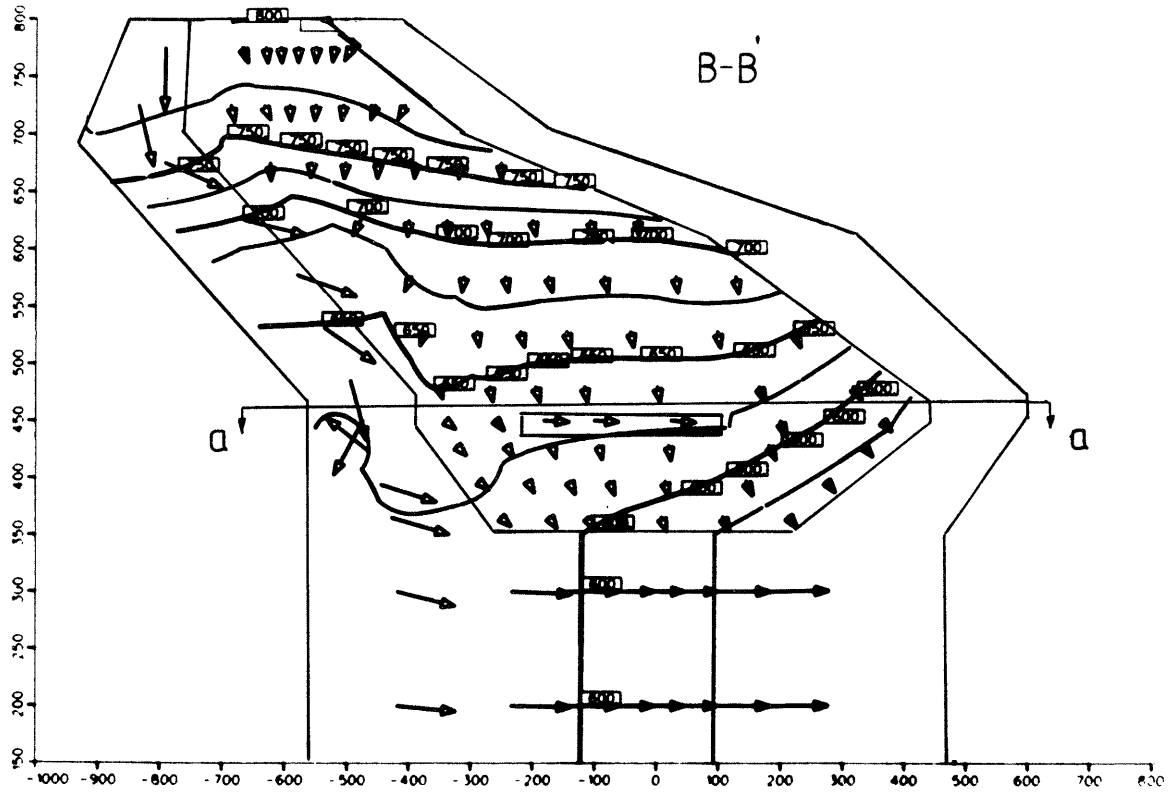

Figure 5.10.3

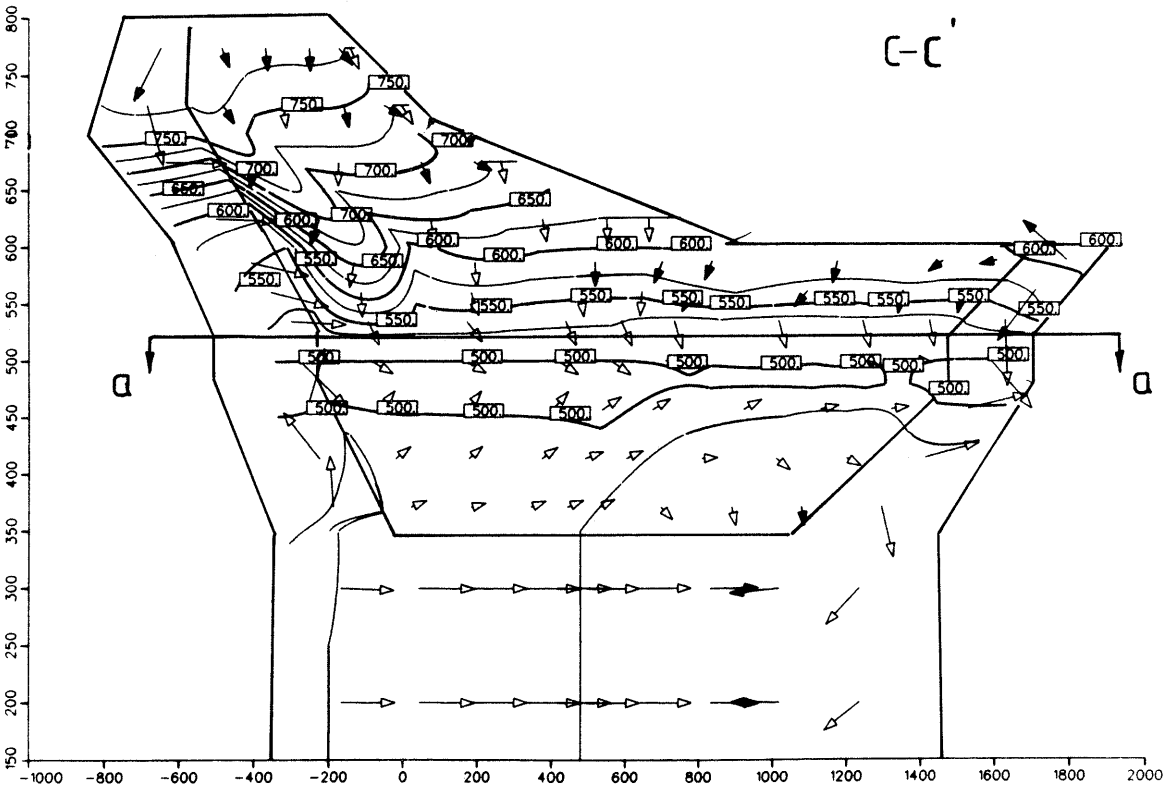

Figure 5.10.4

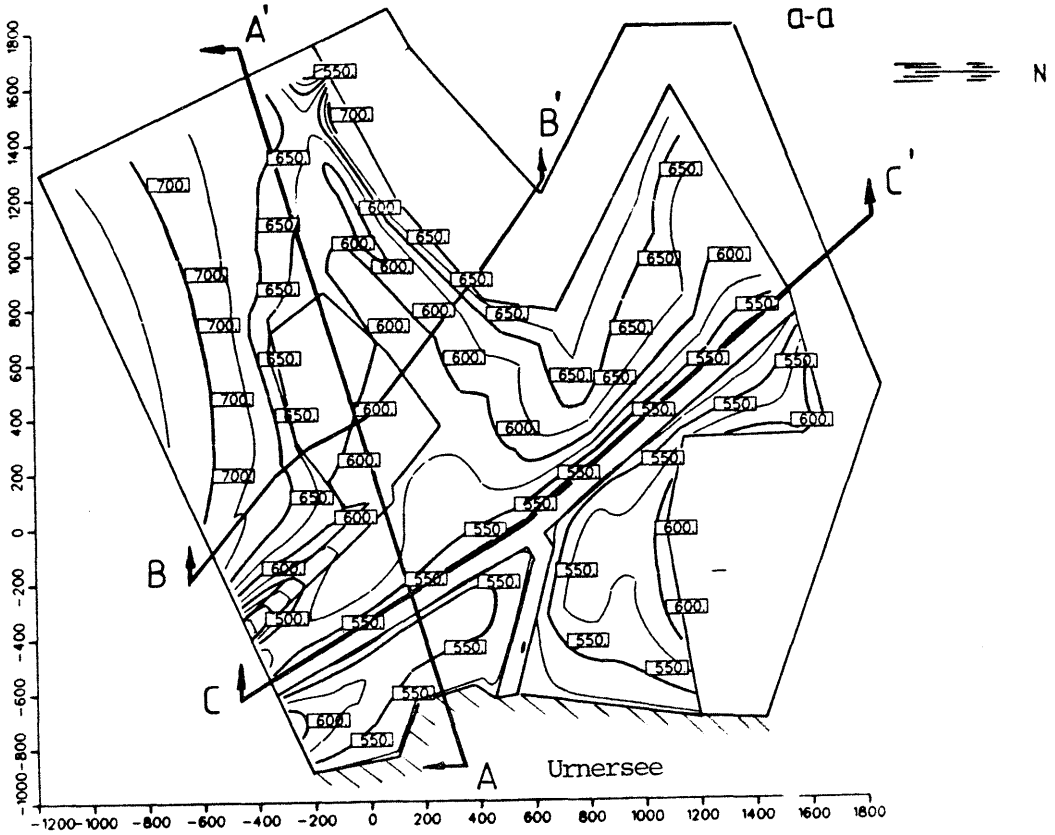

Figure 5.11.1

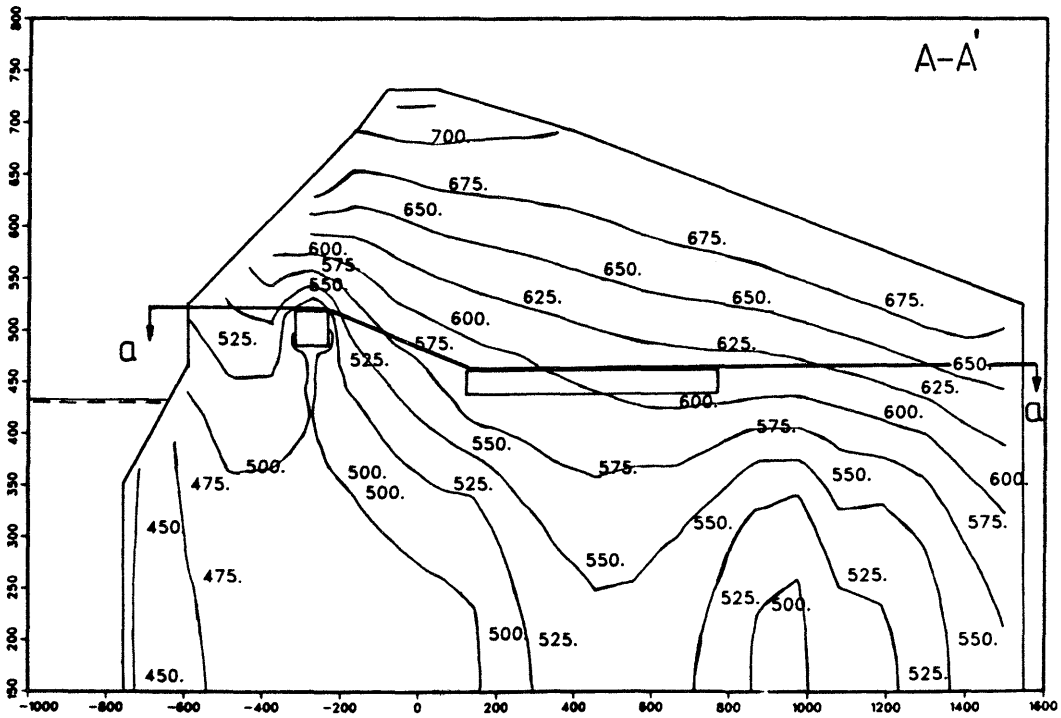

Figure 5.11.2

Figures 5.11.1-4 Isopotentials from run 5.
Figure 5.11.1 shows a horizontal cross-section (aa) through the repository and tunnel planes. Figures 5.11.2-4 show the vertical cross-sections AA, BB and CC indicated in view aa

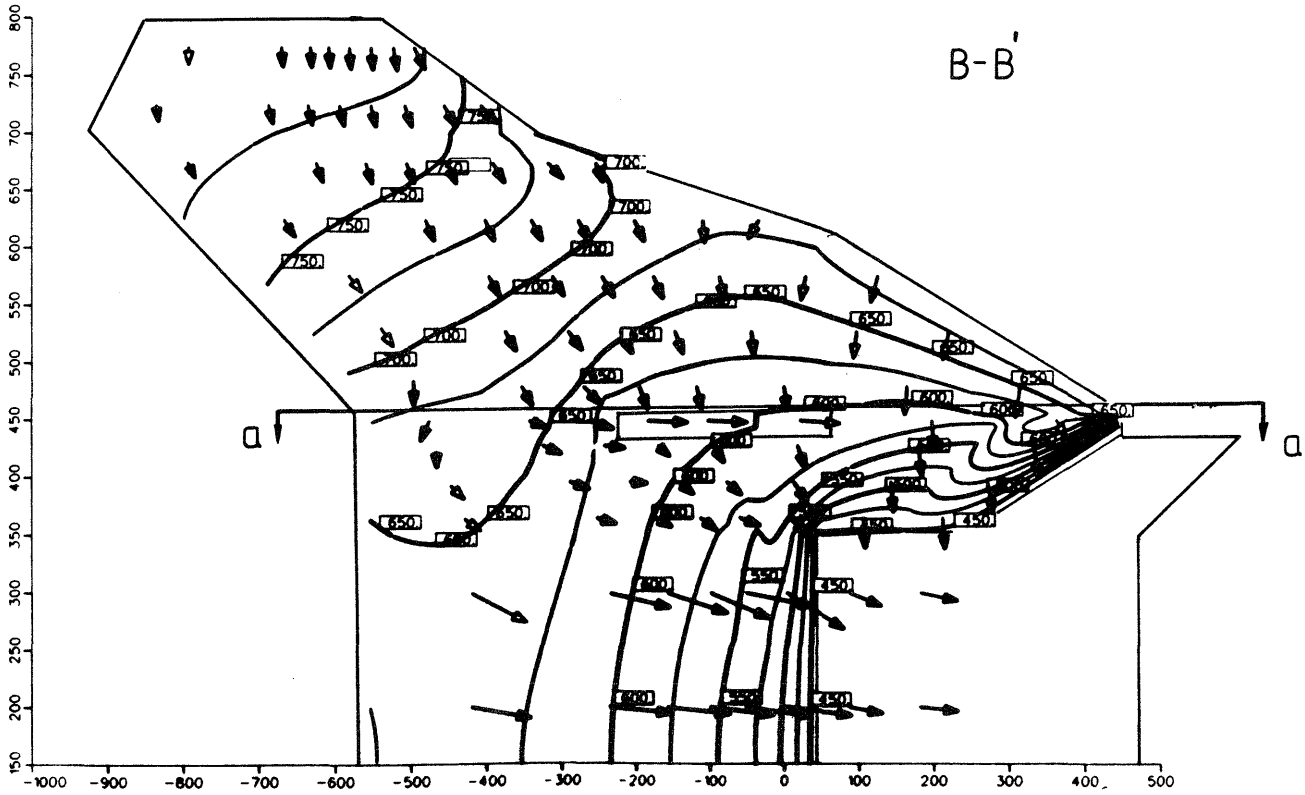

Figure 5.11.3

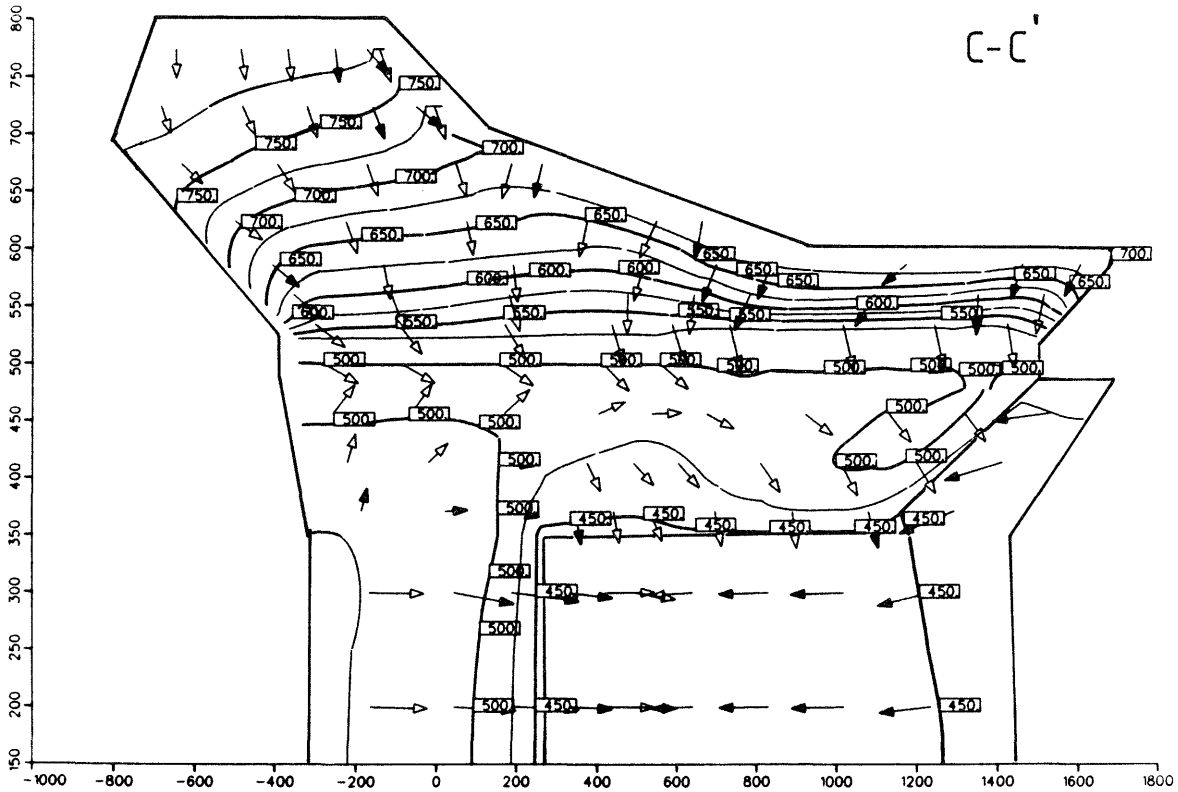

Figure 5.11.4

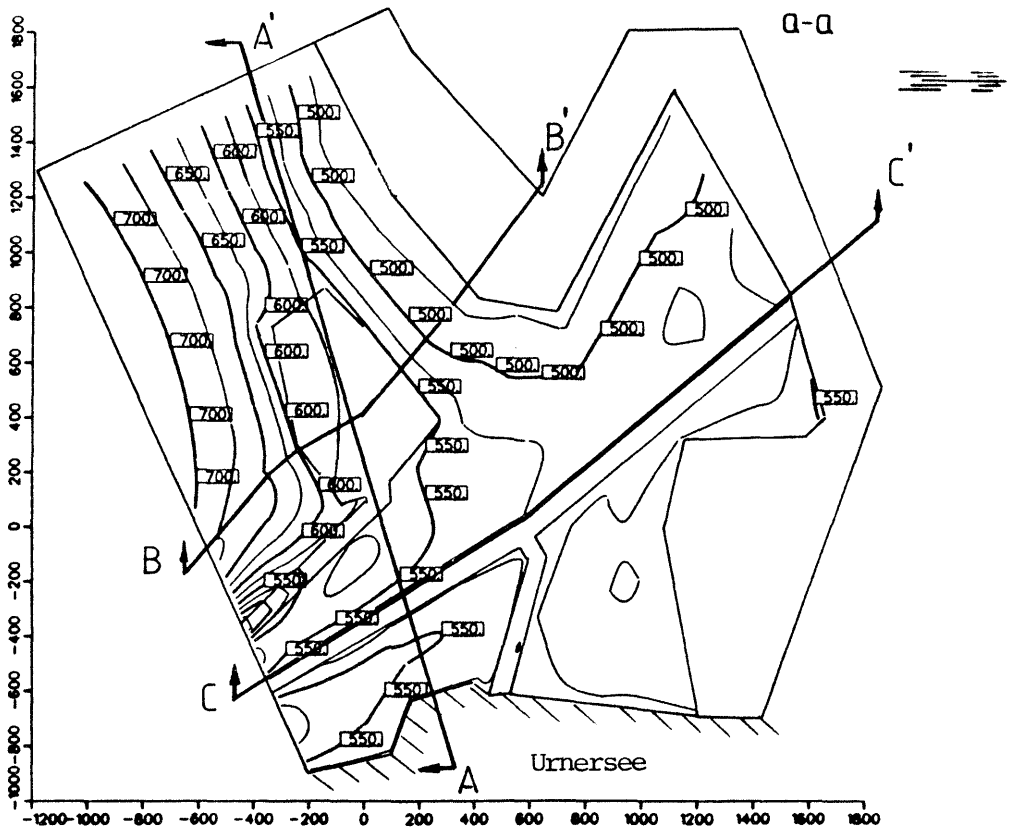

Figure 5.12.1

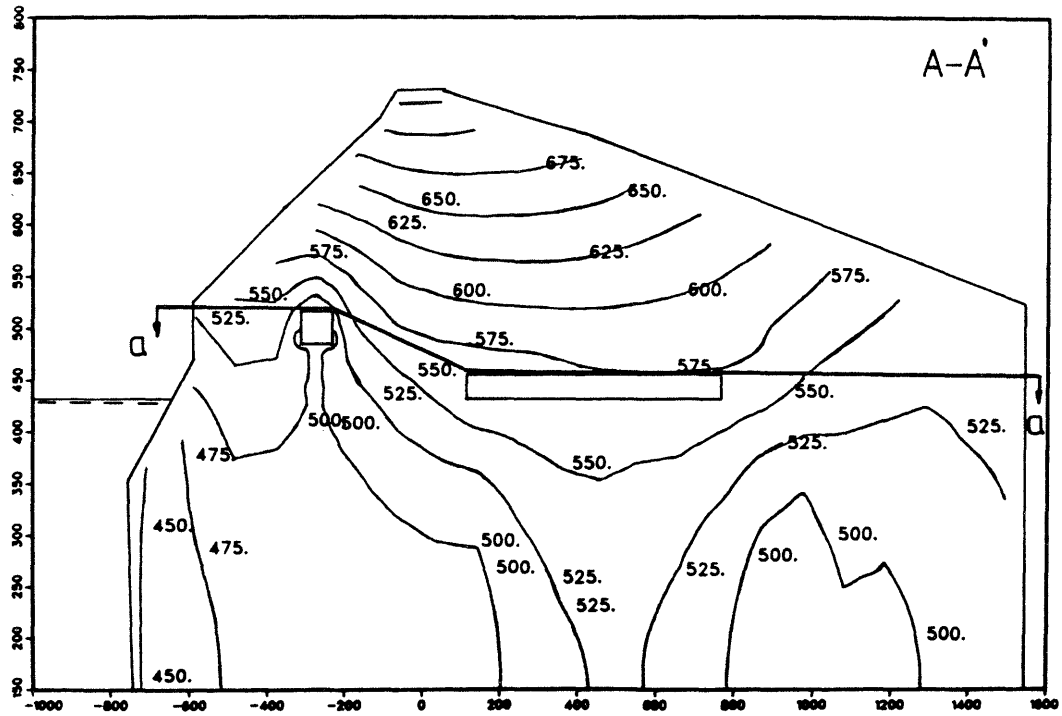

Figure 5.12.2

Figures 5.12.1-4 Isopotentials from run 6.
Figure 5.12.1 shows a horizontal cross-section (aa) through the repository and tunnel planes. Figures 5.12.2-4 show the vertical cross-sections AA, BB and CC indicated in view aa.

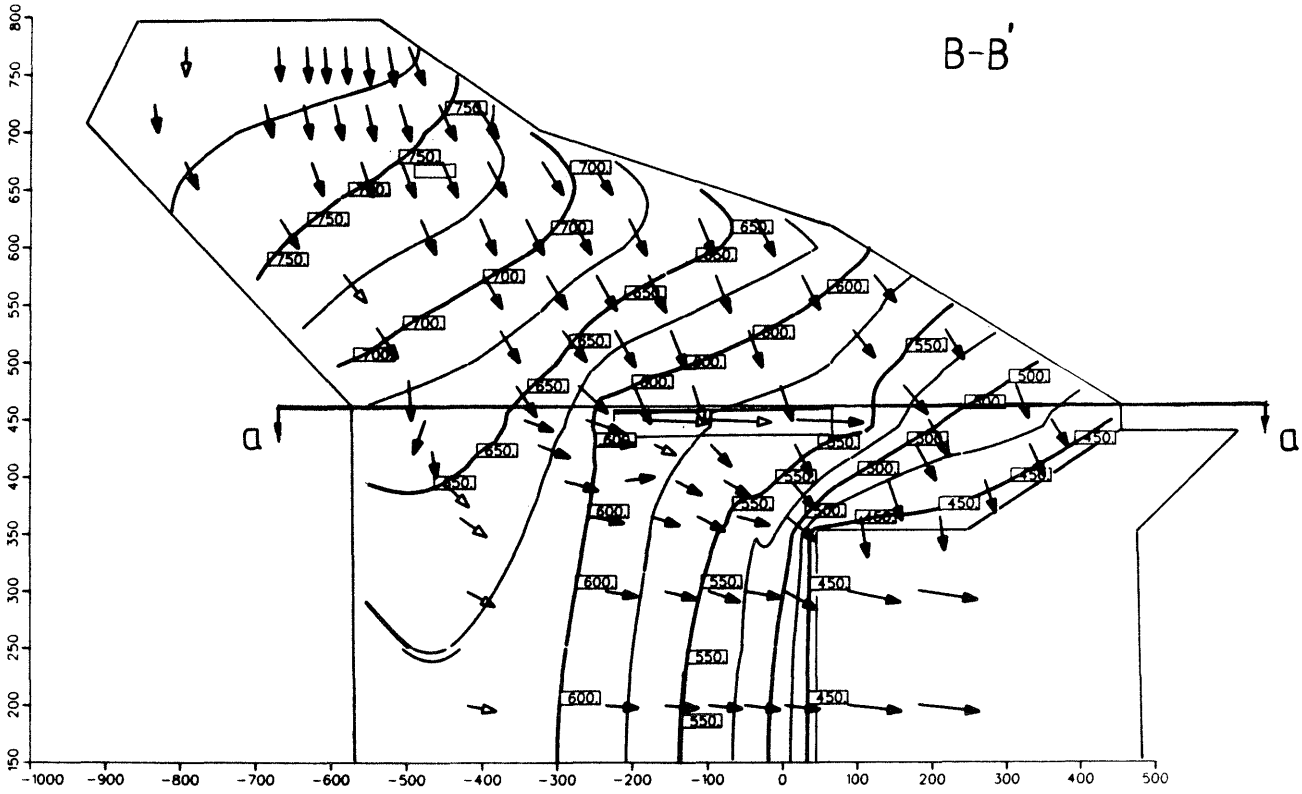

Figure 5.12.3

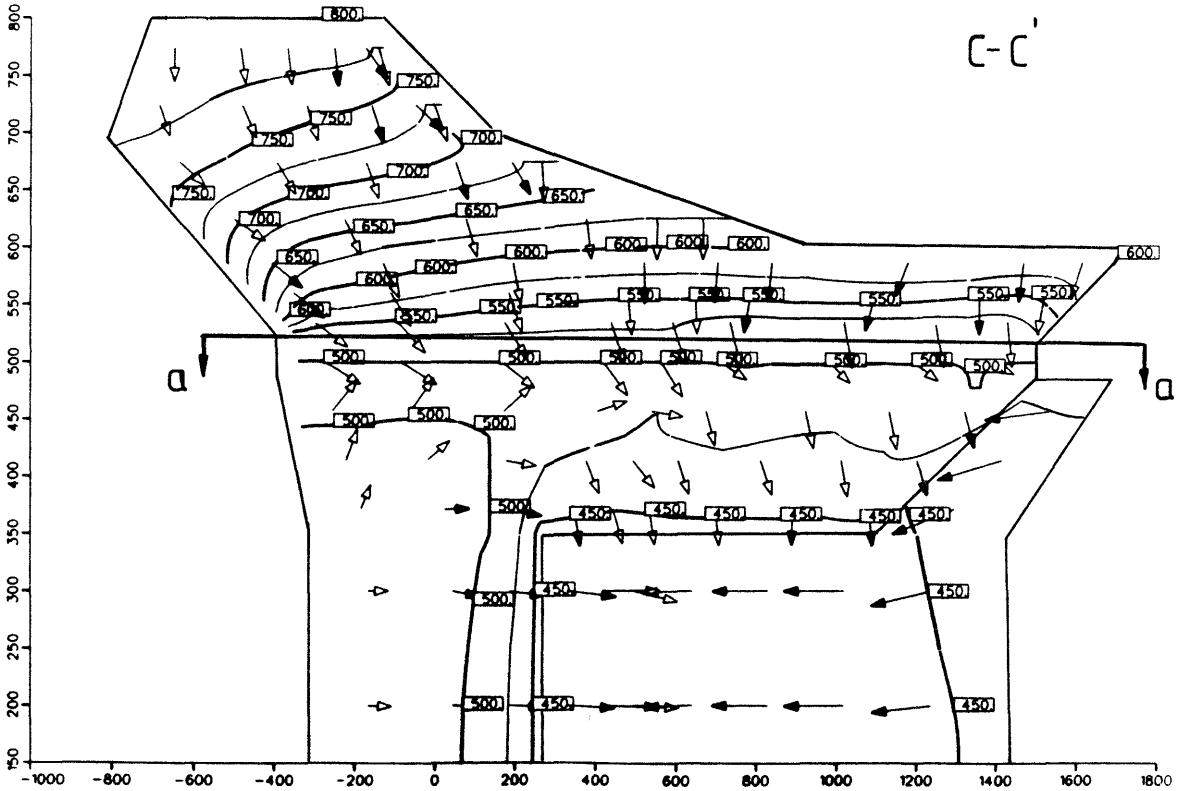

Figure 5.12.4

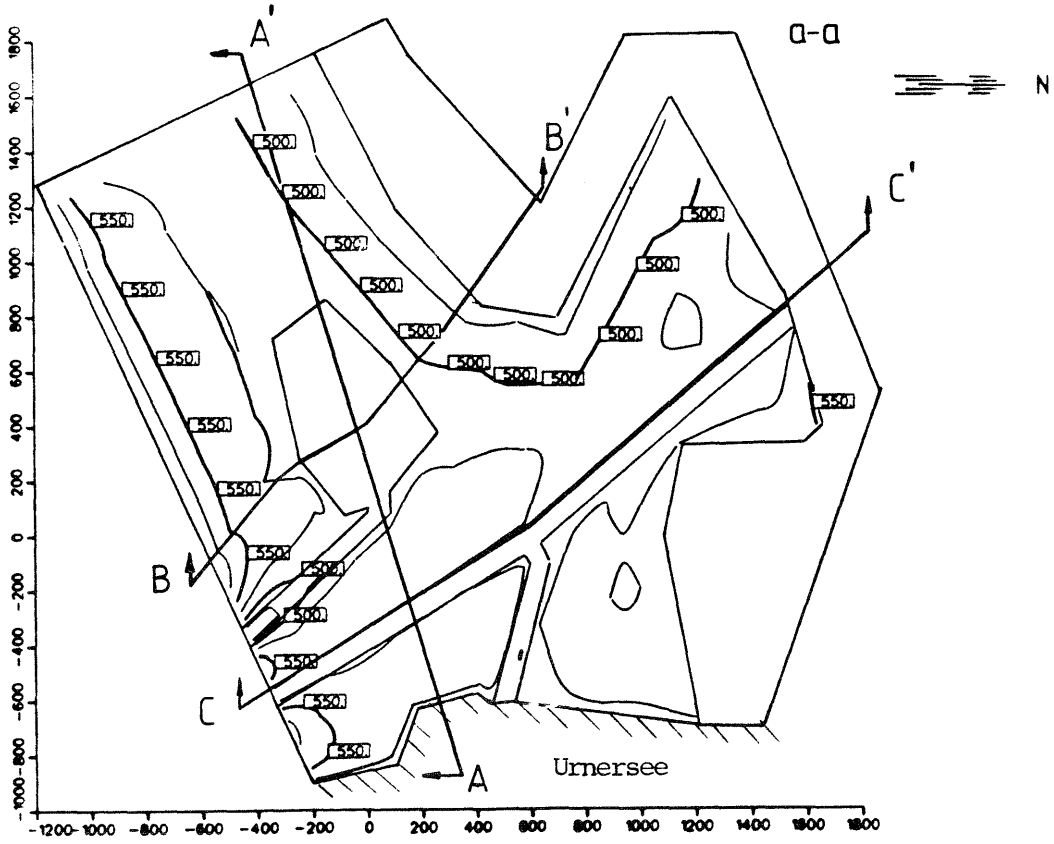

Figure 5.13.1

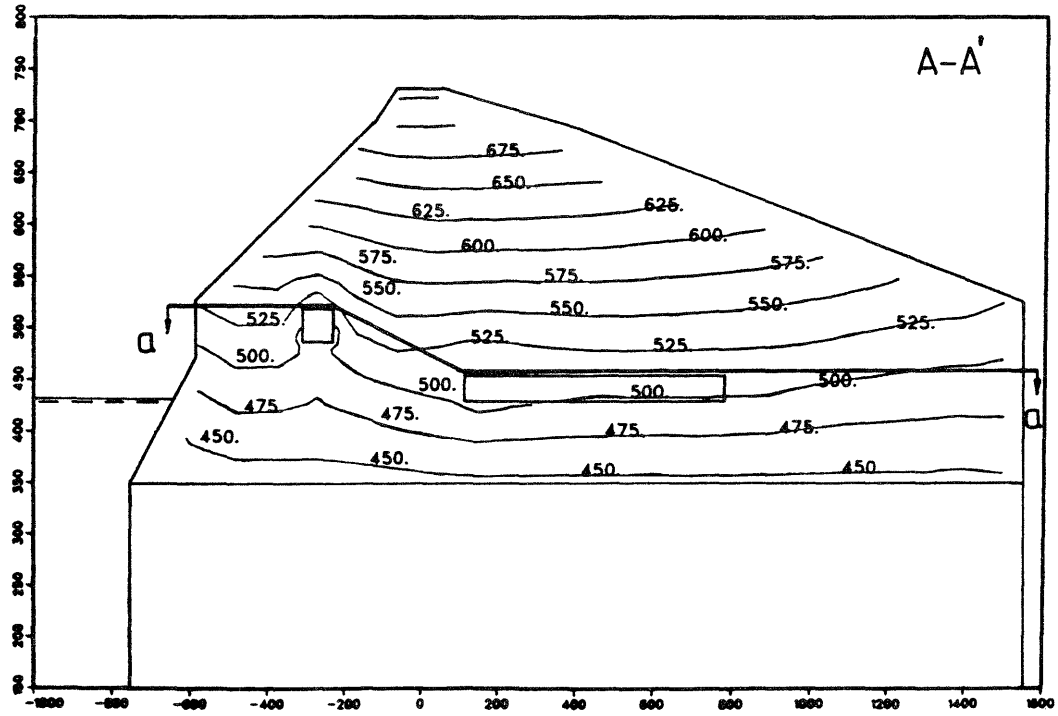

Figure 5.13.2

Figures 5.13.1-4 Isopotentials from run 7.
Figure 5.13.1 shows a horizontal cross-section (aa) through the repository and the tunnel planes. Figures 5.13.2-4 show the vertical cross-sections AA, BB and CC indicated in view aa.

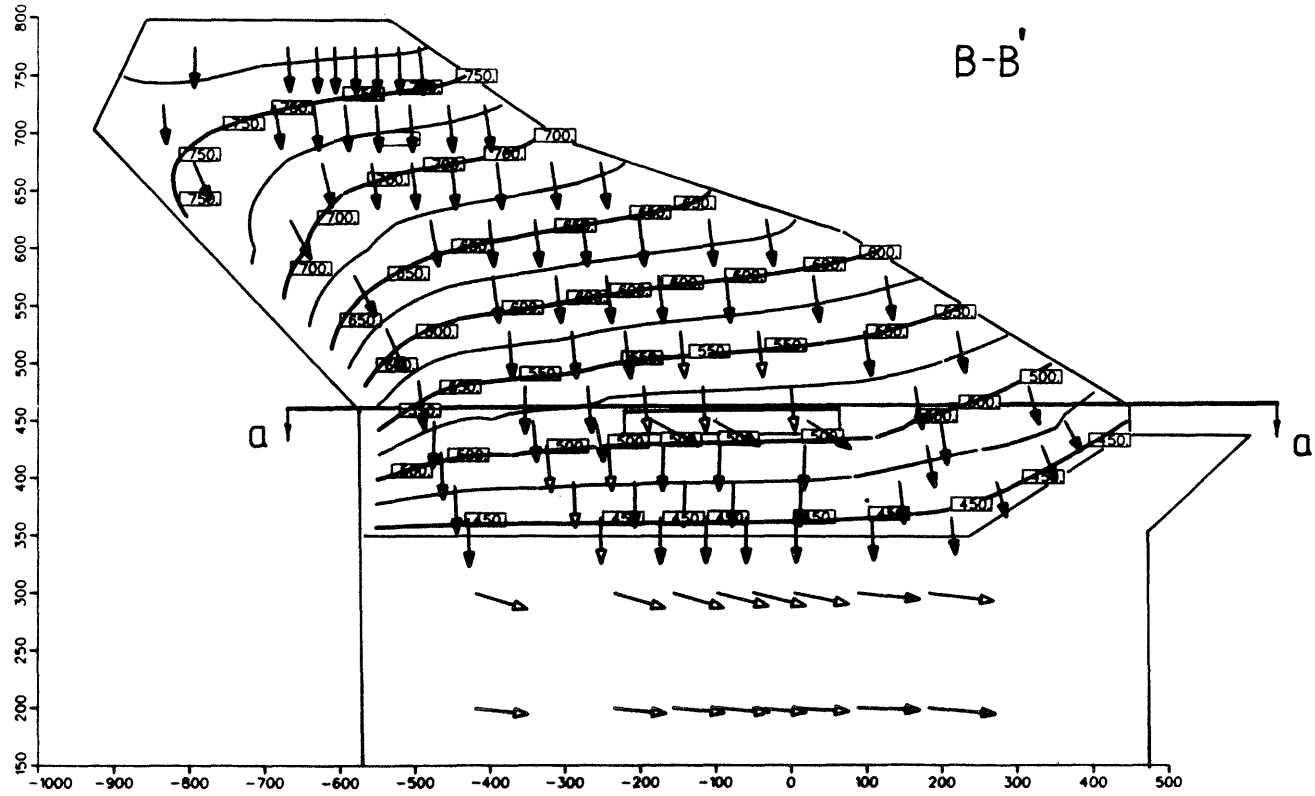

Figure 5.13.3

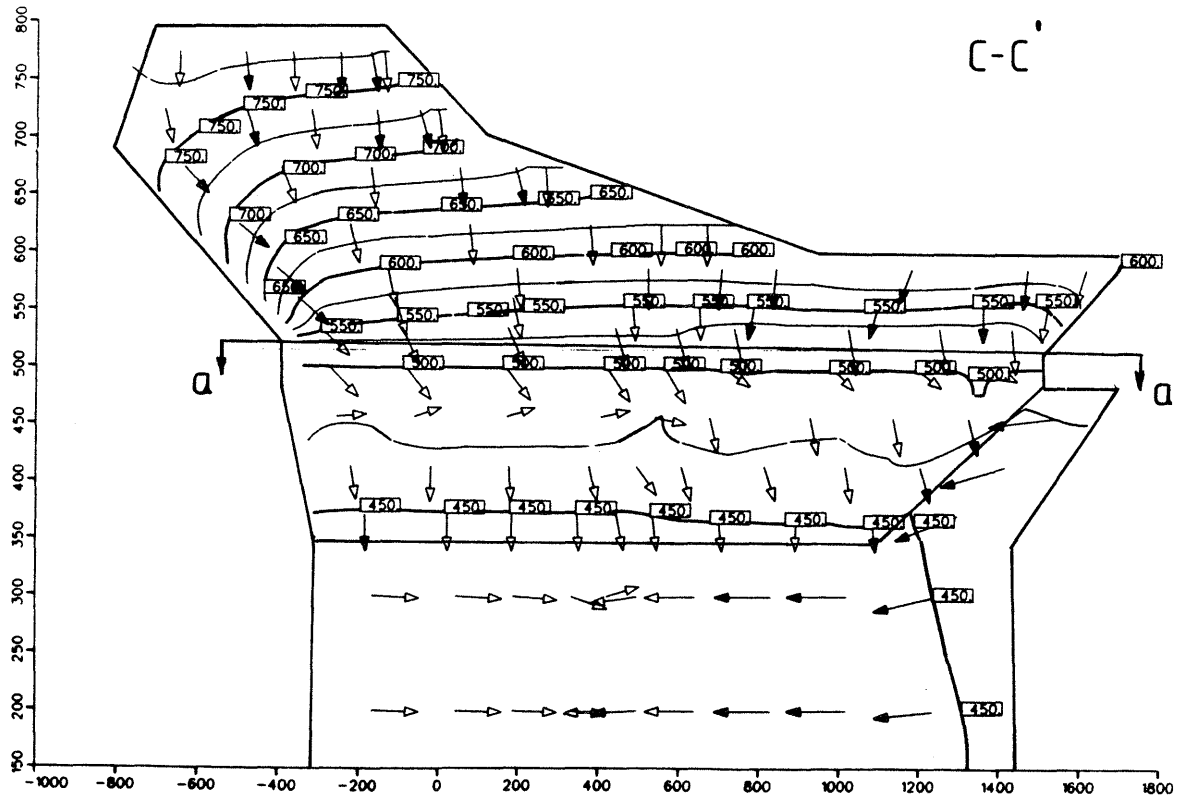

Figure 5.13.4

5.3.2 Groundwater flow rates

The groundwater flow has been calculated at the level of the potential repository, z=450 m.a.s.l.

As mentioned earlier in Section 5.2.1, the modelling of the repository is conservative, which will exaggerate the flow rates.

Figures 5.14-5.20 show the flow rate distribution in the repository for the seven runs. The flow rates in the Figures are summarised in Table 5.2.

Table 5.2 Flow rate (range and representative value) inside the repository at a level of 450 m ($l/(m^2 yr)$).

Run	Range	Representative value
1	5-50	25
2	2-4	3
3	5-25	15
4	5-20	15
5	5-25	15
6	5-25	20
7	2-4	3

The flow rate is in the order of 5-50 $l/(m^2\ yr)$. As can be expected, the water flow increases when the repository elements are assigned a high hydraulic conductivity. However, the increase in flux obtained is less than proportional to the change in hydraulic conductivity because of the lowering of the hydraulic gradient mentioned in the previous section. The difference in conductivity between runs 1 and 2 is a factor of 100 but change in flow rate is only a factor of 10.

An explanation of the comparably low flow rate in run 7 is that the flow direction is more perpendicular to the repository plane in this run; i.e. the continuity requirement puts more stringent constraints on the flow increases than would be the case with parallel flow. This effect has been demonstrated for a hollow cylinder /5/.

The flow rates in the repository are relatively insensitive to the variations of boundary conditions implemented in these series of runs.

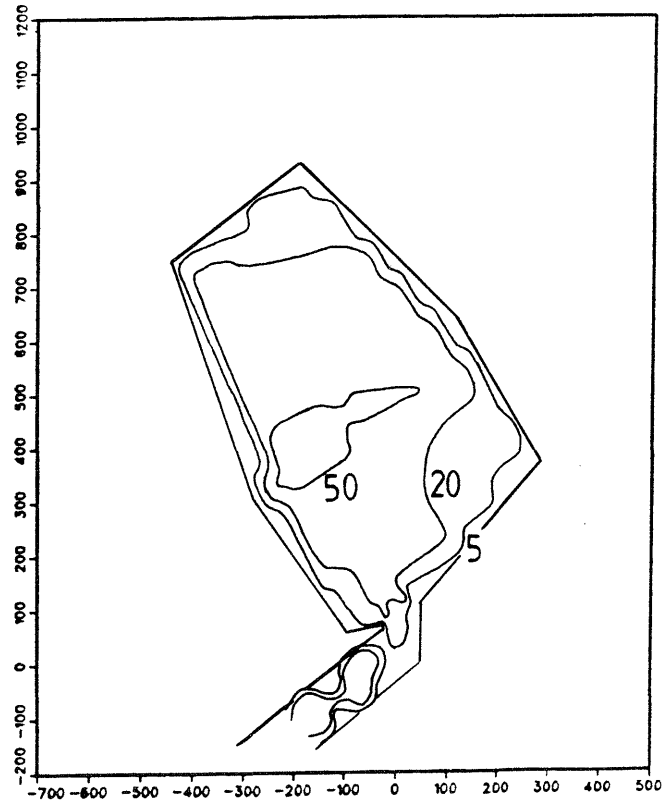

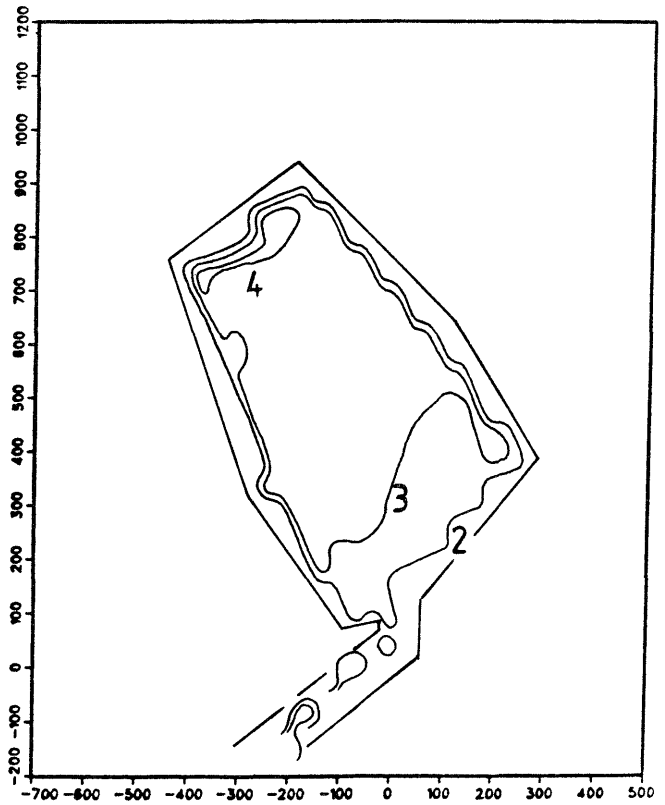

Figures 5.14-5-15 Flow rate distribution within the repository for runs 1 and 2. The isofluxes are in units of $l/(m^2 \cdot yr)$

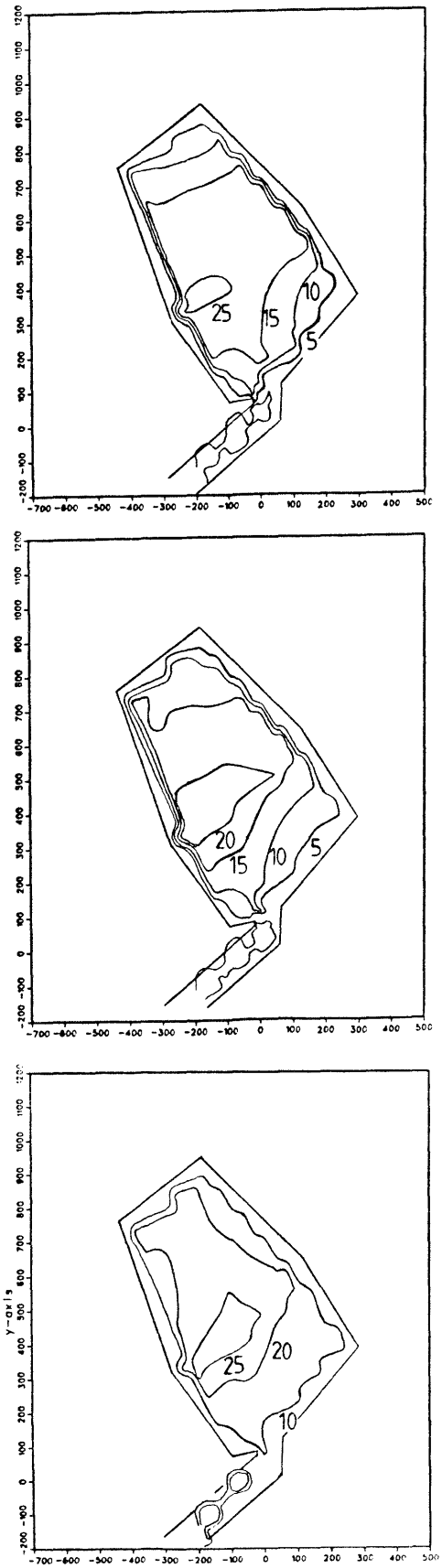

Figures 5.16-5.18 Flow rate distribution within the repository for runs 3-5. The isofluxes are in units of $1/(m^2 \cdot yr)$

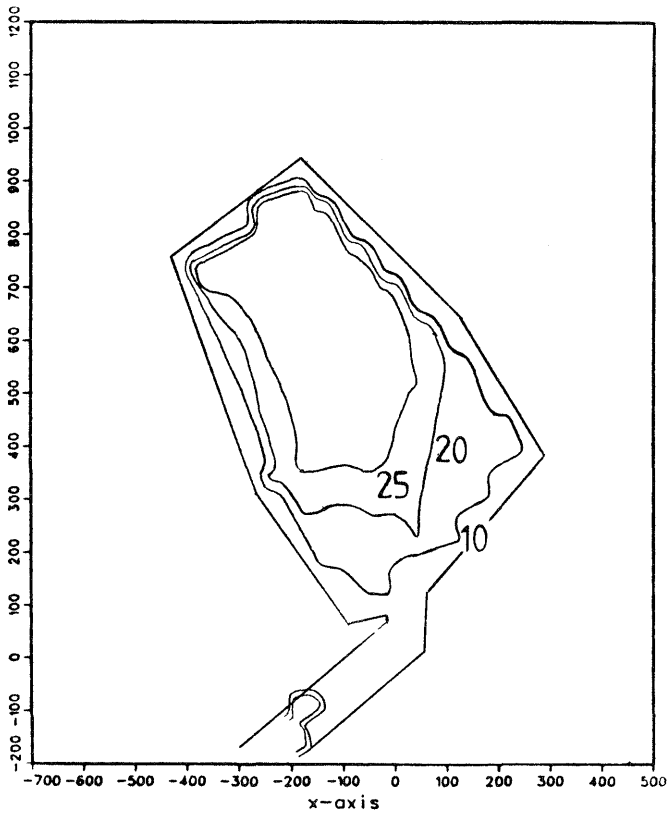

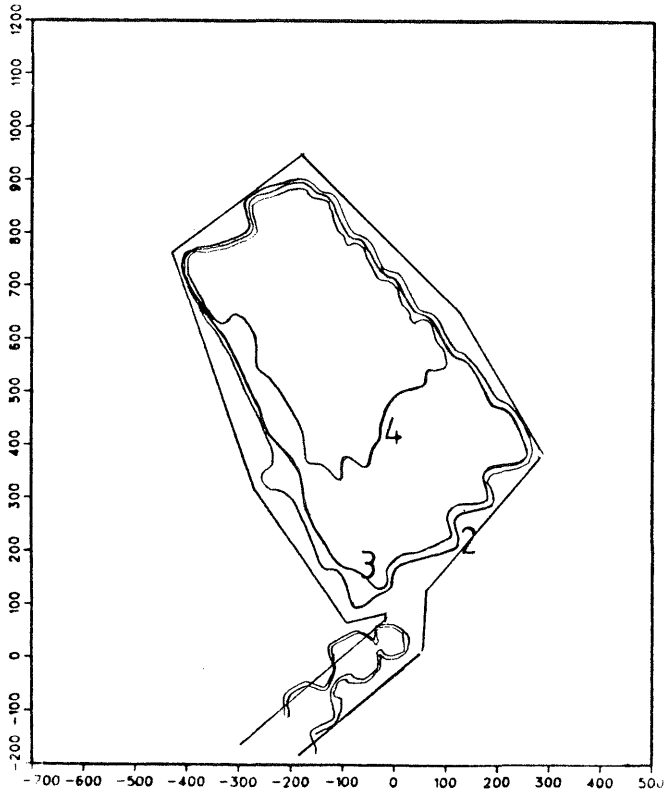

Figures 5.19-5.20 Flow rate distribution within the repository for runs 6-7. The isofluxes are in units of $1/(m^2 \cdot yr)$

5.3.3 Trajectories and groundwater travel times

For all seven runs presented in this report, six trajectories have been tracked from 450 m.a.s.l. The starting points of the trajectories are located in the area of the potential repository, Figure 5.21. The travel lengths and the particle travel times are summarised in Table 5.3. The Table also shows average hydraulic gradients calculated as the average flow rate (porosity x travel length/travel time) divided by the appropriate hydraulic conductivity. The pathways are shown in Figures 5.22-5.28.

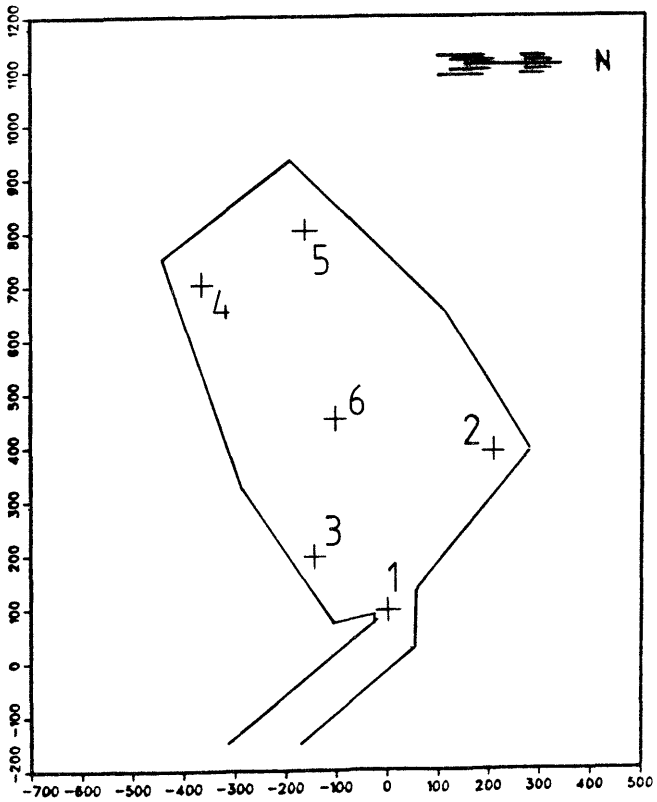

Figure 5.21 View of the trajectory starting points inside the repository. The indicated position numbers correspond to the trajectory numbers in Table 5.3.

The travel times in the marl have been calculated assuming that all flow occurs in the more permeable discontinuities of the marl body, corresponding to 3% of the cross-sectional area (Section 5.2.4).

The part of the porosity which is hydraulically conductive, the kinematic porosity, is assumed to be 3% for all material groups.

As can be seen in Figures 5.22-5.28, most of the trajectories go straight down to the underlying pervious stratum then turn off towards the eastern or the western boundaries where they exit from the model. It should be pointed out that the flow direction in the underlying strata is very sensitive to the boundary conditions applied. Both the flow direction and the magnitude of the flow in these strata might be artificial in these calculations. For this reason the limestone part of the trajectories has been left out of Table 5.

By comparing the path lines in Figures 5.22-5.28 and the calculated values in Table 5.3, the following conclusions can be drawn:

- The level of the water table in the pervious surrounding layers is of importance for the Darcy velocity in the marl underneath the repository. A high level of the water table decreases the gradients between the repository and the underlying pervious stratum, which implies lower fluxes in the marl

- The Tertiary shale causes the path lines to go deeper before they enter the pervious layers. The particle travel time is, however, not significantly affected

- Differences in path length inside the repository mainly depend on the hydraulic conductivity assigned to the repository elements and to the direction of the flow vector in relation to the repository plane

- None of the trajectories exited into the Seelisberg tunnel.

The distance between the repository and the underlying pervious layer has, as mentioned earlier, been underestimated, which also means that the calculated particle travel times in Table 5.3 are underestimated. The distance between the repository and the pervious layer should, according to the current understanding of the site geology, be about 1.7 times longer than modelled. As mentioned earlier, the hydraulic head in the pervious layer is mainly determined by the boundary conditions applied to this layer and thus largely independent of the level of the bottom marl surface. Assuming that the hydraulic head in the repository is also insensitive to the thickness of the marl underneath the repository, the gradient should be

0.57 times the calculated gradient and the travel times thus underestimated by a factor of 1.7/0.57=3. If the pressure drop from the Choltal to the underlying strata is distributed equally over the distance, the travel time reduction factor should be about 2.

Table 5.3 Path lengths (m) and groundwater travel times (years) for six trajectories. The travel times are calculated seperately for the path through the actual repository and for the path through the host rock. The latter travel time is calculated assuming that flow occurs only in discontinuities.

Run no.	Trajectory no.	repository part			host rock part		
		path length (m)	travel time (years)	average gradient (m/m)	path length (m)	travel time (years)	average gradient (m/m)
1	1	-----		Oscillating -----			
	2	60	250	0.0023	80	34	0.66
	3	160	280	0.0054	100	67	0.43
	4	320	250	0.0122	100	116	0.24
	5	160	150	0.0101	100	74	0.39
	6	340	270	0.0120	84	46	0.50
2	1	40	180	0.21	80	36	0.48
	2	40	34	1.12	80	44	0.52
	3	40	38	1.00	100	77	0.36
	4	20	17	1.12	100	82	0.35
	5	20	17	1.11	100	67	0.43
	6	20	16	1.19	100	73	0.39
3	1	-----		Oscillating -----			
	2	60	340	0.0170	80	51	0.43
	3	80	170	0.0437	140	131	0.30
	4	240	440	0.0521	110	204	0.15
	5	220	440	0.0481	110	196	0.16
	6	220	350	0.0607	100	77	0.37
4	1	200	1230	0.015	100	91	0.31
	2	40	1790	0.021	80	32	0.72
	3	100	270	0.035	80	48	0.47
	4	120	2430	0.047	100	93	0.31
	5	60	1560	0.037	100	60	0.47
	6	140	230	0.058	100	60	0.47
5	1	120	1200	0.010	100	69	0.41
	2	40	84	0.045	80	13	1.79
	3	180	400	0.043	180	36	1.43
	4	180	250	0.068	260	65	1.15
	5	40	68	0.056	160	27	1.67
	6	220	310	0.068	160	28	1.93
6	1	60	1500	0.004	180	75	0.69
	2	60	100	0.057	80	18	1.25
	3	200	420	0.045	140	41	0.97
	4	240	240	0.095	160	50	0.92
	5	60	70	0.082	380	58	1.87
	6	200	230	0.083	220	150	0.42
7	1	40	3100	0.001	80	27	0.85
	2	40	220	0.017	80	29	0.78
	3	20	120	0.016	100	36	0.81
	4	20	110	0.017	100	39	0.74
	5	20	150	0.013	100	41	0.70
	6	20	130	0.015	100	41	0.69

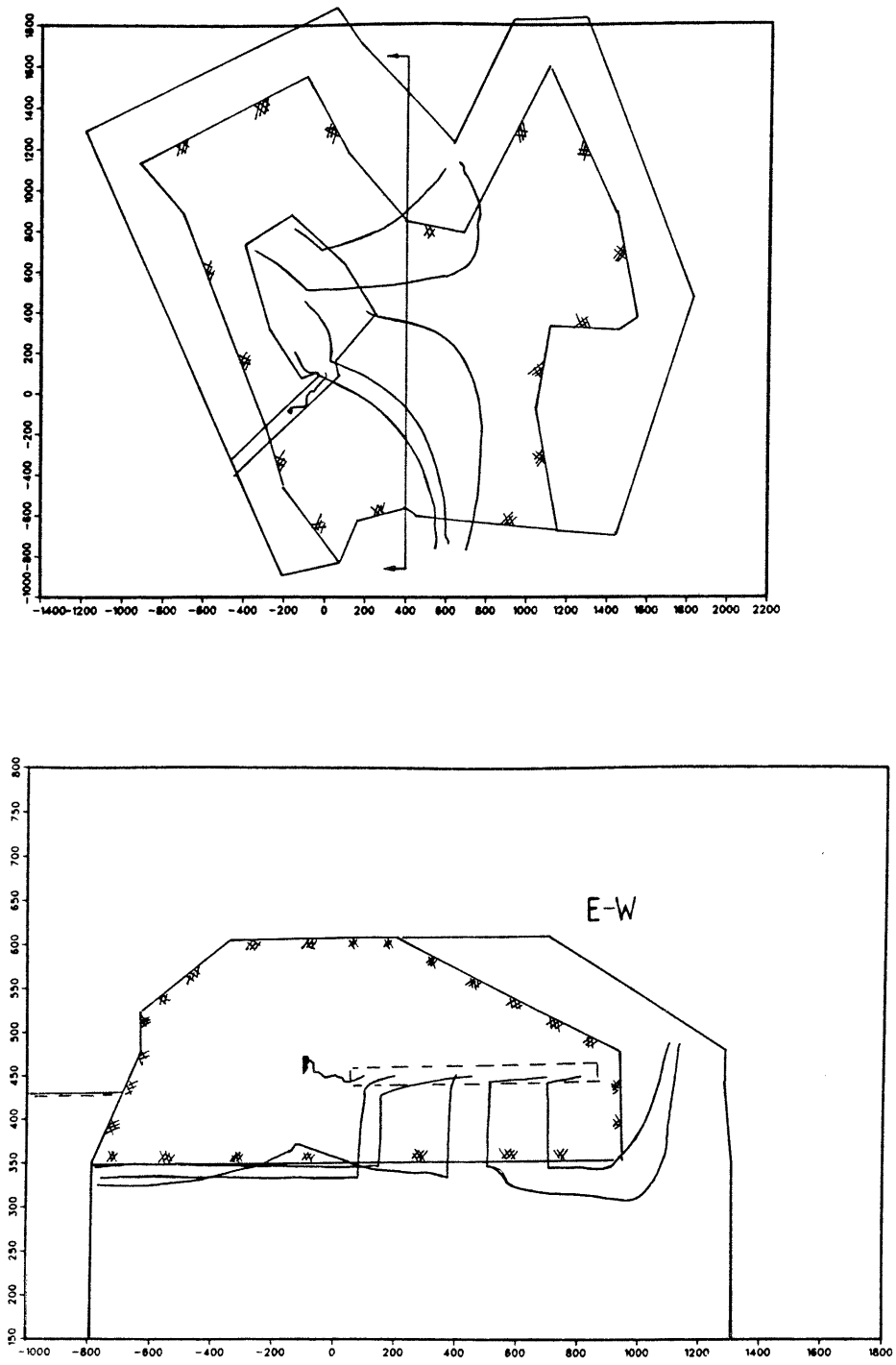

Figure 5.22 Path lines from the repository for run 1 in a horizontal and vertical projection

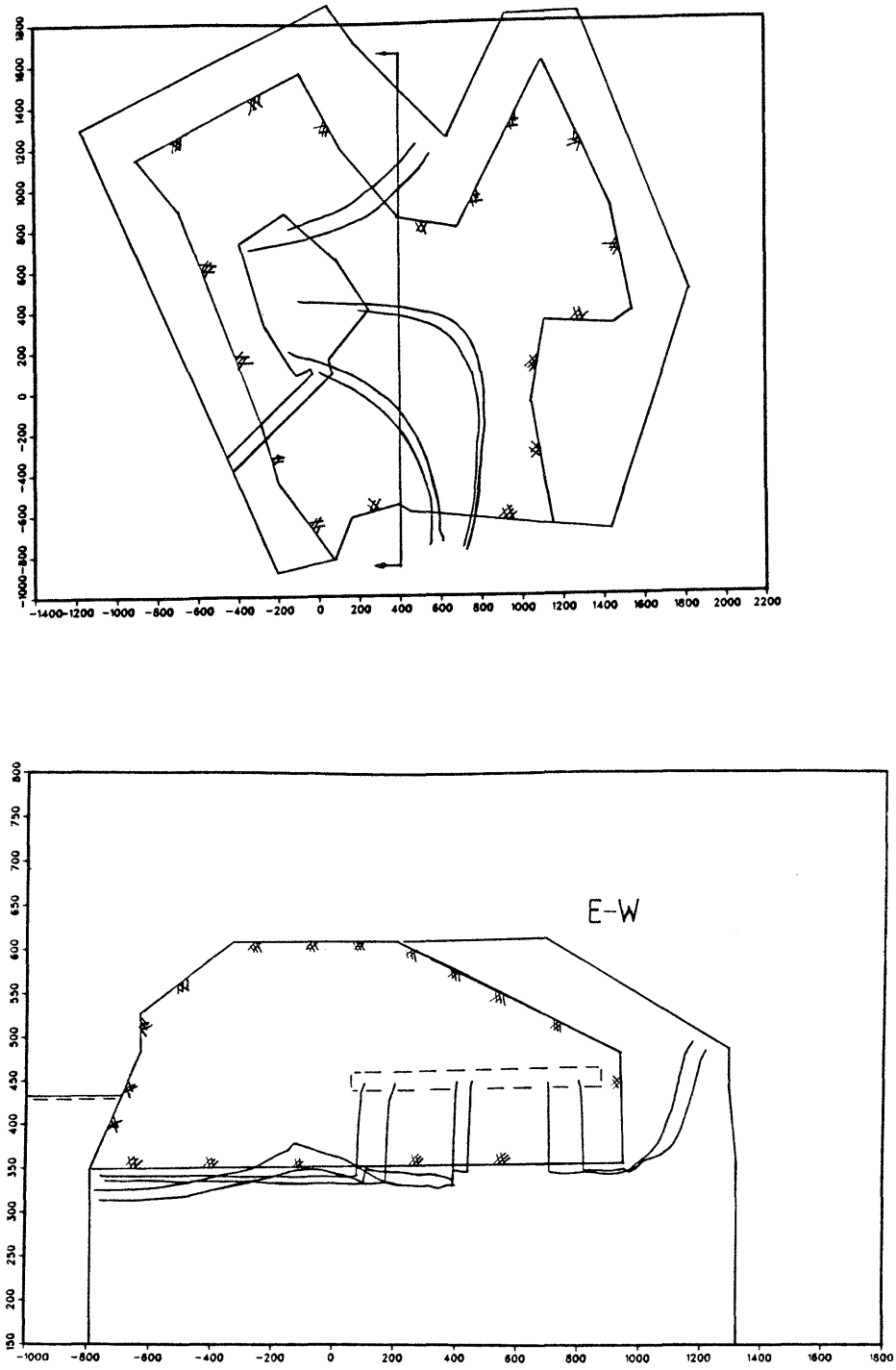

Figure 5.23 Path lines from the repository for run 2 in a horizontal and vertical projection

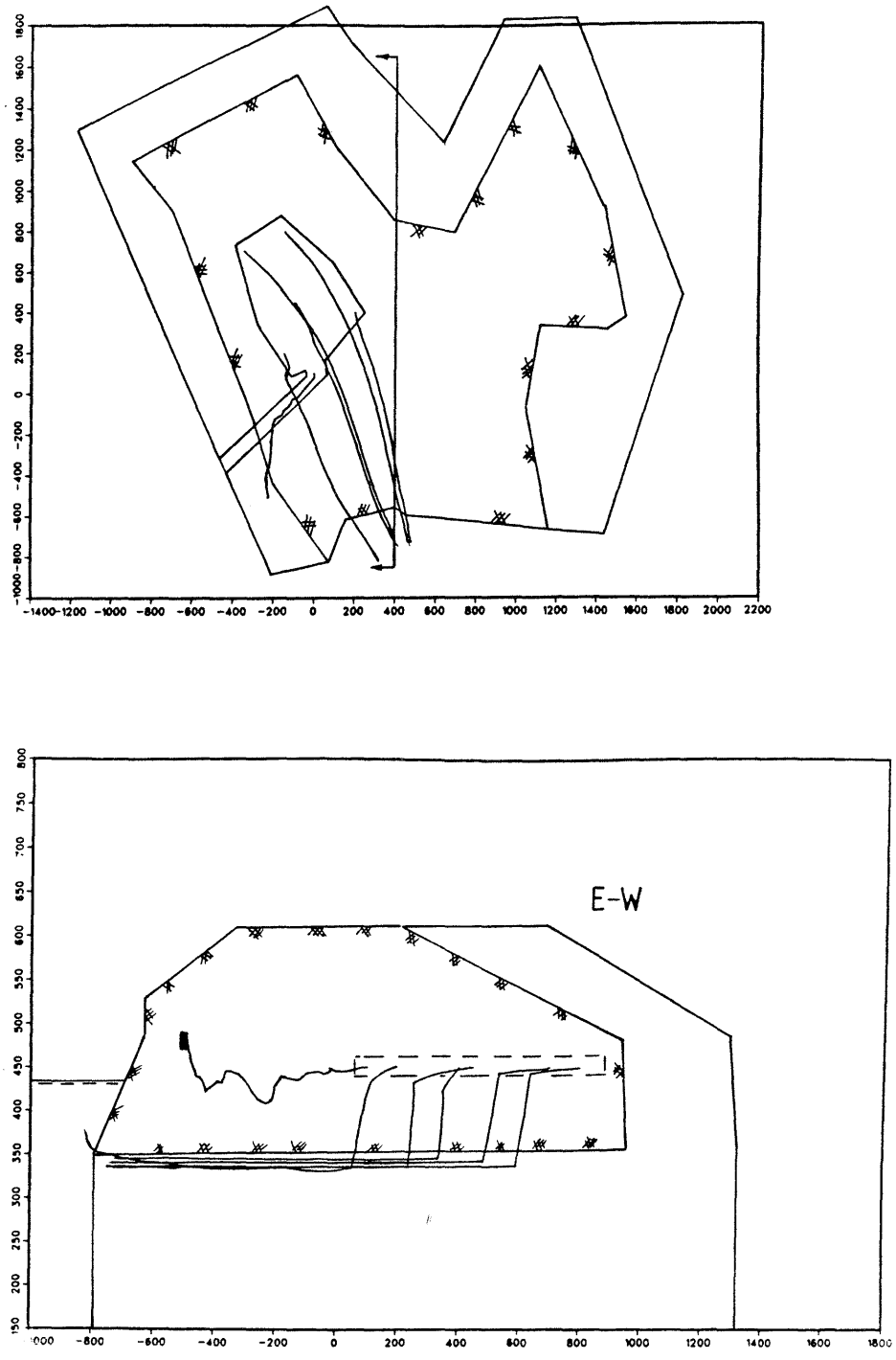

Figure 5.24 Path lines from the repository for run 3 in a horizontal and vertical projection. The instability in path line no. 1 is caused by local mass conservation disturbances and does not end in the Seelisberg tunnel. The path line is ending in a numerically induced sink.

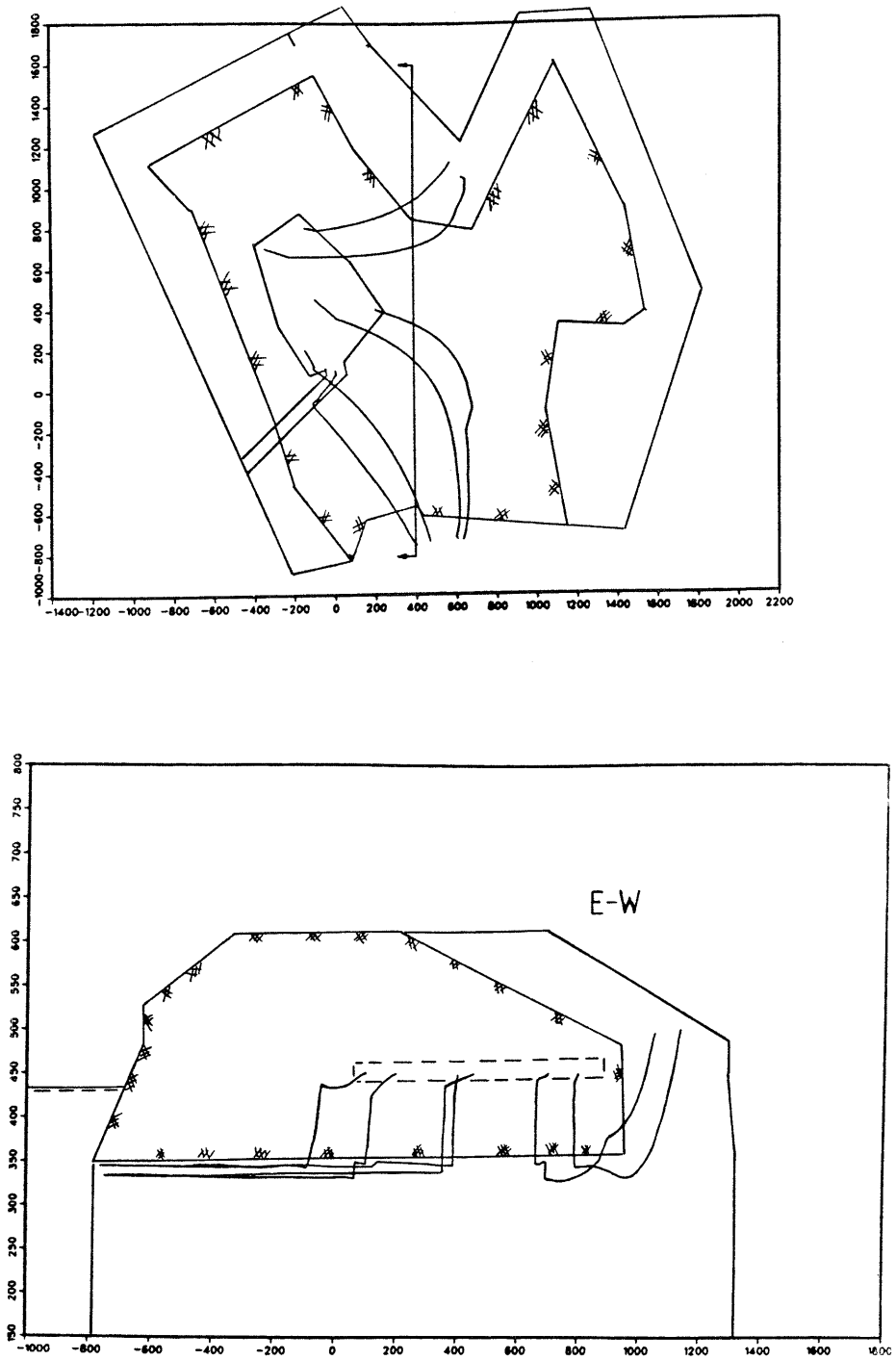

Figure 5.25 Path lines from the repository for run 4 in a horizontal and vertical projection

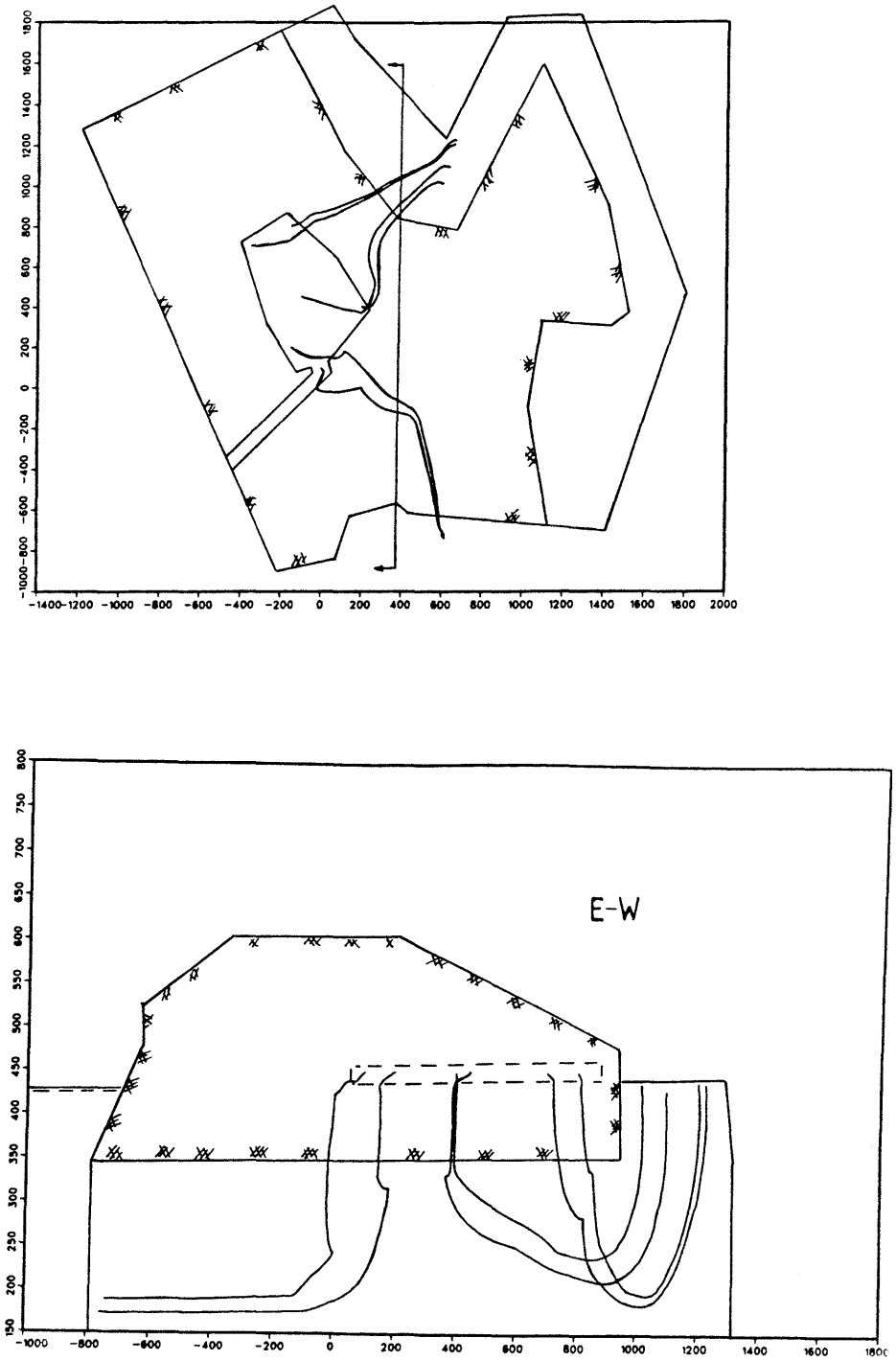

Figure 5.26 Path lines from the repository for run 5 in a horizontal and vertical projection

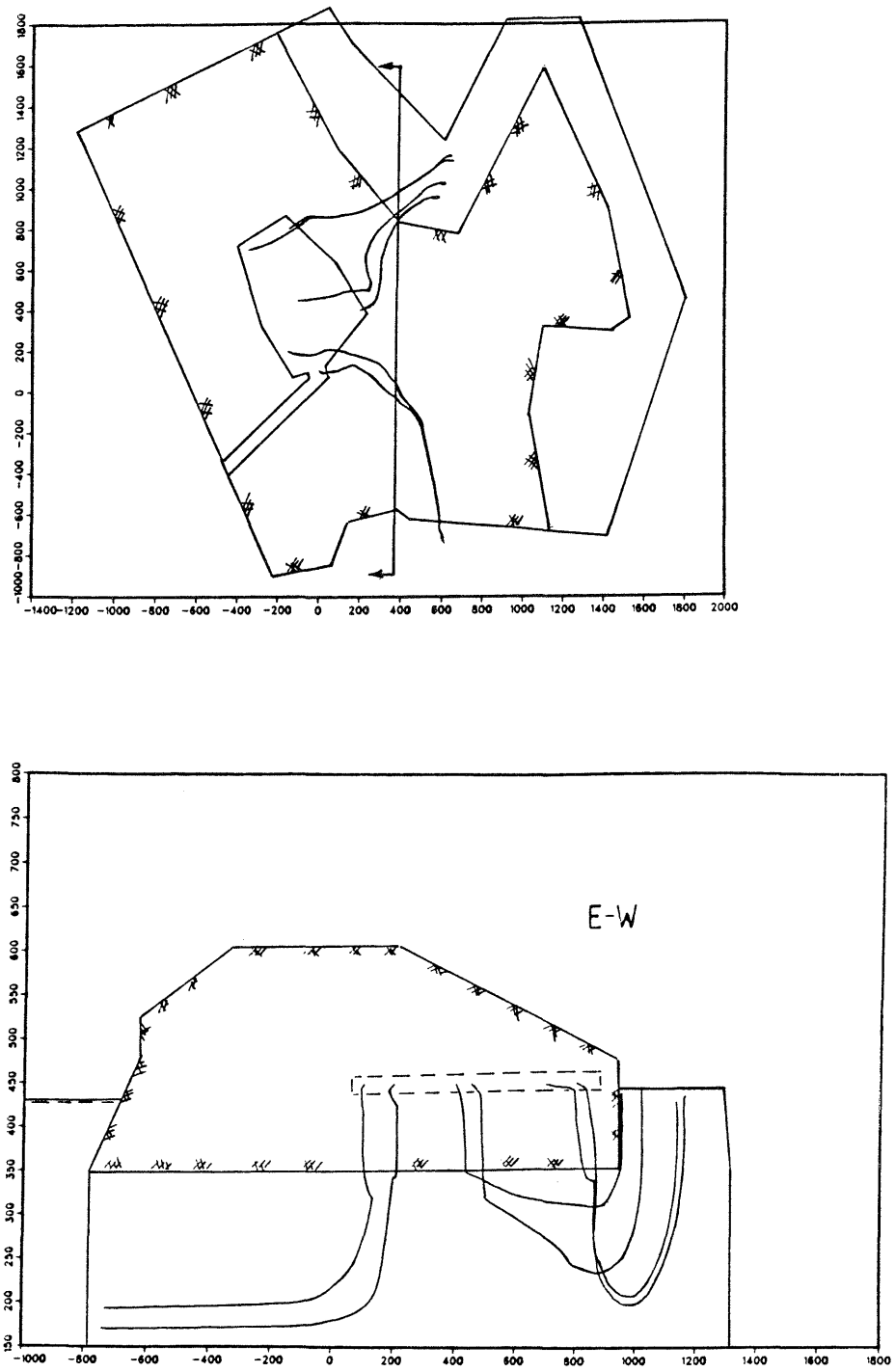

Figure 5.27 Path lines from the repository for run 6 in a horizontal and vertical projection

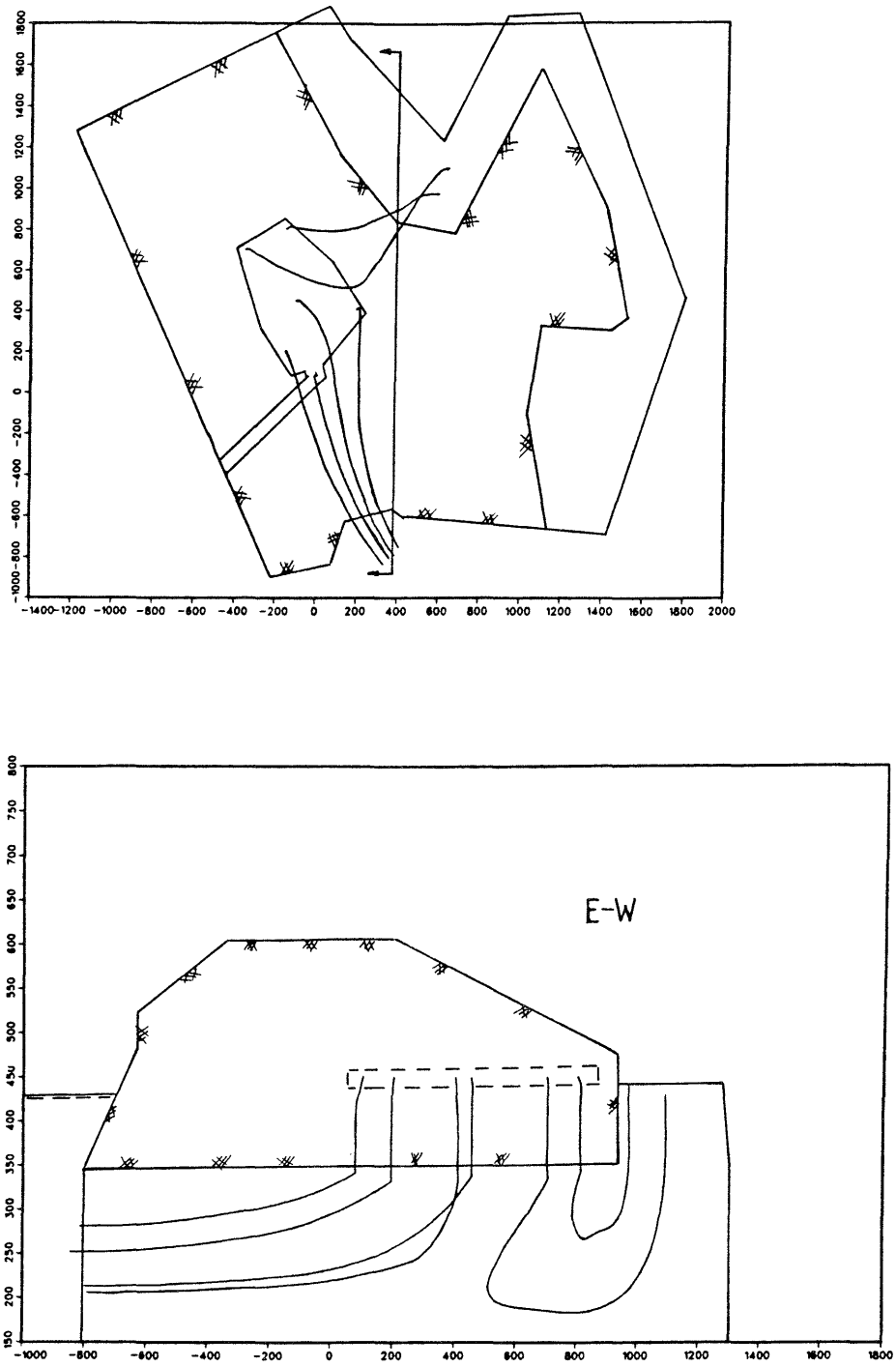

Figure 5.28 Path lines from the repository for run 7 in a horizontal and vertical projection

5.4 Relevance of the results

5.4.1 Groundwater recharge into the marl

The groundwater recharge, i.e. the rate of percolation needed to maintain the water table at the top surface, is calculated as the total recharge of the upper face of the marl surface (above the Urnersee) divided by the area of the corresponding surface, Table 5.4. In runs 1-4, part of the recharge area is covered by the pervious boundary layer. The values in Table 5.4, however, refer to the recharge into the marl.

Table 5.4 Calculated groundwater formation rates and recharge areas.

Run	Recharge rate(mm/yr)	Recharge area (km^2)
1	1.48	2.10
2	1.97	2.10
3	2.68	2.20
4	2.00	2.11
5	2.88	2.40
6	1.54	2.42
7	1.88	2.43

The percolation rate is in the range of 1.5-3 mm/yr for the seven runs, which corresponds to about 0.1-0.3% of the precipitation in the area.

5.4.2 Mass conservation in the solution

The mass balance deviation is a measure of the numeric quality of the solution.

A relative mass balance is calculated for each element in the mesh from the following equation:

$$\Delta_e = \frac{\sum_i F_i}{\sum_i |F_i|}$$

where; Δ_e = relative mass balance deviation for element e

F_i = the flow across element face i and the summation is made over all faces of element e

The elements are classified in order of their deviation in Table 5.5 below.

Table 5.5 Mass balance for the Oberbauen runs.

Run	Percentage of elements deviating from mass conservation with			
	<1%	1-10%	10-20%	20-100%
1	23.9	51.3	13.0	11.8
2	26.9	50.0	12.7	10.4
3	22.0	46.3	15.9	15.9
4	24.4	49.1	12.4	14.1
5	23.7	51.0	14.3	11.0
6	27.9	49.9	12.9	9.3
7	44.7	42.7	6.8	5.8

Elements with high deviation are located in areas where the conductivity contrast is high and where steep gradients are found. Another factor that affects the solution quality in the negative direction is the abundance of geometrically disturbed elements. This is, however, probably not the major reason for poor mass conservation in these meshes.

5.5 Discussion

The finite element calculations of the hydrogeology at the Oberbauen site show the importance (influence) and the sensitivity of the different parameters and boundary conditions to the flow situation.

The model input data are, due to the poorly founded geological investigations, afflicted with uncertainties. They are foremost:

- The boundary condition in the surrounding pervious boundary elements; i.e. the level of the water table in the limestone layers

- The material parameters of the subregional stratum (strata) underneath the marl body; i.e. the hydraulic conductivity of this formation(s).

The finite element mesh describes the geometry of the modelled domain in a simplified way. Some conservative assumptions have been made during the modelling work, such as:

- The flake representation of the storage tunnel system, which is modelled as a large decompressed zone. This approach will tend to exaggerate the flow rate within the repository

- The assumed marl thickness in the model underneath the repository was smaller than is to be expected. This fact will increase the particle travel time through the host rock by up to a factor of 3, compared to the calculated travel times

- The assumption that the groundwater table in the surrounding layers is equal (approximately) to the level of the Urnersee can be considered as a conservative estimate. This presumption causes the largest possible difference in hydraulic head between the repository and the underlying pervious formations, which implies high gradients and high Darcy velocities in the interlying marl formation.

The calculated flow in the critical area between the repository and the underlying formations is mainly determined by the boundary conditions in the western permeable boundary elements. The results of the calculations show that the difference in hydraulic head between the repository and the underlying pervious formations causes the path lines to go almost vertically downwards to the underlying stratum. A high water table in the western boundaries decreases the difference in head, which implies lower gradients and fluxes within the marl. Another effect of the western

boundary condition is the influence on the direction of the particle pathways in the underlying stratum. A high level of the water table causes the trajectories to exit from the model at the eastern boundary, while a lowering of the water table causes some of the trajectories, mainly in the western part of the repository, to exit at the western boundary.

The general flow within the marl body has a northbound component depending on the higher groundwater level at the southern boundary. When the elements at the southern boundary (above 350 m.a.s.l) are considered impervious, this component is eliminated and the flow becomes almost perpendicular to the repository plane. The introduction of the Tertiary shale recreates the northerly flow component.

The flow rates within the repository are principally determined by the conductivity assigned to the repository elements and by the direction of the flow vector in relation to the repository plane. A general flow direction parallel to the repository plane implies the highest flow rate.

REFERENCES

1. Thunvik R, Braester C,"Hydrothermal conditions around a radioactive waste repository", SKB-KBS Technical report 80-19, 1980.

2. Thunvik R, "Calculation of fluxes through a repository caused by a local well", SKB-KBS Technical report 83-50, 1983.

3. Tripet J-P, Motor Columbus Ingenieursunternehmung, Baden, Switzerland. Personal Communication, 1984.

4. Grundfelt B, "GWHRT - A finite element solution to the coupled ground water flow and heat transport problem in three dimensions", SKB-KBS Technical Report 83-51, 1983.

5. Neretnieks I, "Transport of oxidants and radionuclides through a clay barrier", KBS-TR 79, 1978.

REFERENCES TO NTB-REPORTS

NTB 85-17 Gas formation in a Type B Repository and Gas transport in the Host-Rock; M. Wiborgh, L.O. Höglund, K. Pers, Kemakta Konsult, Schweden.

NTB 85-20 Radionuclide Sorption on Carbonate clayish Rocks; B. Allard, RCG Consultant, Schweden.

NTB 85-29 Hydrogeologische Grundlagen für das Modellgebiet Oberbauenstock; G. Resele, J.P. Tripet, Motor Columbus Ingenieurunternehmung AG, Baden; April 1985.

NTB 85-30 Auflockerungszonen um Stollen und Kavernen im Valanginien-mergel des Oberbauenstocks; M. Gysel, Motor Columbus Ingenieurunternehmung AG, Baden; Januar 1985.